EFFICIENCY AND LEAKAGE ANALYSIS OF A TWIN-SCREW MULTIPHASE PUMP

A Thesis

by

YUSUF TURHAN

Submitted to the Office of Graduate and Professional Studies of
Texas A&M University
in partial fulfillment of the requirements for the degree of

MASTER OF SCIENCE

Chair of Committee,	Gerald Morrison
Committee Members,	Je Han
	Karen Vierow
Head of Department,	Andreas Polycarpou

May 2014

Major Subject: Mechanical Engineering

Copyright 2014 Yusuf Turhan

ABSTRACT

Multiphase twin-screw pumps have become an important alternative to produce the oil and natural gas from wells. In comparison to a conventional multiphase oil production systems, a multiphase twin screw pump provides larger boost with smaller footprint and less maintenance costs. Therefore, it is very crucial to analyze conducted experiments in the past in different ways with respect to demand of the twin-screw multiphase production systems.

The analysis of the Leistritz twin-screw pump data is formed by two sections. The first data is achieved by Texas A&M University Turbomachinery Laboratory with water-air mixture experiment; other data is achieved by Louisiana State University with water-methane experiment. In the first section, these experiments with different working fluids are analyzed. The similarities and differences which are caused by the working fluid difference, the operation differences and the instrumentation differences are considered. Since the experiment results must be limited by the nature of the pump, the experiment setup problems and their reasons are considered in the comparison part. The function of the liquid re-circulation instrumentation significance is highlighted in the first section.

In the second part, the leakage flow whose direction is from the pressure side to the suction side of the pump is investigated. The leakage flow and its properties are modeled with respect to Leistritz screw pump geometry and some thermodynamics and fluid mechanics tools. Furthermore, the leakage models are used to calculate the

mechanical efficiency with the single-phase experiment data. The TAMU experiment results are used to evaluate the accuracy of the leakage models. The leakage models show their accuracy in terms of the volumetric and mechanical efficiency. With considering and applying recommendations, the built leakage models can be used to predict the volumetric and mechanical efficiencies of a Leistritz twin-screw pump.

DEDICATION

Firstly, I dedicate this work to God. Then, to my departed family members: my dad TURGAY TURHAN, my grandmother TEVFIKA TURHAN, my aunt NILGUN BILEN, and my uncle AYDIN AKKOR.

ACKNOWLEDGEMENTS

I would like to thank my committee chair, Dr. Morrison, for his great assistance. It will be unforgettable experience to work with him. Also I would like to thank my committee members, Dr. Han and Dr. Vierow for serving on my committee and for their support.

I would like to thank the graduate students in the Turbomachinery Laboratory for making the Laboratory an adorable place to work. I also would like to thank my roommate Burak Erdogan for his support and patience. Thanks to Mehmet Oren, Abdulkadir Bostanci and Yasir Demiryurek for their friendship.

Thanks to Mustafa Kemal Ataturk for his great leadership and launching abroad scholarship programs for Turkish youth. Also thanks go to Turkish Petroleum Corporation for selecting me as a future worker with a scholarship.

Finally, thanks to my mother, my uncles, my aunt and my grandmother for their help in achieving important education and experience. Special thanks to my father for his support from heaven. Also thanks go to my lovely sister Sinem and cousins Ahsen, Hakan and Sezen. It would be very hard for me without their support.

NOMENCLATURE

A	Cross-sectional Area of Volume Created by Screw
B	Outer Screw Diameter
c	Clearance Diameter
c_{eff}	Effective Clearance
$c_{mixture}$	Mixture Speed of Sound
c_p	Constant Pressure Specific Heat of Air
c_v	Constant Volume Specific Heat of Air
CFD	Computational Fluid Dynamics
f	Darcy Friction Coefficient
F	Fahrenheit
f_c	Correction Factor
GPM	Gallons per Minute
GVF	Gas Volume Fraction
GVF_{exit}	Pump Exit Pump Based GVF
IP	Inlet Pressure
k	Heat Capacity Ratio
L	Tooth Length
LSU	Louisiana State University
l_h	Helical Arc that Describes the Circumferential Gap
$\dot{m}$	Mass Flow Rate

$\dot{m}_{inlet}$	Inlet Mass Flow Rate
n	Pump Speed
PSI	Pounds per Square Inch (Pressure)
P^*	Sonic Pressure
P_{in}	Pump Inlet Pressure
P_{out}	Pump Exhaust Pressure
P_r	Pressure Ratio (P_{out}/P_{in})
Re	Reynolds Number
R_c	Clearance Radius
$\dot{Q}_{actual}$	Total Volumetric Flow Rate of the Fluid Entering the Pump
$\dot{Q}_{air}$	Volumetric Flow Rate of the Air at the Pump Suction
$\dot{Q}_{re\text{-}circulation}$	Volumetric Flow Rate of Re-circulation Fluid
$\dot{Q}_{liq}$	Volumetric Flow Rate of the Liquid at the pump suction
$\dot{Q}_{theoretical}$	Maximum Theoretical Flow Rate
$\dot{Q}_{leakage}$	Leakage Volumetric Flow Rate
$\dot{Q}_{slip}$	Slip Flow in Circumferential Gap
s	Screw Lead
T^*	Sonic Temperature
TAMU	Texas A&M University
V_{ax}	Axial Velocity
V_g	Pump Displacement per Revolution
X	Empirical Pump Factor

ρ_{gas}	Gas Density
ρ_{liquid}	Liquid Density
η_{eff}	Effectiveness
η_{mech}	Mechanical Efficiency
η_{vol}	Volumetric Efficiency
ΔP	Differential Pressure

TABLE OF CONTENTS

Page

LIST OF FIGURES

Page

LIST OF TABLES

Page

1. INTRODUCTION

A conventional multiphase production system generally produces a mixture of oil, gas, water and sand. If the well pressure is enough to pump the mixture to the joint of the production center, the mixture is moved to this place with this energy. However, in some cases the reservoir energy is not sufficient to boost the mixture. At this point, the mixture is separated into phases which requires additional equipment such as separator, compressor and pump. With a multiphase pump, the phase separation is not needed, and then the equipment counted above is not required. With this equipment elimination the production expense can be reduced about 30% [1]. Furthermore, this elimination prevents the system extra maintenance cost and footprint area. [2]

Since the production of natural gas becomes more important nowadays, one of the most important missions of a multiphase pump is to work with high gas volume fraction conditions. In comparison with conventional multiphase production systems, a multiphase pump can work with 0-100% GVF conditions which makes the pump unique. Efforts have been made to increase its efficiency and understand how it works [2]. However, pump manufacturers only provide the single-phase operation performance charts of the pump and this makes it difficult to select the correct pump for the desired multiphase operation conditions [3]. Therefore, multiphase operation experiments with twin-screw pumps and their analyzed results are valuable tools for oil production industry.

In this part, the screw pump technology, the twin screw-pump, multiphase fluids and flow types that are used for leakage models will be explained.

1.1 Screw Pumps

Screw pumps are split into two parts: Single rotor and multiple rotor types. In the single rotor type, the rotor thread meshes with the internal housing threads. Multiple rotor types are split into two parts as well: Single-end and double – end. In both cases only one rotor is driven. While a gear is used to rotate the other rotor in double-end screw pumps, the single-end screw pump configuration enables the other rotor to rotate with the motion of driven rotor [4].

Even though all rotary pumps move the fluid circumferentially, flow pattern of screw pumps is axial. This makes the screw pumps unique and gives numerous advantages as follows [4]:

- It is able to work in a wide range of different conditions such as flow type, pressures, liquid type and viscosity.
- Since its inertia of rotating parts is lower, it can work in high speeds.
- The axial flow pattern results in low internal velocity.
- It can work in multiphase operations.
- Since the mechanical vibration is so low, it can work silently.
- The installation and the maintenance of the pump are relatively easy.
- The pump is able to tolerate solid particles in the pump.

There are some important parameters that govern the performance of a screw pump. They can be counted as follows:

- Inlet Condition: Since a screw pump is not able to pull or lift the fluid, there must be a force to enter the fluid into the pump. Generally, atmospheric pressure is used for this operation.
- Fluids and Vapor Pressure: The vapor or dissolved air pressure may cause the cavitation and this suffers efficiency. Also it may cause noisy operation.
- Viscosity: The viscosity of the fluid has a direct relation with the filling cavity rate. Since fluids with higher viscosity need more time to fill the rotor cavity, the speed selected for the pump should be lower in this situation.
- Outlet Conditions: Outlet conditions such as pipe size are crucial to outlet pressure. For example, with a good selection of pipe size, the operation of pump may be more efficient [4].

1.2 Twin-Screw Pump

The twin screw pump, which is in the subject of interest, is in the double-end screw pump family. It is configured with two opposed screws which have the same size with a common driving rotor. The screws are connected by a gear. The pump has a common inlet and a common outlet. All axial loads on the screws are balanced. Double-end screw pumps are capable of work in a wide range pressure application with large volumetric flow rates. Furthermore, the viscous and the multiphase flow can be handled with the same system. [4]

Fluid is moved by the series of C-shaped cavities which are generated by the rotating screws. Therefore, the pump geometry and pump speed are the only governing

parameters to define theoretical volumetric flow rate of the pump. Figure 1 is the sectional drawing of a twin screw pump.

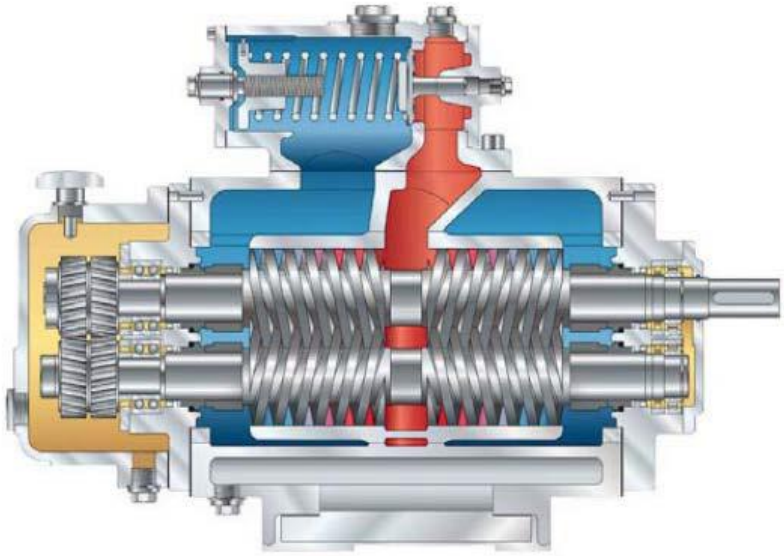

Figure 1 Sectional drawing of a twin screw pump [5]

In order to avoid metal- metal contact in a pump operation, the twin-screw pump is manufactured with tolerances. These tolerances are also called clearances. There are three types of clearances: Circumferential Clearance, Flank Clearance, and Radial Clearance. The pressure rise across the pump causes backflow or leakage across these clearances. This situation suffers both the volumetric and the mechanical efficiency. Therefore, understanding this leakage flow is the most important thing for a multiphase operation to estimate the pump performance. Figure 2 shows these clearances. As seen in the graph, the circumferential clearance is located between the liner and the screw, the root clearance is the tolerance between outer diameter of the screw and root diameter of

the other screw and then the flank clearance is tolerance between flanks of screw rotors [2].

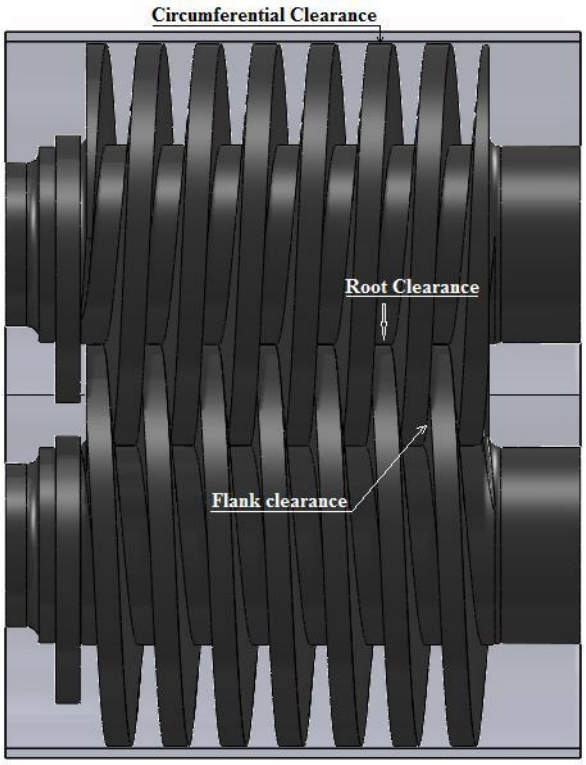

Figure 2 Clearance types of a twin screw pump [2]

1.3 Multiphase Fluids

For a multiphase operation, the multiphase flow type and flow regimes should be known. Firstly, the multiphase fluids are split into two parts: Homogenous multiphase flow, in which includes multiple phases of only one type of liquid and heterogeneous multiphase flows which may include different substances. In oil production area, nearly all operations are conducted with heterogeneous flow because the production mixture includes crude oil, natural gas, sand, water, wax etc. The main governing parameters for

the flow regime are the GVF of the multiphase production and the relative velocities of the flow. Figure 3 illustrates the possible flow regimes for mixed fluid flow. However, it is hard to determine the flow regime in a twin-screw pump because the C shaped cavity adds other forces to the flow and this affects the relative speed of phases [5].

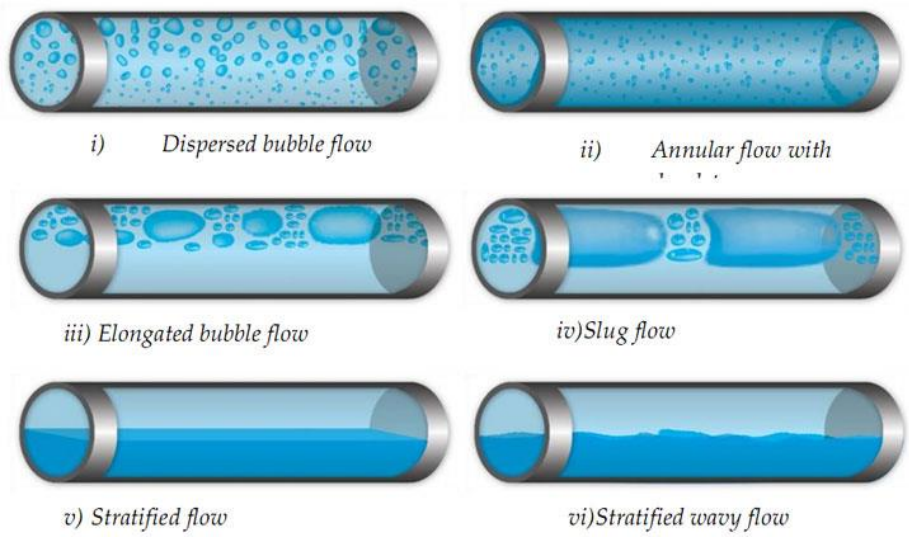

Figure 3 Multiphase flow regimes [5]

1.4 Pipe Flow

The pipe flow model is mainly based on the mass and energy conservation laws. According to this law, the inlet and outlet mass and energy should be equal. Bernoulli Equation can be used for this type of this flow. In addition, with consideration of the inlet and outlet flow properties, the energy consumption due to the friction should be added into the energy equation. The final form of the governing equation for a pipe flow with the fully developed flow assumption is [6]:

$$\left\{P + \frac{1}{2} * \rho * V^2 + \rho * g * z\right\}_{inlet} = \left\{P + \frac{1}{2} * \rho * V^2 + \rho * g * z\right\}_{outlet} + h_{friction}$$

where P is the pressure, ρ is the density of the liquid, V is the velocity of the liquid, g is the gravitational acceleration, z is the height. $h_{friction}$ is the consumed energy due to the friction forces.

A French engineer, Henry Darcy, and a German Professor, Julius Weisbach, found a correlation for the friction power:

$$h_f = f * \frac{L}{d} * \frac{V^2}{2}$$

where f is the Darcy friction coefficient, L is the pipe length, d is the hydraulic diameter of the pipe and V is the inlet velocity. [9] The friction coefficient depends on the flow mode and the pipe geometry. For a plain and circular pipe the Darcy friction coefficient is [7]:

$$f = 0.3322 * Re^{-0.25}$$

where Re is a dimensionless number which is used to detect the flow type such as laminar, turbulent or transition. This detection depends on the flow environment and the friction.

1.5 Choked Flow

For a compressible flow, the speed of sound is one of the main criteria to evaluate the compressibility factor of the pump. If the compressible flow velocity is equal to the speed of sound the flow type is called a choked flow. The flow properties of

the choked flow for air can be found by some thermodynamic correlations as followed. Here, k is the isentropic gas coefficient. The air isentropic gas coefficient is 1.4.

$$\frac{P^*}{P_0} = \left(\frac{2}{k+1}\right)^{k/k-1} = 0.5283$$

$$\frac{T^*}{T_0} = \left(\frac{2}{k+1}\right) = 0.8333$$

where P^* is the sonic pressure in the choked flow and P_0 is the inlet pressure and T^* is the sonic temperature and T_0 is the inlet temperature [6].

2. LITERATURE REVIEW

The multiphase operation with a twin-screw pump became an important research area with the venture of the French Institute of Petroleum in the 1970s. Henceforth, other pioneer petroleum companies joined this research area. Some of them are conducted by a consortium of these companies and some of them are conducted privately. Furthermore, the pump manufacturers put valuable effort into understanding the pump performance in different conditions [3].

This part includes that the twin screw pump analysis in different multiphase operations and the models to predict its performance in various projects. In the first part, the projects with the multiphase operations will be investigated. Their results and conclusions will take place in terms of the pump operation parameters such as efficiencies and flow properties. In the second part, the leakage flow models and their set up process will be explained.

2.1 Multiphase Operation with a Twin-Screw Pump

In order to investigate various projects in a categorical way, the multiphase operation projects with a twin-screw pump will be considered with some pump performance metrics. Basically, the efficiencies of the pumps are able to give us an idea about their performance. There are two types of efficiencies that dictate the pump performance: the volumetric efficiency and the mechanical efficiency. The projects which are in the subject of interest will be explained under the title of these efficiencies.

The main governing parameters which affect these efficiencies will be discussed. The project conductors, the working pump and the operation conditions are tabulated in Table 1. All experiments are conducted in the Texas A&M University Turbomachinery Laboratory.

Table 1 Multiphase Experiments with Twin Screw Pump

Project Conductor	Pump	Operation Conditions
Abhay Ravindra Patil(2013)	Colfax MR-200 Twin Screw Pump	GVF=%50-100
		ΔP= 50,100,150,200,250 PSI
		Inlet Pressure=15,50,75,100 PSI
		Speed= 900,1350,1800 rpm
Ryan Kroupa(2011)	Leistritz Twin Screw Pump	GVF=%0-100
		ΔP= 50,100,150,200,250 PSI
		Inlet Pressure=10,50 PSI
		Speed= 1800,2700,3600 rpm
Theodore Isaac Hatch(2013)	Colfax MR-200 Twin Screw Pump	GVF=%65-92
		ΔP= 50,100,150,200,250,300 PSI
		Inlet Pressure=15,50 PSI
		Speed= 900 rpm

2.1.1 Volumetric Efficiency

The volumetric efficiency is found by the following formula:

$$\eta_{vol} = \frac{\dot{Q}_{actual}}{\dot{Q}_{theoretical}}$$

The fluid which is moved by the pump is always less than the theoretical volumetric flow rate because of the non-touch design of the pump. The volumetric efficiency directly affects the overall pump efficiency because the backflow suffers the

mechanical efficiency. Therefore, it is crucial to work in the high volumetric efficiency range in multiphase operations.

Abhay Patil stated that the volumetric efficiency firstly depends on the inlet pressure. Inlet pressure increase reduced the volumetric efficiency in all particular GVF case. This was an expected result because with the inlet pressure increase, the inlet gas amount was increased. Hence, the leakage was increased as well. However, the best volumetric efficiency was achieved in different GVF conditions for each inlet pressure case. When inlet pressure is increased, the GVF of the mixture should be increased a little bit in comparison to a lower inlet pressure case to get better volumetric efficiency. For example while the best volumetric efficiency value was achieved in the %70 GVF case in 15 PSI inlet pressure case, for 50 PSI inlet pressure case the GVF value should be around %90. This is because in the low inlet pressure case the phase separation is much more because of the density difference and the gas phase needs more liquid for sealing. The speed of the pump was another parameter for the volumetric efficiency. While in single-phase operations the speed increment suffered volumetric efficiency, in multiphase operations the speed increment was beneficial. Since the speed increment increases the centrifugal affects, the gas seals well in high speed cases. This affect can be seen especially in a high inlet pressure case because the leakage due to the differential pressure becomes predominant. Furthermore, the temperature increment across the pump, viscosity and pump geometry influences were reported in this dissertation. Temperature rise in the outlet suffered volumetric efficiency. While viscosity increment was good for volumetric efficiency in low GVF operations, in high GVF operations it

did not affect the volumetric efficiency. Lastly, he compared the Leistritz pump and the Colfax pump. Even though Leistritz pump is more advanced in terms of sealing options, Colfax pump volumetric efficiency was much better. He stated that the pump geometry played significant role for this conclusion because the Colfax pump prevents leakage flow thanks to its geometry [2].

Ryan Kroupa generally agrees with Patil's results in his thesis. An interesting result he achieved for speed is that 2700 rpm and 3600 rpm results were nearly indistinguishable. However, 1800 rpm results were drastically different. The pump did not work in above 150 PSI of differential pressure because this rotational speed was not able to overcome the amount of leakage. Another interesting result is that he found that the volumetric efficiency trends with respect to differential pressure for 0 and %50 GVF was totally different than the high GVF cases (%90-%100). Also, the volumetric efficiency tended to stay constant in all particular GVF and it did not depend on the differential pressure. In addition, he put another effort to work in the %100 GVF and the 250 PSI differential pressure condition which he called the worst scenario for a multiphase operation. He mainly focused on the temperature effect on the volumetric efficiency and he conducted an experiment with the temperature parameter. Low temperature is 120 F and high temperature is 180 F. As can be seen in Figure 4, the temperature rise had a dramatic effect on the volumetric efficiency [5].

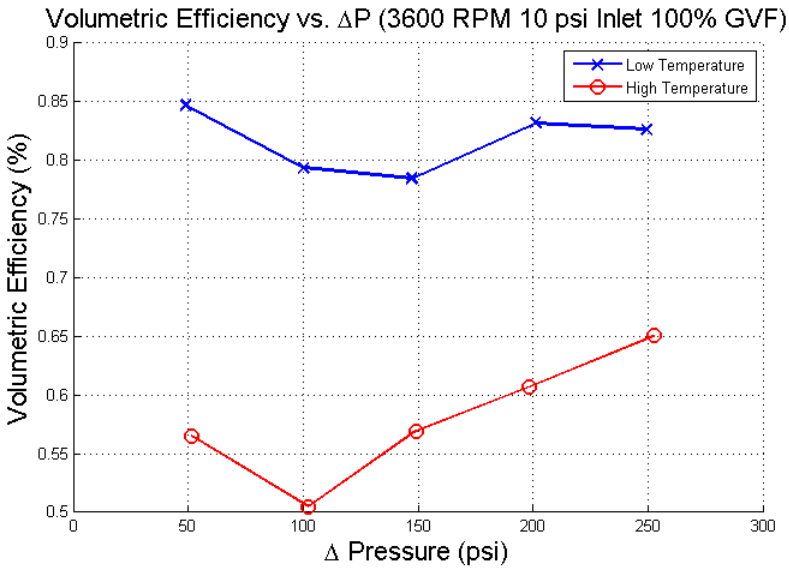

Figure 4 Temperature rise effect on volumetric efficiency [5]

Theodore Isaac Hatch found that the volumetric efficiency more depends on the pressure rise across the pump. The differential pressure makes it hard to push all inlet fluid to exhaust and this induces the larger leakage volumetric flow rates in high GVF operations. The pressure rise dependency can be seen in the higher inlet pressure case as well. The contours of volumetric efficiency purely depend on the pressure rise of the pump especially in higher inlet pressure cases. As can be seen in Figure 5, there is no sign for volumetric efficiency change with respect to GVF. Moreover, he compared open-loop facility and the closed-loop facility in the same operation conditions. Even though the working fluid temperature is more in the closed-loop facility and it suffers the volumetric efficiency, the closed-loop facility is more efficient in terms of the volumetric efficiency in all conditions such as the inlet pressure, differential pressure and GVF [3].

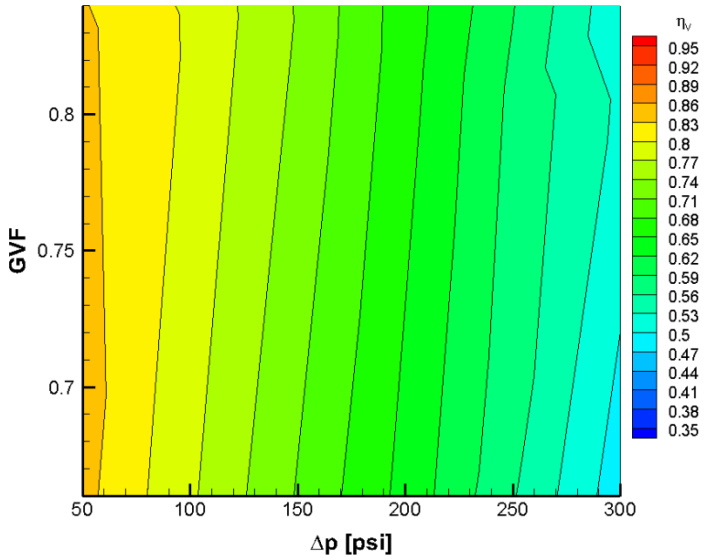

Figure 5 Volumetric efficiency in higher inlet pressure operation [3]

2.1.2 Effectiveness and Mechanical Efficiency

Mechanical efficiency can be calculated by the following formula:

$$\eta_{mech} = \frac{P_{actual}}{P_{electrical}}$$

where P_{actual} is the power imparted to the fluid by the pump and $P_{electrical}$ is the power supplied to the pump providing a constant rotation speed [2]. Mechanical efficiency is the most important metric to evaluate the pump performance. Basically, the system sustainability can be examined with the mechanical efficiency. However, the mechanical efficiency can be found after the operation of the pump. In order to get a theoretical efficiency metric before operations, the effectiveness can be used. Effectiveness is:

$$\eta_{effectiveness} = \frac{P_{model}}{P_{hydraulic}}$$

where P_{model} is the power calculated by the summation of the liquid compression and the gas compression power with respect to thermodynamic gas compression models such as isothermal or polytropic. $P_{hydraulic}$ is the calculated power which is assumed that all entered fluid to the pump is incompressible fluid. Basically, effectiveness presents how the gas compressibility affects the pump efficiency.

Abhay Patil indicated that for the gas compression model, GVF plays a significant role. In the low GVF operations the liquid is sufficient to seal the gas and the compression heat can be absorbed by the liquid. Therefore, the isothermal model can be used for gas compression. However, temperature rise takes place in high GVF operations and the polytropic compression becomes the gas compression model in these operations. In the isothermal model the polytropic index equals 1 and in the isentropic model the polytropic index equals ratio of specific heats. The polytropic index increment is beneficial for both the effectiveness and mechanical efficiency. The best effectiveness values were achieved in the higher inlet pressure but lower differential pressure and lower GVF conditions. The mechanical efficiency increased with the inlet pressure increment because the inlet mass flow rate induced the greater work for pump. Especially in high GVF operations, the mechanical efficiency mostly depends on the GVF value and pressure rise across the pump contribution becomes negligible. The pump speed was another parameter for its performance as well. The pump speed increment increased the mechanical efficiency. Furthermore, in order to compare multiphase screw pumps and the conventional multiphase systems, Patil compared the results of the pump and an isentropic compressor. According to his results, a

conventional isentropic compressor consumes much more power for the same amount of gas compression. This is another sign to present the multiphase pump efficiency. Figure 6 shows the comparison of the multiphase pump and the isentropic compression in terms of power output per kilogram of gas [2].

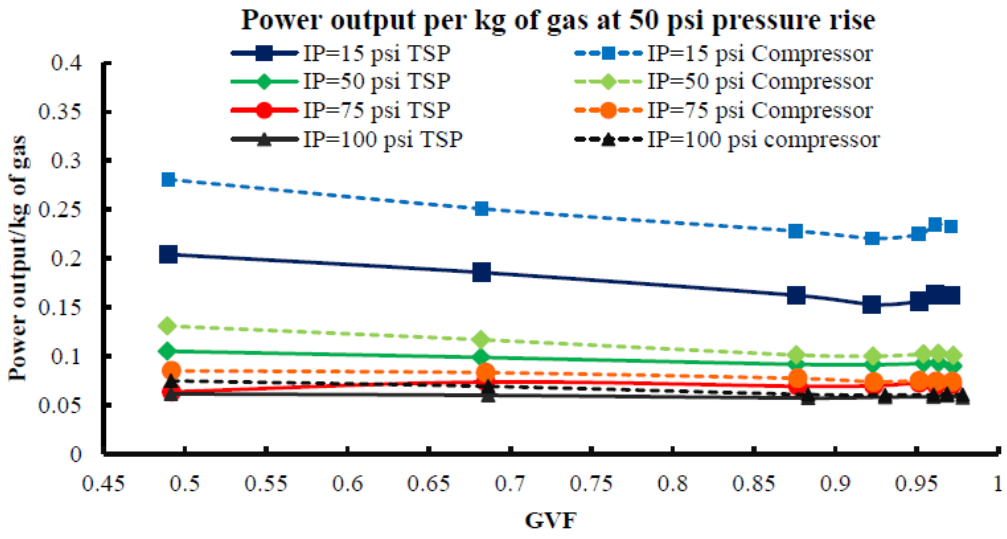

Figure 6 Power output per unit mass of gas at different inlet pressures [2]

In addition, the temperature rise did not play a significant role for the mechanical efficiency because there is not so much difference between the isothermal and the polytropic gas compression models. The viscosity change did not affect the mechanical efficiency either. Lastly, as expected, the Leistritz pump had smaller mechanical efficiency because of a large leakage flow in comparison with the Colfax pump [2].

Ryan Kroupa brought another point of view for the inlet pressure dependency of the mechanical efficiency. He showed with his experiment that the electrical power consumption only depended on the pressure rise across the pump linearly and the inlet

pressure had no effect on it. Therefore, the mechanical efficiency was greater in the higher inlet pressure case because the work done by the pump was greater. Since the only purpose of the multiphase pumping is to move the fluid with an identified exhaust pressure, the heat rise is not desired. In higher pressure and higher GVF operations, he observed that the inlet temperature effect becomes notable and the mechanical efficiency decreases [5].

Theodore Isaac Hatch agrees with the mechanical efficiency change with the operation conditions as stated in the projects above. He found that the closed-loop facility is better in terms of the volumetric efficiency, and this phenomenon is true for mechanical efficiency as well. The mechanical efficiency in closed-loop system behavior was very similar to the open-loop system behavior. Figure 7 shows both the similarity in contours and better efficiency result. In the figure, the left contour shows the mechanical efficiency of the closed-loop facility and the contour placed at the right shows the mechanical efficiency of the open-loop facility. As can be seen in the graph the closed-loop facility provides better mechanical efficiency [3].

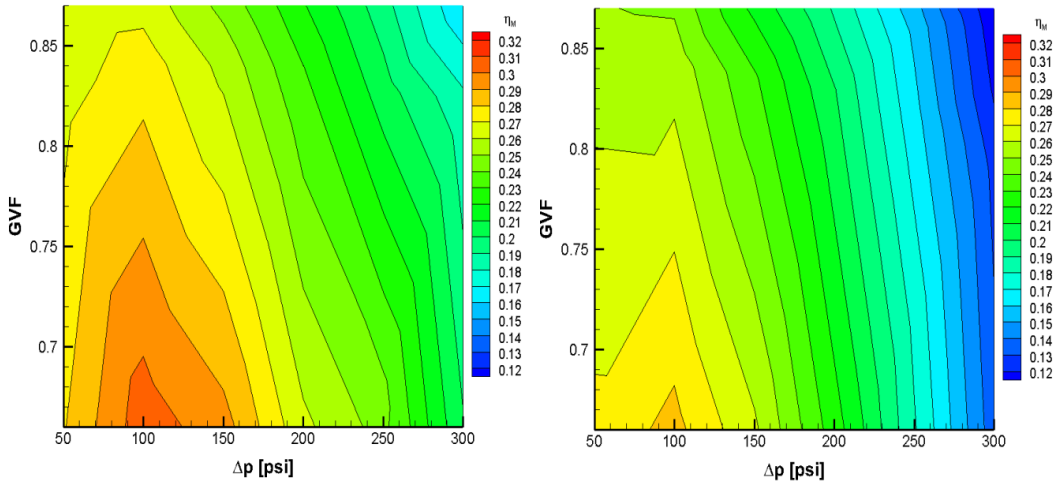

Figure 7 Mechanical efficiency comparisons of closed-loop facility and open-loop facility [3]

2.2 Twin Screw Pump Leakage Models

As stated before, the leakage has a direct effect on the pump performance and it is very important to predict the leakage amount for pump operations. In the literature there are several works for the leakage flow and its modeling. Since the geometry is very complex, the pump operation conditions are different, and the interaction between the phases and the chamber takes place, the assumptions are very important to build models. As will be explained the main difference of the leakage models are their approach to interaction between the screws and the mixture.

2.2.1 Vetter-Wincek (1993)

Vetter and Wincek provided a computer model for their leakage model and they conducted an experiment to validate their model. The experiments were conducted with two screw pumps with timing gear and free clearances and they considered the

contamination with abrasives. The computer model is mainly based on the geometric properties which are roughness, rotation and eccentricity effects. For two-phase operation, they assumed that the clearances are filled by only liquid and the gas compression occurred because of the liquid back flow. They achieved the same results in the experiment with the computer program for one-phase flow. Because of the increasing gas content the performance of the computer program becomes doubtful. As expected, the liquid-filled clearance theory cannot be acceptable in high GVF operations [7].

The clearance leakage flow is split into three parts: the circumferential clearance, the radial clearance and the flank clearance. Theoretical leakage volumetric flow rate is calculated with the fully developed and the stationary flow assumption and the inlet and the outlet losses are neglected. The calculation part includes two components: the differential pressure component and the rotational component. The clearance geometry does not stay constant because of the existing differential pressure. Hence, the elastic-shaft bending should be considered. Also because of the centrifugal forces, authors assumed that the clearance leakage flow was separated into single-phases. Therefore, there was no gas leakage flow and all clearances were filled by liquid. Finally, these important results are achieved by the authors [7]:

- The circumferential clearance had biggest portion of the internal leakage flow with approximately 80 percent and the radial clearance had 15 percent of the total internal leakage flow. Flank clearance had only 5 percent of the internal leakage flow.

- As can be seen in Figure 8, the single-phase operation had linear pressure distribution and it does not depend on the speed. However, the multiphase operation, which is in very high gas/liquid ratios, shows its compressible effects on the differential pressure distribution. Hence, most of the compression takes place in the last screws.
- As expected, the authors had more accurate results in single-phase operation with the theoretical calculation.
- The authors concluded that the totally-liquid filled clearances may not always be applicable in all operation conditions, especially above 80 percent GVF conditions.

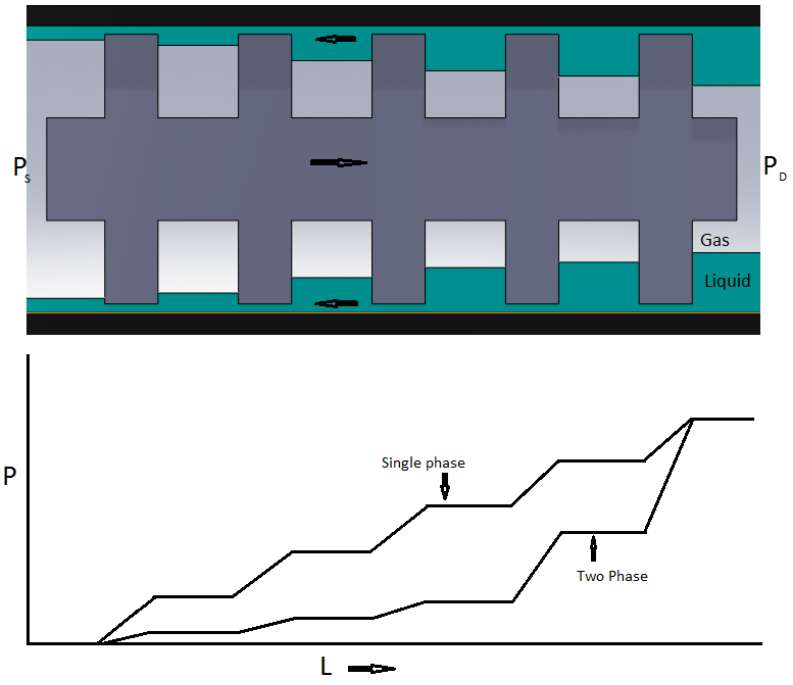

Figure 8 Vetter and Wincek leakage model and the pressure distribution across the screw [7]

2.2.2 Feng et al (2001)

Feng et al. developed their leakage model with respect to the position of the rotor. The clearances were categorized with respect to the filled fluid type. As can be seen in Figure 9, L is referred to the lobe tip and S is referred to the blowhole. They assumed that L_3 and L_4 are filled by the liquid due to the centrifugal forces. Other clearances which S_1, S_2, S_3, S_4, L_1 and L_2 are filled by the mixture. Here L_1 and L_2 are called contact lines.

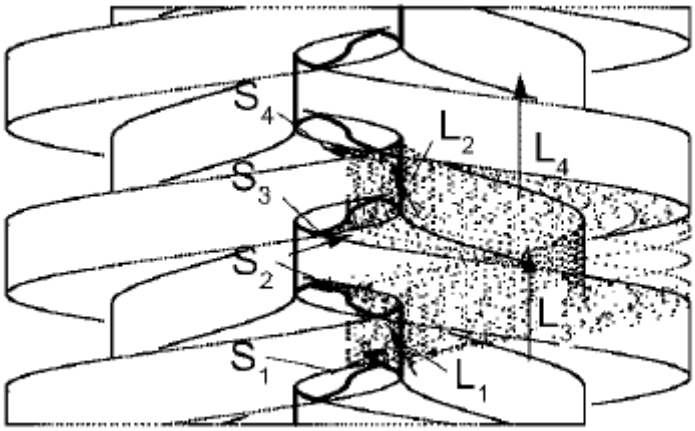

Figure 9 Visualization of clearances [8]

Lobe tip clearance leakage mass flow rate is calculated with the incompressible, viscous, laminar flow assumptions [8]:

$$\dot{m}_l = \frac{\rho_l * \pi * d_l * h^3 * \Delta P}{12 * \mu_l * L}$$

Blowhole clearance leakage flow is modeled as a two-phase flow through an orifice. The following formulation was used [8]:

$$\dot{m} = \frac{c * \alpha * \varepsilon * A(\varphi) * \sqrt{2 * \rho_l * \Delta P}}{(1-x) * \Theta * x\sqrt{\rho_l / \rho_g}}$$

where c is devised from experiments, α is the expansion coefficient, A(φ) is the cross-sectional area of the blowhole x is the mass ratio of gas to oil and Θ can be found by Lin`s correlation. Finally the contact line leakage flow is calculated by the adiabatic two-phase flow in narrow channels between two plates. With the following formula the contact line leakage flow can be calculated [8]:

$$\dot{m} = c * A \sqrt{\frac{2 * \Delta P * D_H * \rho_L}{4 * \phi_L^2 * f_L * (1-x)^2 * \Delta Z + D_H * \left[1 + x * \left(\frac{\rho_L}{\rho_G} - 1\right)\right]}}$$

where ϕ_L is the friction multiplier which is calculated by Lockhart-Martinelli type of correlation, f_l is the friction factor of the liquid and ΔZ is the equivalent height [8].

With the assumptions and calculations, the model gave accurate results with respect to their experiment. As can be noted in Figure 10 the calculated results and the measured results are very close in the high GVF and the high inlet pressure condition [8].

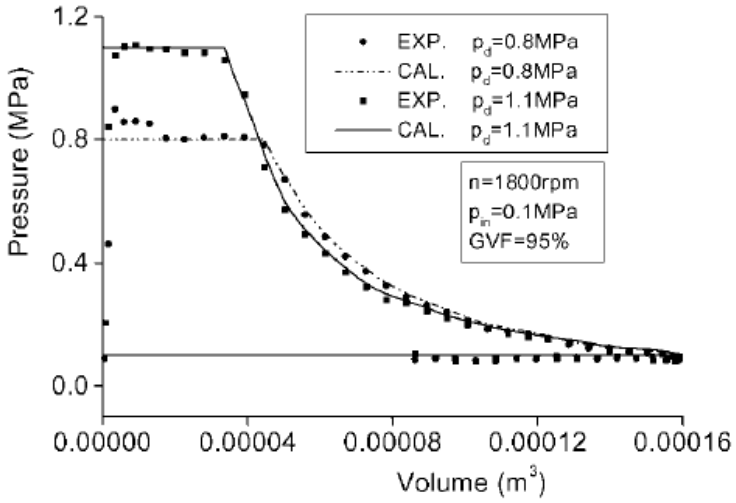

Figure 10 Calculated results and experiment results comparison [8]

2.2.3 Martin (2003)

Mercedes Martin from Texas A&M University developed a model with simple geometrical approximation. He used single-phase water data to predict the leakage amount in the pump and modified it to the multiphase operations. He created a term which is called "effective clearance" purely depends on the characteristic curve of the pump. The following assumption were made for the model [9]:

- The leakage is only in circumferential clearance. The length of the circumferential clearance can be calculated by a geometrical correlation. Figure 11 shows the basic dimensions of the screw.

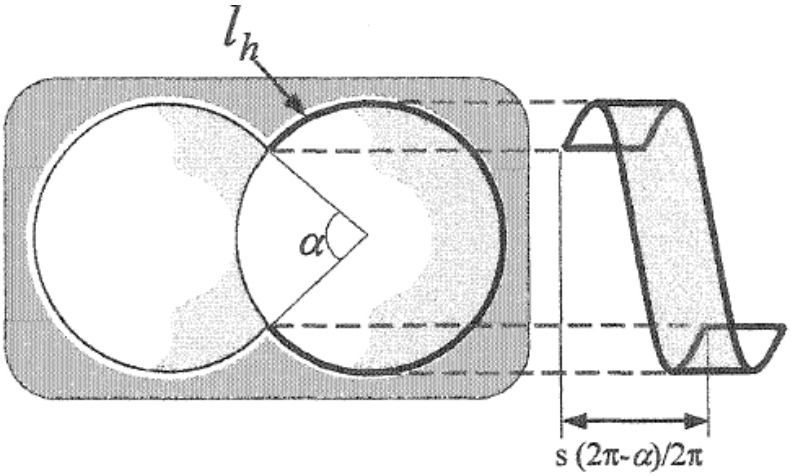

Figure 11 Circumferential path of the leakage [9]

Here, l_h is calculated by the following formula:

$$l_h = (2 * \pi - \alpha) * \sqrt{\left(\frac{s}{2 * \pi}\right)^2 + R_c^2}$$

where α is the portion of the circumferential channel interrupted by the screw meshing [9].

As seen, the height is much smaller than the wideness. Therefore, the flow can be assumed as two dimensional laminar flow. This is also known as Poiseuille flow between parallel plates. With the following formulas the slip volumetric flow rate can be calculated:

$$C_{eff} = 4 * l_h * \left\{\frac{c^3}{0.033 * \rho^{0.75} * \mu^{0.25} * s}\right\}^{0.57}$$

where c_{eff} is the effectiveness clearance. Also it should be noted that the liquid part of the mixture physical property values are used in the formula above. The effectiveness clearance is used in the following formula to predict the leakage volumetric flow rate.

$$\dot{Q}_{slip} = f_c * l_h * \frac{c_{eff}^3 * \Delta P}{6 * \mu * s}$$

where f_c changes with respect to flow type. When the flow is laminar, it equals to the 1. In the turbulent flow condition it equals to the 5. Basically Martin concluded that the turbulent flow assumption can be made with the low viscosity fluids such as water [9].

The developed model by Martin gave parallel results from experiments in relatively lower GVF conditions. From %50 to %90 GVF the model accuracy was acceptable. However, above %90 GVF the accuracy of the model became doubtful [9].

2.2.4 Rabiger (2006)

Most of the leakage models considered that the liquid part of the mixture is able to absorb the side effects of the gas compression part. However, in high GVF operations the compressibility and some thermodynamic effects such as pressure drops, choked flow conditions should be considered [10].

For the thermodynamic model of the pump was considered as formed subsequent chambers. And each chamber was considered as a control volume. As can be seen in Figure 12, there is inflow and outflow to the leakage from the mixture in the chamber. Each letter is referred as an amount of bulk or energy and their thermodynamic properties as follows:

- **a-** Gas Inflow: It has the constant specific enthalpy.

- **b-** Liquid inflow: It has the constant specific enthalpy.
- **c-** Gas compression because of the liquid inflow: Gas temperature increasing
- **d-** Liquid outflow: It may have variable specific enthalpy.
- **e-** Gas expansion by liquid outflow: Gas temperature decreasing.
- **f-** Gas outflow: It may have variable specific enthalpy.
- **g-** Gas- liquid heat transfer: It occurs through the interfacial area.

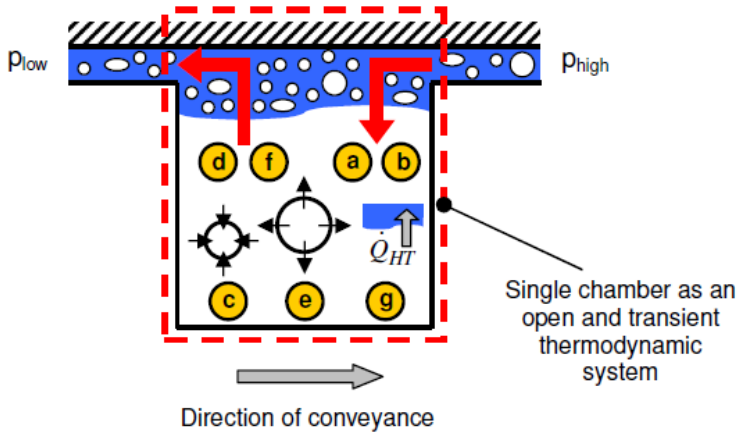

Figure 12 Chamber control volume [10]

With the assumptions counted above the mass and the energy conservation laws were applied to the subsequent chambers. Also it should be noted that for the temperature or the pressure change the isentropic model assumption was used. The heat transfer between phases was modeled by the simple stratified flow assumption and the identical temperature in the end of the heat transfer assumption. Figure 13 shows how the phase temperatures change in a single time step [10].

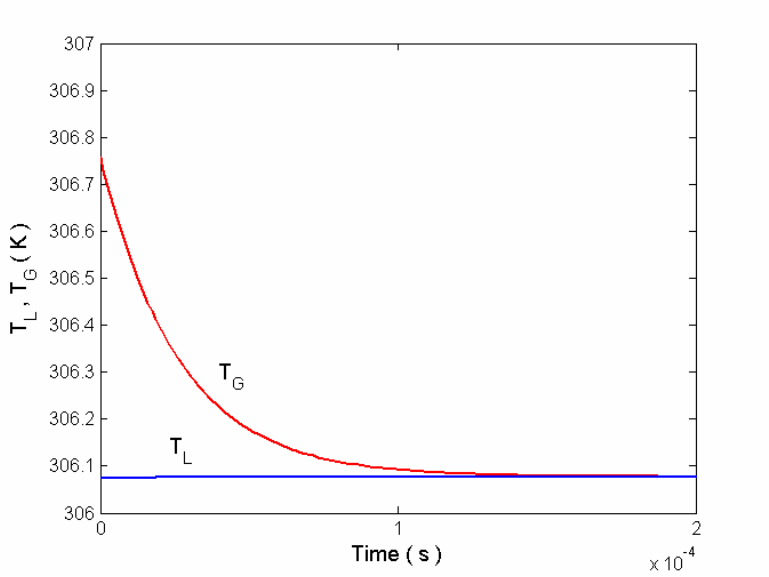

Figure 13 Temperature change in a chamber in a single time step [10]

The flow in the perimeter and the radial gap was modeled in a rectangular clearance with fully developed flow and the mass, momentum and the energy conservation equations were applied. Also, the model was able to work in the extreme condition for critical flow which is the case of the static pressure difference is so high between subsequent chambers [10].

The pump inlet properties with estimated inlet velocity were used in the calculations above and then the model was controlled by the outlet properties of the pump. The achieved results can be counted as follows [10]:

- The leakage flow lost their sealing effect in high GVF operations because of the density and viscosity decrease.
- The maximum temperature increase was observed between the inlet and the first chamber because of the heated leakage for both phases.

- As can be seen in Figure 14, the GVF was decreasing in each chamber because of the liquid amount in the leakage flow.

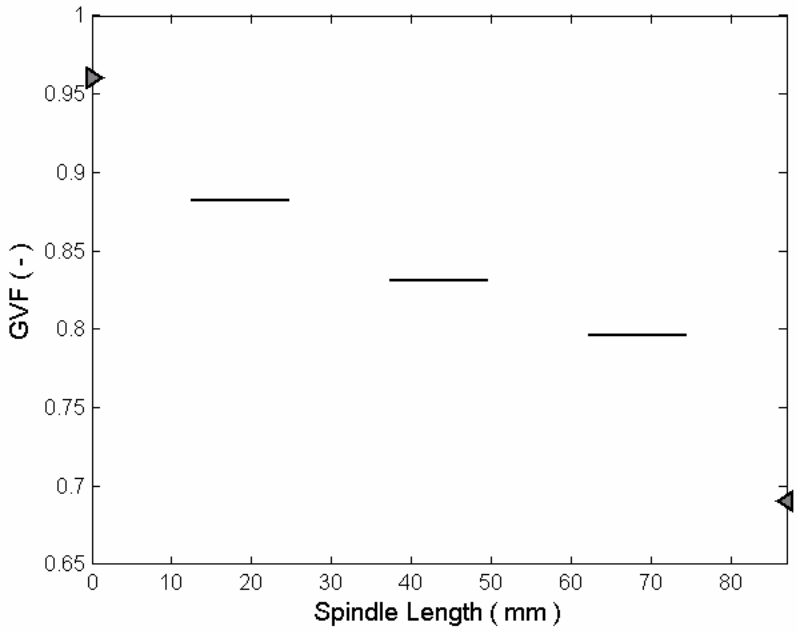

Figure 14 GVF change across the screw [10]

2.2.5 Beijnum (2007)

A graduate project which was written by M. van Beijnum in Technische Universiteit Eindhoven is about to CFD Simulation of Multiphase Twin Screw Pump. The experiment and the numerical solution are conducted in three different cases:

1. Non-rotating screws with single-phase flow
2. Rotating screws with single-phase flow
3. Rotating screws with multiphase flow

In the project, the leakage flow was considered in two parts: Through an annulus with rotating cylinder, the flow between the screw and housing and through a straight-through labyrinth seal. Theoretically leakage flow rate which can be calculated by an experiment is

$$\dot{Q}_{leakage} = k_2 * \Delta P * D^2$$

where D is the screw diameter and k_2 is an empirical constant which depends on the geometry and the working fluid [11].

The leakage mass flow rate was simplified and equations are built with respect to the experiment case. For the first case which is non-rotating screws with single-phase flow, the flow was assumed as Hagen-Poiseuille flow in a cylindrical annulus and the axial velocity for a screw was found by following equation:

$$V_{ax} = \frac{\Delta P * s^2}{12 * \mu * L}$$

where ΔP is the pressure difference for each tooth, s is the clearance between the screw and the liner, μ is the viscosity of the liquid and L is the screw length. Since $5\,{}^{1}/_{3}$ screw threads seal 4 cavities the total differential pressure is divided by 4 for ΔP in this case [11].

For the second and the third case the following general formula was used for the pressure drop:

$$\frac{\Delta P}{\rho} = \left(\lambda \frac{L}{s} + \delta_{i0}\right) \frac{(V_{ax})^2}{2}$$

where λ is the resistance coefficient which is a function of the axial Reynolds number and the tangential Reynolds number and δ_{i0} is the resistance factor for the inlet and the outlet. The axial Reynolds number and the tangential Reynolds number were calculated by the following equations:

$$Re_{axial} = \frac{\rho * v_{ax} * s}{\mu}$$

$$Re_{tangential} = \frac{\rho * w * R * s}{\mu}$$

where w is the rotational speed of the pump and R is the radius of the geometry. In the second case in which rotating screws with single-phase flow the resistance factor is 0 because in the single-phase flow no-resistance can be assumed. In the third case in which multiphase flow is considered the resistance factor is 1.5. Since the main purpose of the research is the leakage CFD modeling, generally the mesh system and the numerical solution was discussed and evaluated. The following table includes the comparison of numeric model with the calculated values that were found by equations above. As noted in Figure 15, pressure difference increment causes the leakage mass flow rate increment. Furthermore, pressure difference increment reduces the accuracy of the numeric model [11].

Δp $[kPa]$	$\dot{m}$ $[kg/s]$	$\langle v_{ax} \rangle$ $[m/s]$			Re	$\dot{m}_2$ / $\dot{m}$ [%]
		laminar	turbulent	numeric		
1.5	4.7	0.072	0.38	0.0745	19	0.6
3	6.6	0.14	0.57	0.15	38	0.8
6	9.4	0.29	0.84	0.29	73	1.1
12	12.9	0.57	1.2	0.57	144	1.6
24	18.3	1.1	1.8	1.08	273	2.1
48	26.2	2.2	2.7	1.9	482	2.6
96	37.6	4.1	4.0	2.9	740	2.8
192	52.4	7.3	5.8	4.0	1005	2.7
288	62.5	10.2	7.3	5.0	1262	2.8
384	75	12.7	8.6	6.0	1514	2.8

Figure 15 Comparison of experiment and numeric results [11]

3. RESULTS AND DISCUSSION

3.1 Overview of Data Analysis

This section includes the results and discussion of the investigation of this thesis. The first section will analyze Texas A&M University Turbomachinery Laboratory Leistritz Twin-Screw Pump Research by Ryan Kroupa and Louisiana State University Twin-Screw Pump Research. The second section will present the leakage flow model for Texas A&M University Turbomachinery Laboratory Leistritz Twin-Screw Pump Research by Ryan Kroupa data.

The first section begins with analyzing Texas A&M University Turbomachinery Laboratory Twin-Screw Pump research which was conducted by Ryan Kroupa and Louisiana State University research. Both programs were conducted with the same pump but different working fluids. While Texas A&M University research was conducted with the air-water mixture, LSU data included the fresh water-methane and oil-methane multi-phase operations. Since three different multi-phase operations data are available, the working fluid dependency of the twin-screw pump is analyzed in this report.

In the second section, the leakage flow that reduces the volumetric and mechanical efficiency is modeled. Step by step leakage model stages will be explained in this section. The research aims to develop a correlation which provides the volumetric and the mechanical efficiency with only knowledge of single-phase operation.

The first section is based on the TAMU water-air and LSU water-methane experiments for the twin-screw pump. Firstly, it is required to take an in depth look at these experiments. The following tables are parameter matrixes which are driven by experimenters for each investigation. Since the LSU experiment is conducted only at 3600 rpm, for comparison, only 3600 rpm results of TAMU experiment is considered.

Table 2 TAMU Experiment Parameter Matrix

GVF %	ΔP(PSI)	Inlet P(PSI)
0	50	10
50	100	50
90	150	
95	200	
98	250	
99		
100		

Table 3 LSU Experiment Parameter Matrix

GVF %	ΔP(PSI)	Inlet P(PSI)
50	50	25
90	100	65
95	150	165
98	200	265
100	250	315

While Table 2 shows the TAMU experiment parameter matrix Table 3 shows the LSU experiment parameter matrix. Even though TAMU experiment has single-phase operation, LSU experiment does not have single-phase operation. Both experiments are

set with the same differential pressure values. Inlet pressures are totally different for both investigations. As presented in the following sections, this difference should be considered for the comparison of experiment results.

Before the following sections, the control volumes should be well-explained. The pump has a liquid re-circulation system and its function is adding a specific amount of liquid into the inlet of the pump. Therefore, the total volumetric flow rate which enters the pump is known in the experiment. The difference between the skid and pump based control volumes is this liquid-recirculation volumetric flow rate. While in the skid based control volume the liquid re-circulation volumetric flow rate is not used in the calculations; in the pump based control volume, it is used.

GVF values in the tables are skid based values. Since the liquid re-circulation is added in the pump based GVF calculation, the pump based GVF values are always smaller than the GVF values in the tables. With the assumption that the liquid is separated in the knockout-boot with %100 efficient, the pump based efficiencies are very crucial to determine pump properties.

The main comparison parameter for these LSU experiment results and TAMU experiment results are volumetric efficiency, process efficiency and mechanical efficiency. Since the pump and the experiment setup are essentially the same with different working fluids, the same or close efficiencies should be expected in the same or close conditions. As it will be explained in the following sections, LSU and TAMU data results are not similar.

In the second section, TAMU data is used to determine the leakage flow and mechanical efficiency. The leakage model is built with some assumptions. The experiment results are used to compare leakage flow models with actual results. Therefore, the model is built in this comparison process. The main function of this model is basically detecting the leakage flow rate in multi-phase operations. Leakage flow amount is a key parameter which dictates the volumetric and the mechanical efficiency. Also, in the final part of the second section, the mechanical efficiency correlation is generated with the only single-phase operation experiment result. This enables a user of the pump to determine the volumetric and the mechanical efficiency of the pump in multi-phase operations with the knowledge of single-phase work result.

3.2 TAMU and LSU Experiment Data Comparison

As explained in the previous section, the main parameter for comparison is efficiencies. In the following sections, the efficiencies and its calculation process will be explained. The lack of single-phase test of the LSU experiment data should be considered.

3.2.1 Volumetric Efficiency

The volumetric efficiency is calculated by the following equation:

$$\eta_{vol} = \frac{\dot{Q}_{actual}}{\dot{Q}_{theoretical}}$$

The actual volumetric flow rate depends on the control volume as mentioned in the previous section. If the control volume is selected as the skid based, the re-circulation volumetric flow rate is not added in the actual volumetric flow rate.

The theoretical volumetric flow rate purely depends on the geometry and the speed of the pump. Therefore; the theoretical volumetric flow rate is constant for a definite speed because of the constant geometry properties of the pump. Theoretical volumetric flow rate is found with the following equations:

$$\dot{Q}_{th} = V_g * n$$

Here, V_g represents the volume and is calculated by the following equation:

$$V_g = \frac{B^2 * s * X}{4 * 10^8}$$

Figure 16 is the skid based volumetric efficiency of the TAMU data for the 10 PSI inlet condition and Figure 17 is the skid based volumetric efficiency of the LSU data for the 25 PSI inlet condition. These figures show the general distribution of the volumetric efficiency with respect to GVF and the pressure rise. As noted in figures, the maximum and the minimum points of both data are in different places. In the TAMU data; the maximum volumetric efficiency values are achieved in the minimum pressure rise and GVF area. In this case, the minimum volumetric efficiency results are in the higher pressure rise but lower GVF area. These results can be expected because of the nature of the pump. Pump works efficiently in volumetric manner in single-phase and low pressure rise condition. In high GVF conditions, the large amount of recirculation liquid is added to the pump but this addition does not show itself in the efficiency calculation. Therefore, the volumetric efficiency is low in this condition. In the LSU data; while the maximum volumetric efficiency is observed in high GVF and low

pressure rise condition, the minimum volumetric efficiency results are observed in both high GVF and pressure rise condition.

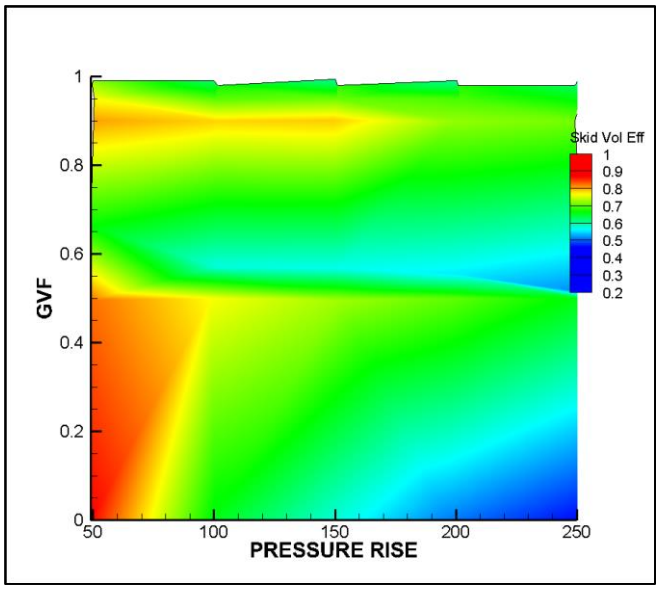

Figure 16 TAMU Inlet 10 PSI skid based volumetric efficiency

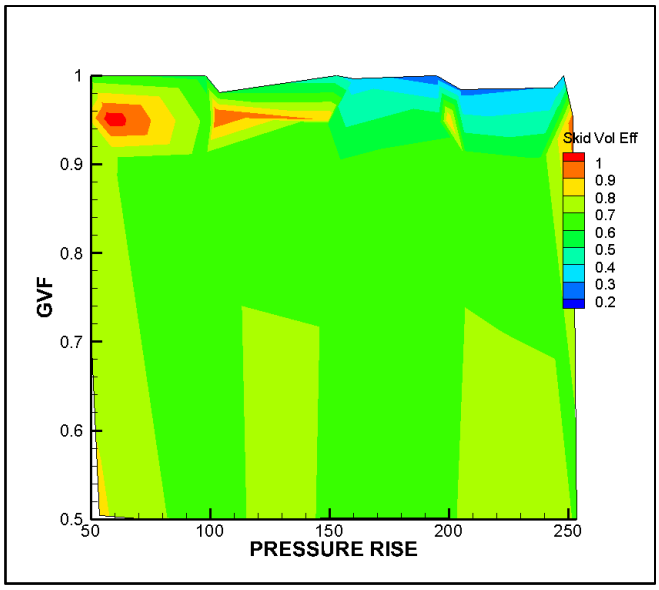

Figure 17 LSU Inlet 25 PSI skid based volumetric efficiency

Figure 18 is the skid based volumetric efficiency of the TAMU experiment data for 50 PSI inlet case and Figure 19 is the skid based volumetric efficiency of LSU data for 65 PSI inlet condition. The behavior of the pump is expressed in higher pressure inlet conditions in terms of the skid volumetric efficiency in these figures. In the high pressure inlet condition, the maximum and the minimum volumetric efficiency points almost match. Also the volumetric efficiency distribution difference is notable in the high pressure inlet case. While the TAMU experiment data volumetric efficiency changes from 0.4 to 0.8, the LSU data volumetric efficiency change can be observed from 0.15 to 0.95.

As expected, higher volumetric efficiency is achieved in the low different pressure and the low GVF conditions in both cases. In the LSU data, low volumetric efficiency is observed in the high GVF and the high pressure rise condition that contrasts with the TAMU data, in which low skid based volumetric efficiencies are observed in the low GVF and the high differential pressure condition which is similar to inlet 10 PSI condition. Even though the inlet pressure effects show up in results, the minimum and the maximum skid based volumetric efficiency match in both cases shows that there is a consistency in the TAMU experiment results. Furthermore, in the high GVF and the pressure rise condition, the higher inlet pressure case suffers volumetric efficiency.

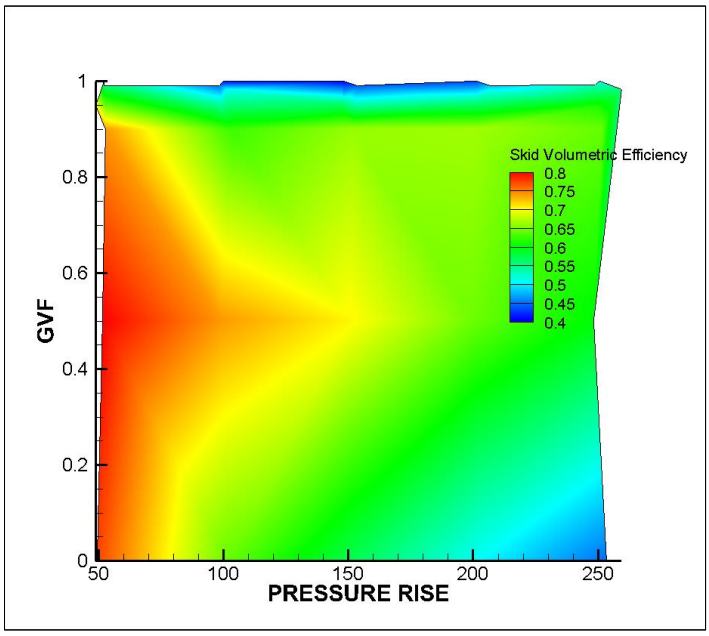

Figure 18 TAMU Inlet 50 PSI skid based volumetric efficiency

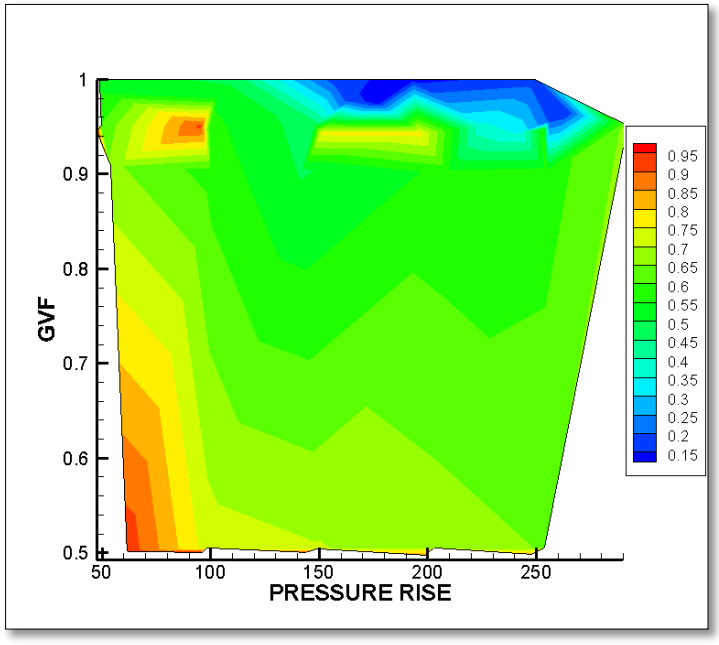

Figure 19 LSU inlet 65 PSI skid based volumetric efficiency

Figure 20 shows the pump based volumetric efficiency of the TAMU data for 10 PSI inlet condition and Figure 21 shows the pump based volumetric efficiency of the LSU data for 25 PSI inlet condition. As expressed above, the liquid re-circulation volumetric flow rate is added to the actual volumetric flow rate. The liquid re-circulation is used to prevent the pump from heat rise. Therefore, in high GVF conditions the liquid re-circulation amount is much higher than single-phase or low GVF conditions.

Volumetric efficiency distribution of the TAMU data for inlet 10 PSI can be admitted as smooth and as expected that it is parallel to the skid based volumetric efficiency for 10 PSI. The working principle of the pump can explain this smoothness. In the low GVF conditions, the temperature rise is low so the liquid re-circulation need is low as well. Conversely, in the high GVF condition, while the liquid amount is low the temperature rise is high so that the liquid re-circulation amount is high. Therefore, the actual volumetric flow rate is always balanced in the pump based control volume. The pump based volumetric efficiency is approximately %30-40 greater than the skid based volumetric efficiency. This shows the stability of the data.

Figure 21 shows that the pump based volumetric efficiency is very similar to the skid based volumetric efficiency of the LSU data in the same inlet pressure. The distribution of the volumetric efficiency conflicts with the expression in the previous paragraph. The reasons and experiment problems will be discussed in the following sections.

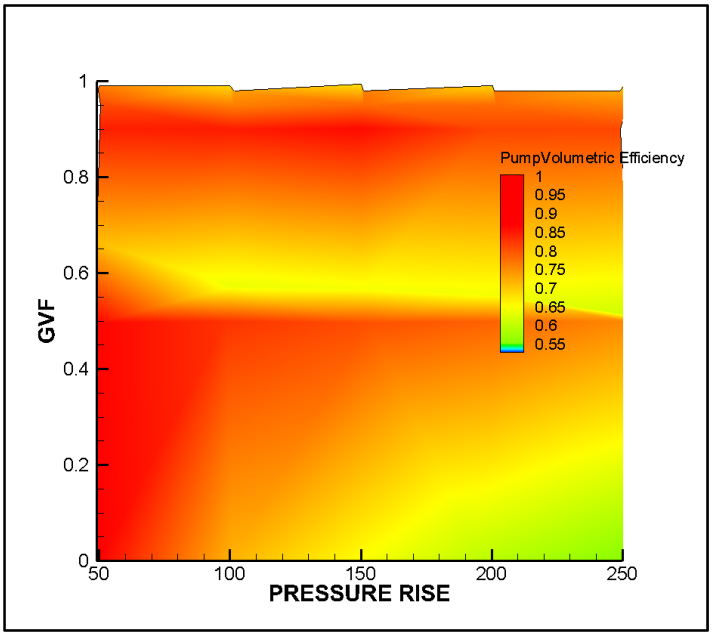

Figure 20 TAMU inlet 10 PSI pump based volumetric efficiency

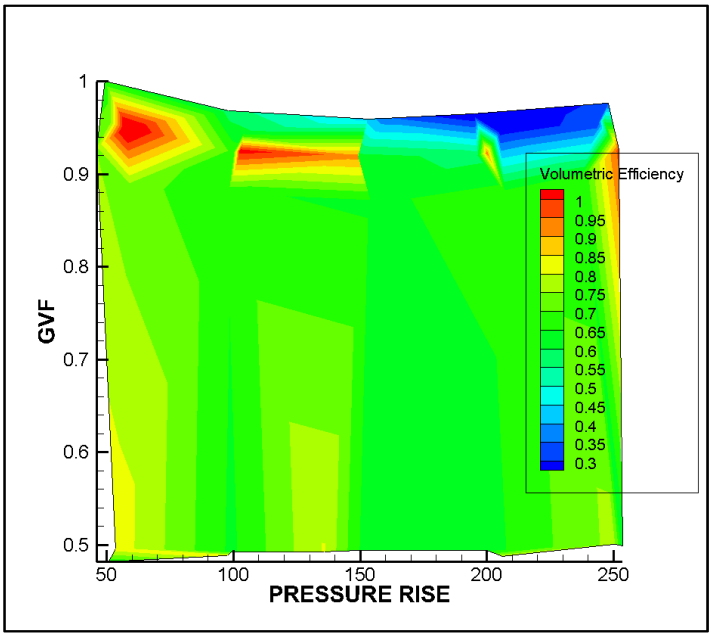

Figure 21 LSU Inlet 25 PSI pump based volumetric efficiency

Figure 22 is the pump based volumetric efficiency of the TAMU data for 50 PSI inlet case and Figure 23 is the pump based volumetric efficiency of the LSU data for 65 PSI inlet case. In comparison to the skid based volumetric efficiency results for both experiments, the liquid re-circulation affect can be observed from the graphs.

As expressed in the lower inlet pressure condition, the pump volumetric efficiency distribution is balanced as well. However, the volumetric efficiency is lower in the higher inlet pressure case because of the leakage flow in the pump. The leakage flow is greater in the high inlet pressure condition and this leakage suffers the pump based volumetric efficiency. The leakage flow and its reasons will be explained in the leakage flow models section.

The LSU pump based volumetric efficiency for 65 PSI graph yields inconclusive results to evaluate data in physical manner. As noted in the TAMU paragraphs, consistent efficiency values especially in the pump based case shows the nature of the pump.

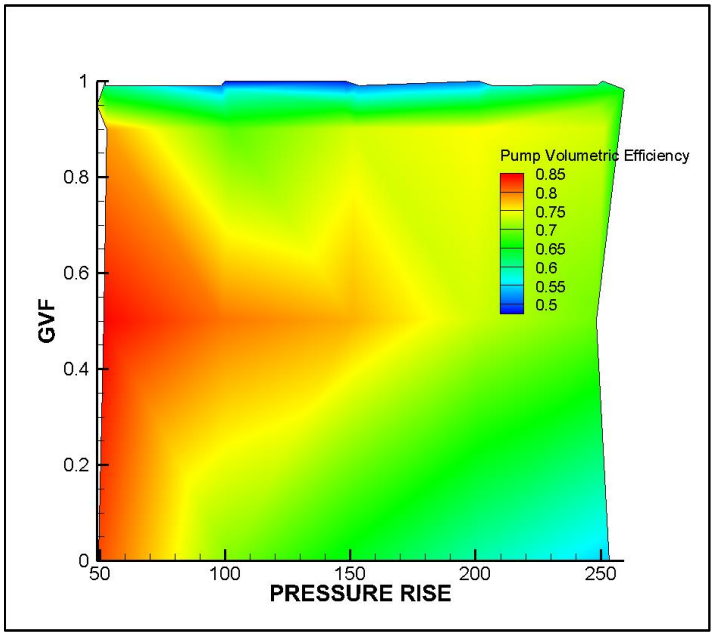

Figure 22 TAMU Inlet 50 PSI pump based volumetric efficiency

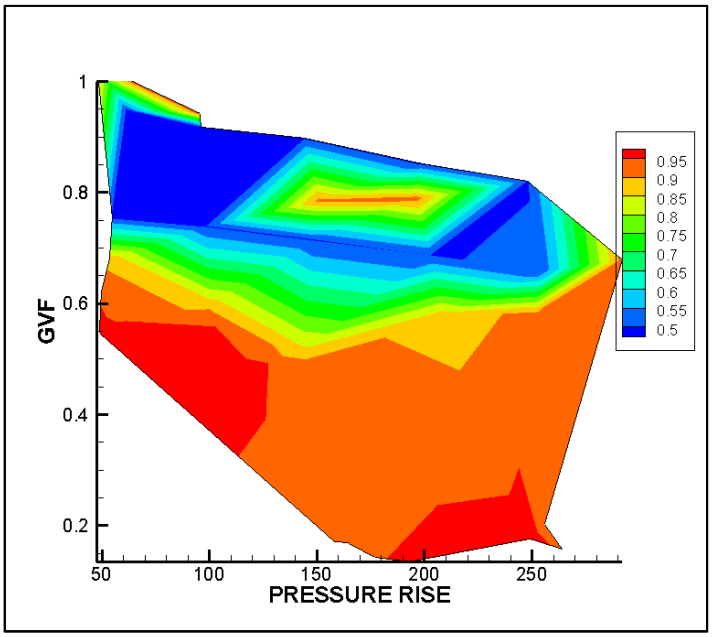

Figure 23 LSU Inlet 65 PSI pump based volumetric efficiency

Figure 24 and Figure 25 are skid based volumetric efficiencies for the TAMU and the LSU data for the low inlet pressure cases. These graphs, basically shows how the skid based volumetric efficiency changes with the increased differential pressure in a specific GVF value in the low pressure inlet condition. Even though the general distributions seem extremely different in both cases, approximately same trends for the low GVF values can be observed in these graphs. The LSU experiment data yields sharp decreases in high GVF case.

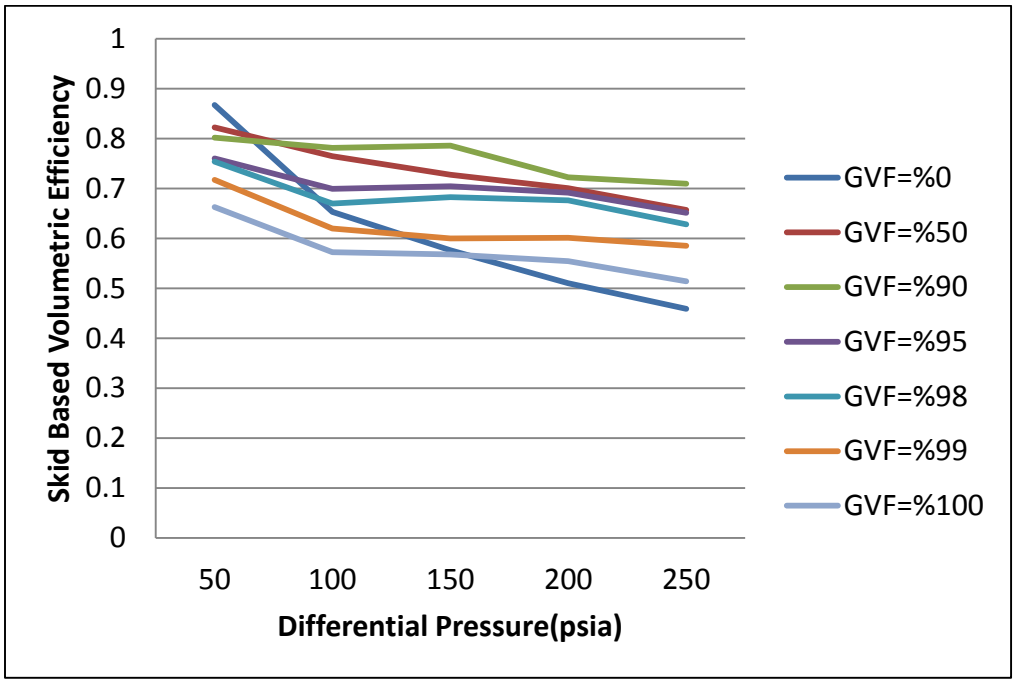

Figure 24 TAMU skid based volumetric efficiency for low pressure inlet

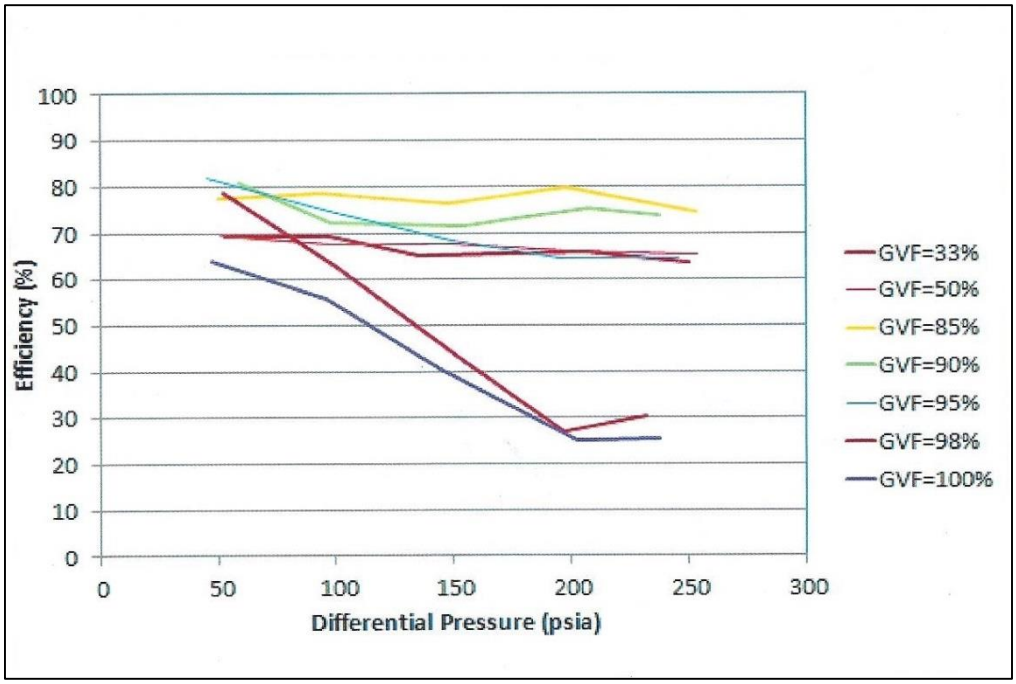

Figure 25 LSU skid based volumetric efficiency for low pressure inlet

Figure 26 and Figure 27 show the skid based volumetric efficiencies for the TAMU and the LSU data for the high inlet pressure cases. The conflicts and similarities for low inlet pressure cases are nearly same in the high pressure case too. While it can be observed that for the low GVF values, similar results are achieved, the skid based volumetric efficiency for the high pressure inlet LSU experiment data is much more suffered than the TAMU experiment data.

Figure 28 illustrates the skid based volumetric efficiency of the LSU and the TAMU data for GVF %98 case. The air/water case represents the TAMU data and the oil/water case represents the LSU data. As seen in the graph, for the same inlet cases under 150 PSI differential pressure cases yield nearly the same results in both experiments. The gas/water data shows a sharp decline in volumetric efficiency at above

100 PSI differential pressure. Therefore, above 150 PSI differential pressure case gives distinctive results. These distinctive results can be caused by the experiment condition differences, the pump working fluid differences and the experiment equipment deficiencies.

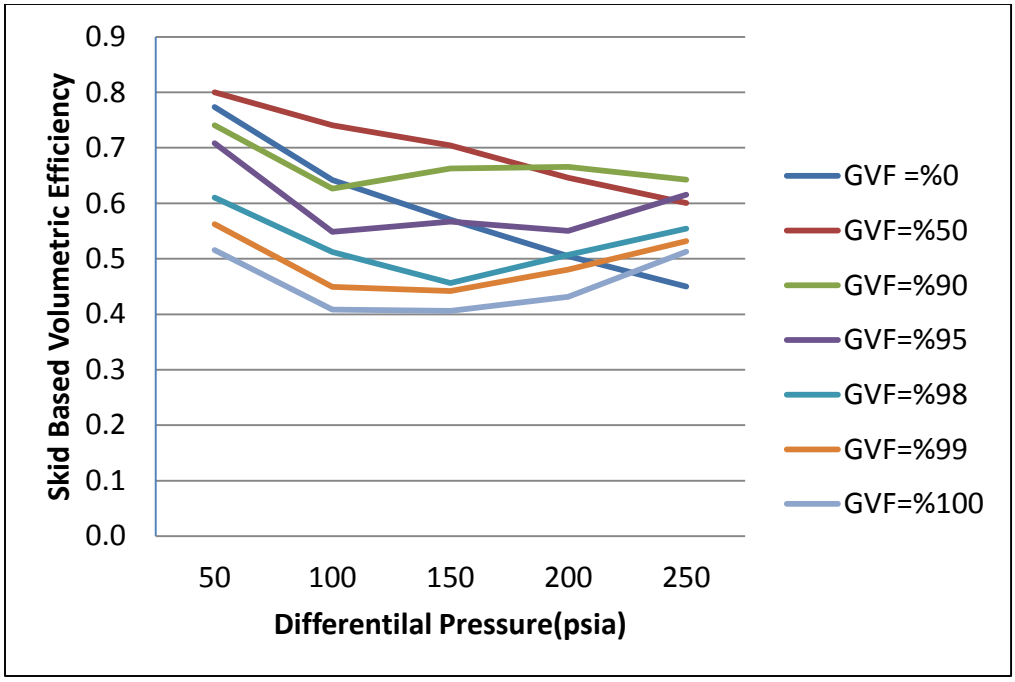

Figure 26 TAMU skid based volumetric efficiency for high pressure inlet

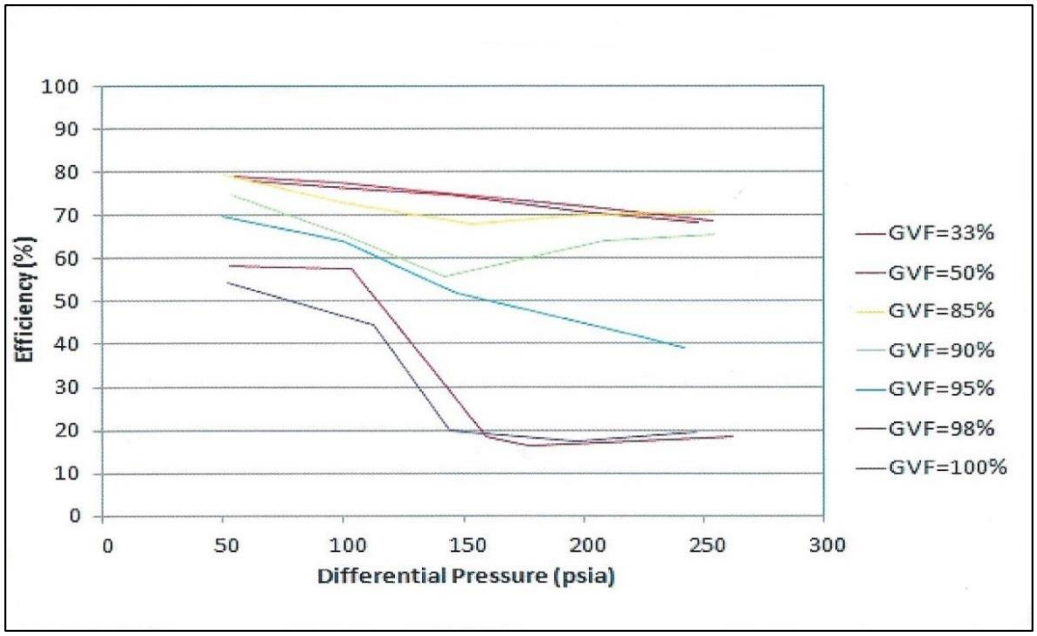

Figure 27 LSU skid based volumetric efficiency for high pressure inlet

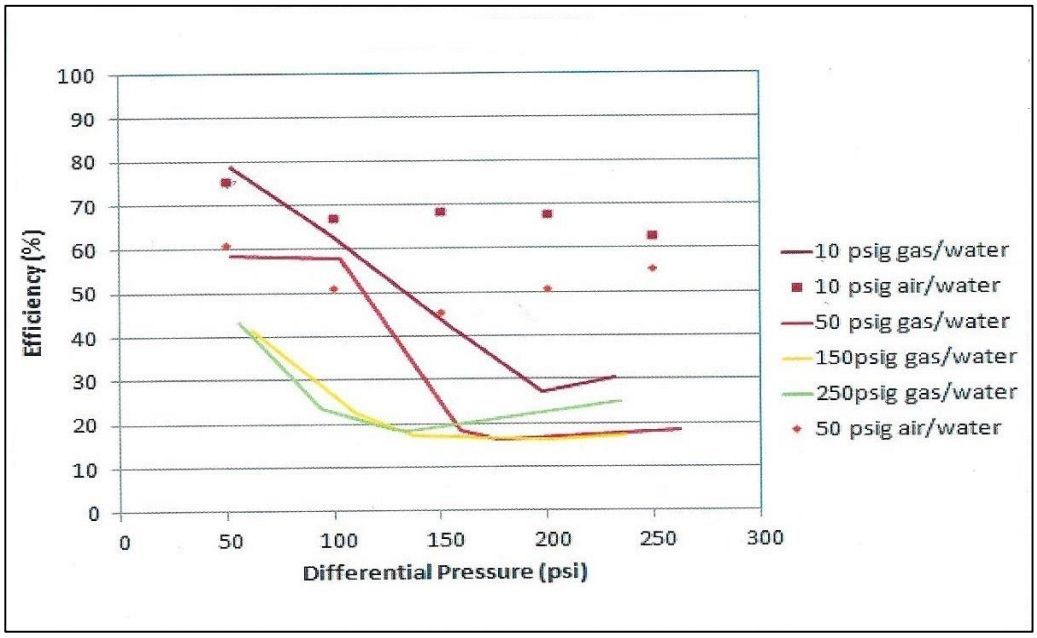

Figure 28 Skid volumetric efficiency for LSU and TAMU data –GVF skid based 98% case

Figure 29 shows the pump based volumetric efficiency of the TAMU data for the low pressure inlet case and Figure 30 shows the pump based volumetric efficiency of the LSU data for the low pressure inlet case. As presented in the skid based control volume that while the TAMU experiment data yields similar volumetric efficiency values in the pump based control volume, the LSU experiment pump based volumetric efficiency is suffered especially in the high GVF conditions.

As Figure 31 shows, the main difference in both cases is due to the variation of the liquid re-circulation amount. The dashed lines are for the TAMU experiment data and the continuous lines are for the LSU data. While differential pressure increment causes more liquid re-circulation addition to the pump control volume for the TAMU experiment, the LSU liquid re-circulation amount tends to stay stable in all GVF and differential pressure cases. Therefore, in the high differential pressure conditions, the LSU pump based volumetric efficiency decline stands out.

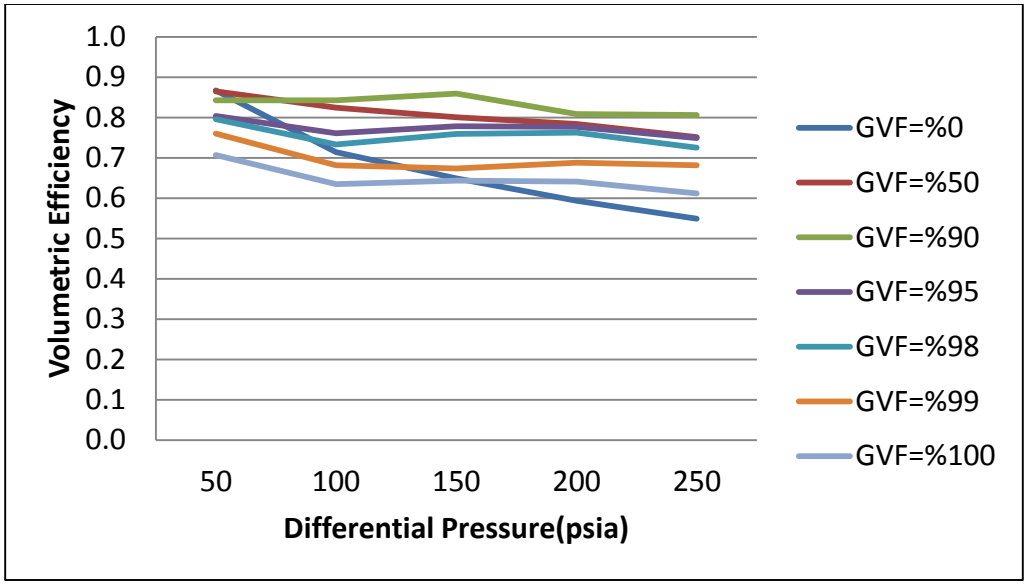

Figure 29 TAMU pump based volumetric efficiency for low pressure inlet

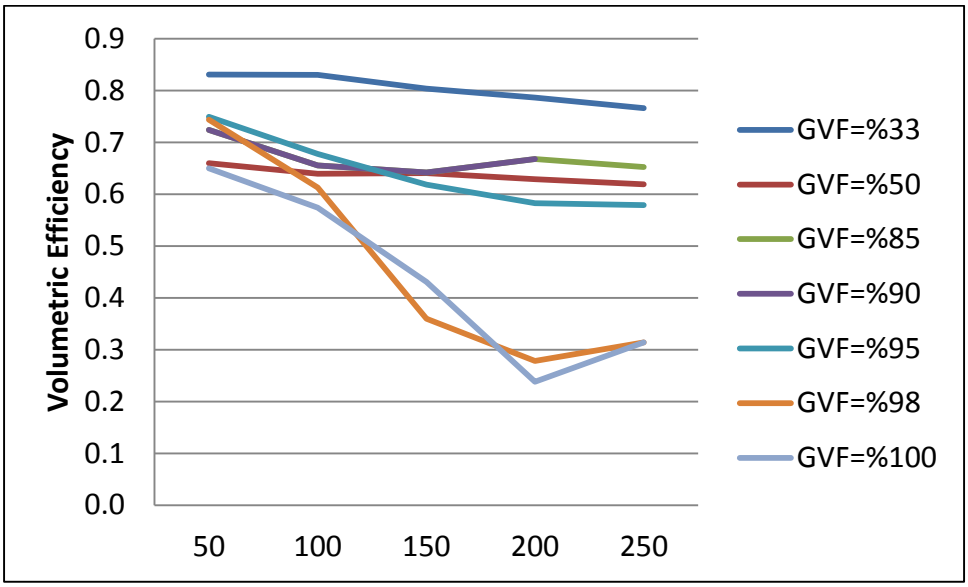

Figure 30 LSU pump based volumetric efficiency for low pressure inlet

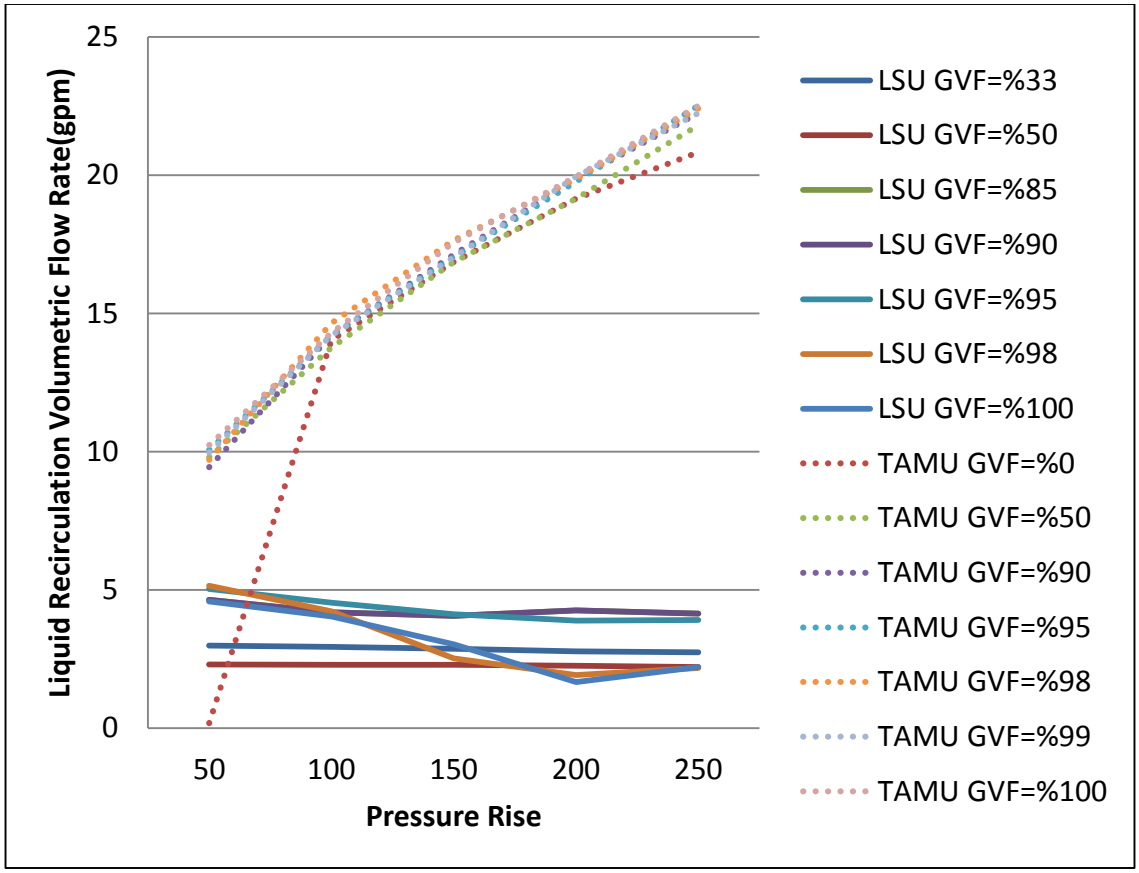

Figure 31 Liquid re-circulation amount comparison for LSU and TAMU data for low pressure inlet condition

Figure 32 shows the pump based volumetric efficiency of the TAMU experiment data for the high pressure inlet case and Figure 33 shows the pump based volumetric efficiency of the LSU experiment data for the high pressure inlet case. In comparison to the low pressure inlet case, the volumetric efficiency is more suffered in the high pressure inlet case. However it can be observed that the lines have nearly same descents and rises in both inlet conditions. This presents that the volumetric efficiency decreases with the inlet pressure increment but it does not affect the behavior of volumetric efficiency change with respect to the differential pressure.

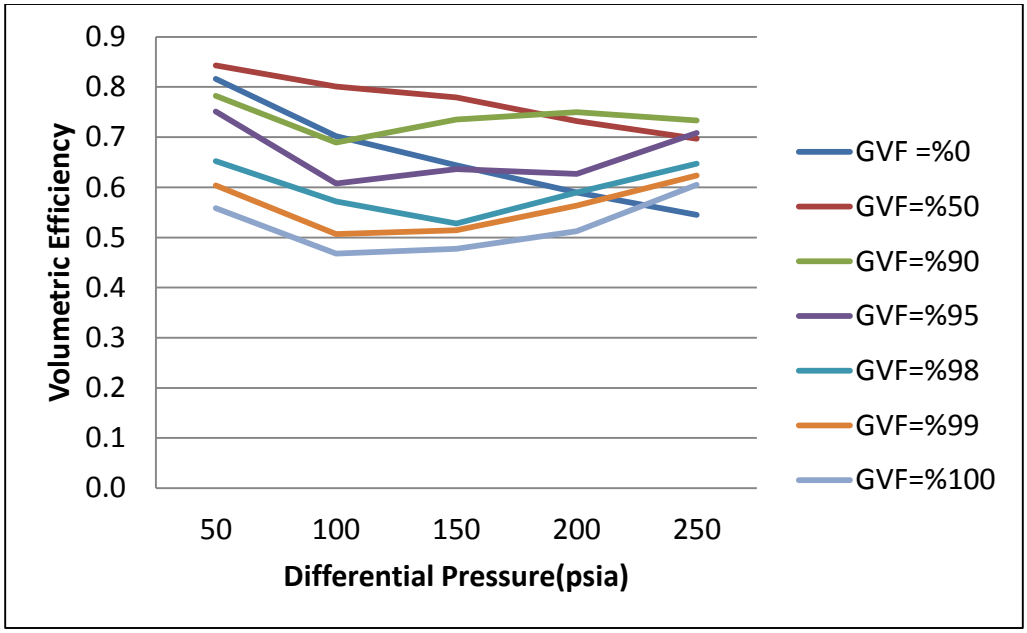

Figure 32 TAMU pump based volumetric efficiency for high pressure inlet

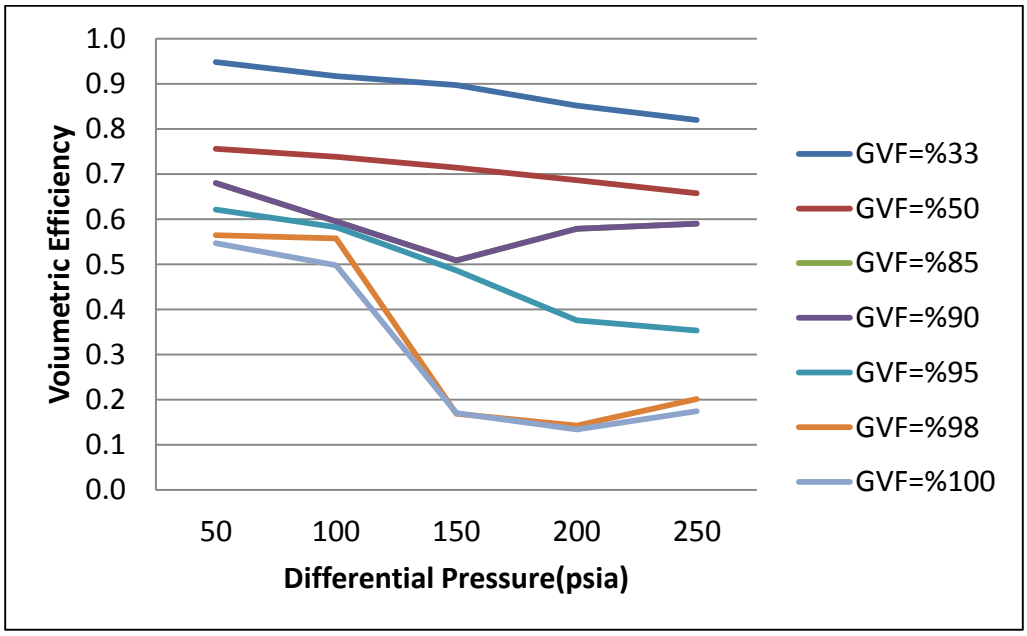

Figure 33 LSU pump based volumetric efficiency for high pressure inlet

Figure 34 shows the liquid re-circulation amount of the high pressure inlet for both experiments. The dashed lines are for the TAMU experiment data and the continuous lines are for the LSU experiment data. The distribution of the liquid re-circulation presents that it does not depend on the GVF values for both cases. The TAMU experiment liquid re-circulation amount is based on the differential pressure. Nearly linear increment for volumetric efficiency can be observed with respect to the differential pressure increase. The LSU experiment liquid re-circulation amount is not based on the GVF inlet pressure or the differential pressure. Nearly the constant liquid re-circulation amounts can be observed.

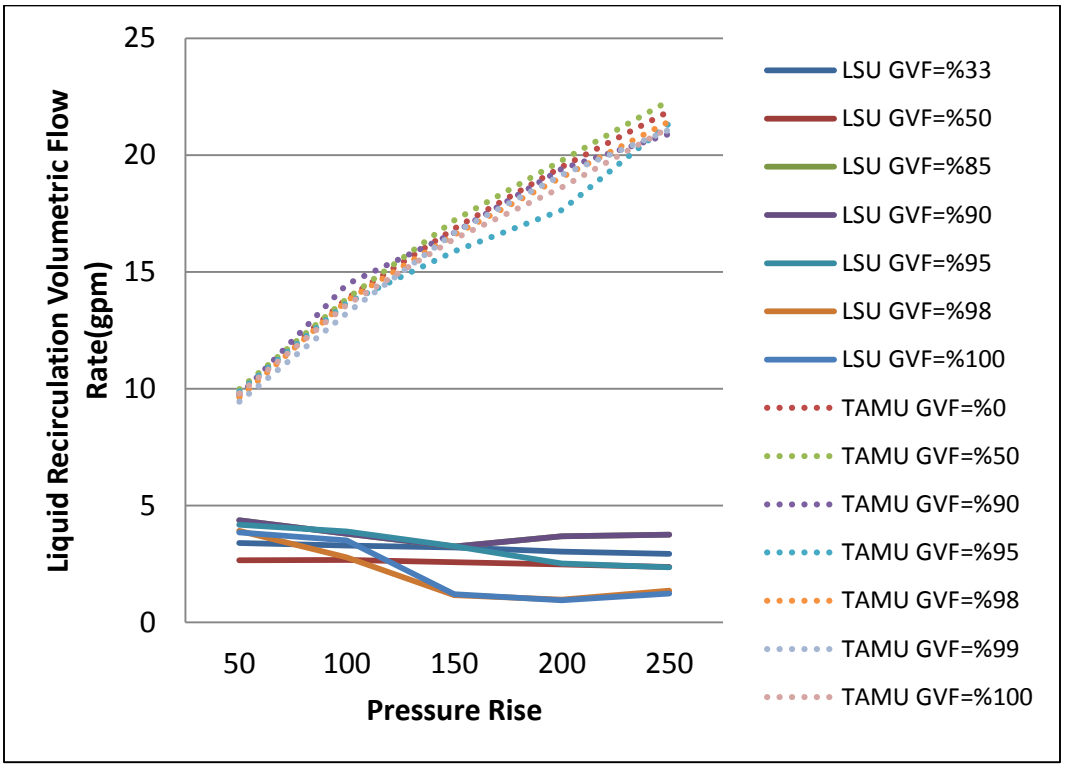

Figure 34 Liquid re-circulation amount comparison for LSU and TAMU data for high pressure inlet condition

Since the liquid recirculation amount depends on the differential pressure in the TAMU data, the pump based GVF changes with respect to the differential pressure. Figure 35 is TAMU pump based GVF for low pressure inlet and Figure 36 is TAMU pump based GVF for high pressure inlet. Especially, high GVF operations are showed in the graph. As can be seen, the pump based GVF more depends on the inlet pressure. It can be observed that the high inlet pressure case more depends on the differential pressure. While in the low inlet pressure case the pump based GVF is less than the skid based GVF approximately %4-7 in the high inlet pressure case the pump based GVF is less than the skid based GVF approximately %10-15.

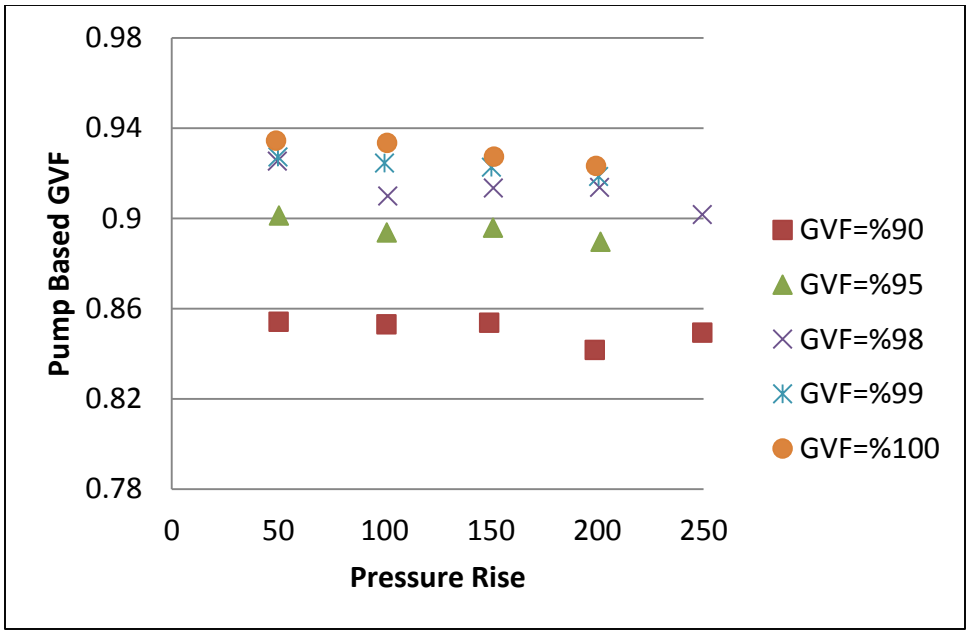

Figure 35 TAMU pump based GVF for low pressure inlet

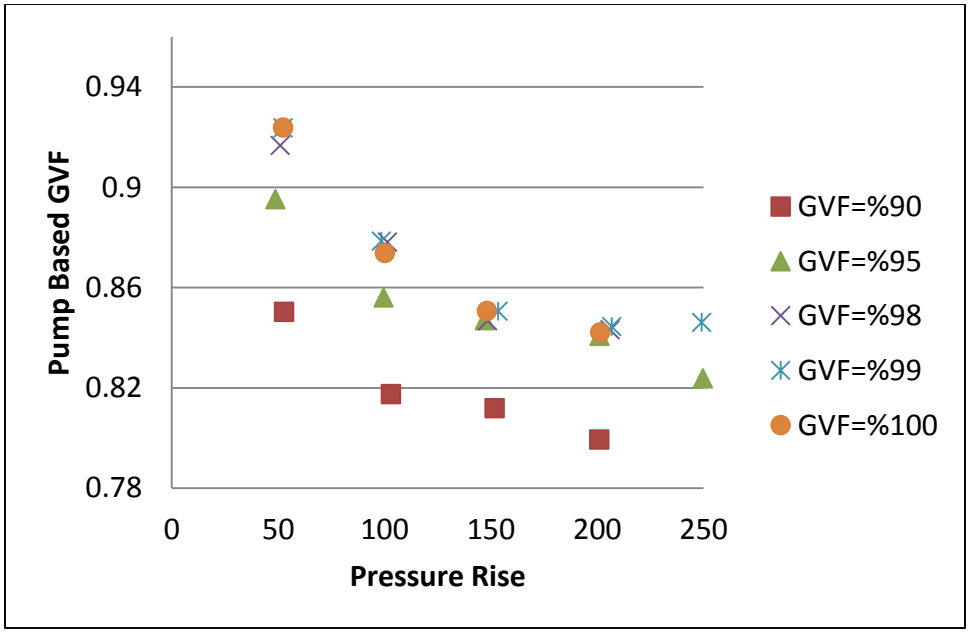

Figure 36 TAMU pump based GVF for high pressure inlet

3.2.2 Mechanical Efficiency and Effectiveness

Mechanical efficiency represents the productivity of the pump in terms of the given energy. The mechanical efficiency can be calculated by the following equation:

$$\eta_{mech} = \frac{P_{actual}}{P_{electrical}}$$

The actual power equals to the sum of the compression power of the liquid and the compression power of the gas. Since the liquid part of the multi-phase flow can be assumed as incompressible flow the liquid power compression is calculated by the following equation:

$$P_{liquid} = \dot{Q}_{liquid} * \Delta P$$

where $\dot{Q}_{liquid}$ is the volumetric flow rate of the pump and ΔP is the pressure rise across the pump. The liquid re-circulation volumetric flow rate is added if the control volume is selected as the pump based.

The calculation of the gas power compression can be based upon thermodynamic theories which are isothermal, isentropic and polytropic. These compression models are used with the assumption of ideal gas.

When the inlet and the exhaust temperature are very close in value, the isothermal compression theory can be applicable. Especially, in the low GVF values, using this compression theory is very reasonable because the liquid in the pump is sufficient to cool the gas part. In contrast, in the high GVF values, the isothermal compression is not applicable because of a significant temperature rise between the pump inlet and the pump exit. The following equation is built for the isothermal gas compression model:

$$P_{gas,isothermal} = \dot{Q}_{gas} * P_{in} * \ln(\frac{P_{out}}{P_{in}})$$

The isentropic compression model is another model that is used for the investigation. Basically, the isentropic compression assumes that no entropy generation takes place. The general governing equation is for isentropic process is:

$$P * v^k = Constant$$

where P is the pressure, v is the specific volume for gas and k is the heat capacity ratio for the gas. The heat capacity ratio is a physical property of the gas and it is found by the following equation:

$$k = \frac{c_p}{c_v}$$

For calculation of the isentropic compression power, the following formula is used:

$$P_{gas,isentropic} = \frac{k}{k-1} * \dot{Q}_{gas} * P_{in} * \left[\left\{\frac{P_{out}}{P_{in}}\right\}^{\frac{k-1}{k}} - 1\right]$$

For a given the inlet and outlet temperature and the pressure, the polytropic process is always more desirable model for an engineer. This is because the polytropic process is also used in irreversible systems which involve heat transfer. Since the investigation data provides the inlet and the outlet temperature and the pressure values, the polytropic compression power is also calculated. The governing equation of the polytropic process is:

$$P * v^n = Constant$$

With the ideal gas equation and the governing polytropic equation, the polytropic index n is found by the following equation:

$$n = \frac{\ln\left[\frac{P_{in}}{P_{out}}\right]}{ln\left[\frac{P_{in}*T_{out}}{P_{out}*T_{in}}\right]}$$

The polytropic compression gas power equation is:

$$P_{polytropic} = \frac{n}{n-1} * \dot{Q}_{gas} * P_{in} * \left[\left\{\frac{P_{out}}{P_{in}}\right\}^{\frac{n-1}{n}} - 1\right]$$

The electrical power which is the denominator in the mechanical efficiency calculation is measured by the VFD. The load power calculation is based on the

working fluid and it is used in order to maintain the set constant rotational speed of motor. (Kroupa)

For the mechanical calculation, the gas power compression model should be selected first and this model is used to calculate the actual power.

The effectiveness is also another measurement to express the compression process efficiency. The effectiveness is a totally theoretical calculation which does not need the load power of the pump. The effectiveness is:

$$\eta_{effectiveness} = \frac{P_{actual}}{P_{theoretical}}$$

The actual power is calculated with the liquid compression power and the gas compression power models. The theoretical power which represents the power added if the total flow through the pump was incompressible is calculated by the equation below,

$$P_{theoretical} = \left(\dot{Q}_{gas} + \dot{Q}_{liquid}\right) * \Delta P$$

As can be seen in the effectiveness calculation, with the knowledge of the inlet and the outlet pressures and the inlet gas and the inlet liquid volumetric flow rates, the effectiveness can be calculated without any information of load power. The effectiveness can be used to calculate the mechanical efficiency of the pump as will be expressed in the following section.

The mechanical efficiency comparison for the LSU experiment data and the TAMU experiment data will be discussed in the following paragraphs and graphs. The isothermal and the polytropic processes are used in order to calculate the actual compression power. As expressed above the isothermal compression power is useful for

low GVF values and the polytropic process is a reasonable compression model with the knowledge of the inlet and the outlet properties. While the isothermal mechanical efficiency presents that the isothermal compression model is used for the gas compression, the polytropic mechanical efficiency presents that the polytropic compression power is used for gas compression.

Rather than using the skid based control volume, the pump based control volume is used for comparison TAMU and LSU data. This is because the liquid re-circulation part of the multiphase fluid is also compressed in the pump and this power should be added to the actual power. Therefore, there is no meaning to evaluate the skid based mechanical efficiency.

Figure 37 is the TAMU Inlet 10 PSI pump based isothermal mechanical efficiency graph and Figure 38 is the LSU Inlet 25 PSI pump based isothermal mechanical efficiency graph. As expected, the mechanical efficiency has maximum value in the low GVF and the high differential pressure condition in both experiments. While the TAMU experiment data shows an anticipated contour, the LSU experiment gives unreasonable results such as maximum mechanical efficiency in high GVF and low pressure rise. The reasons which expressed in the volumetric efficiency part may cause this kind of result.

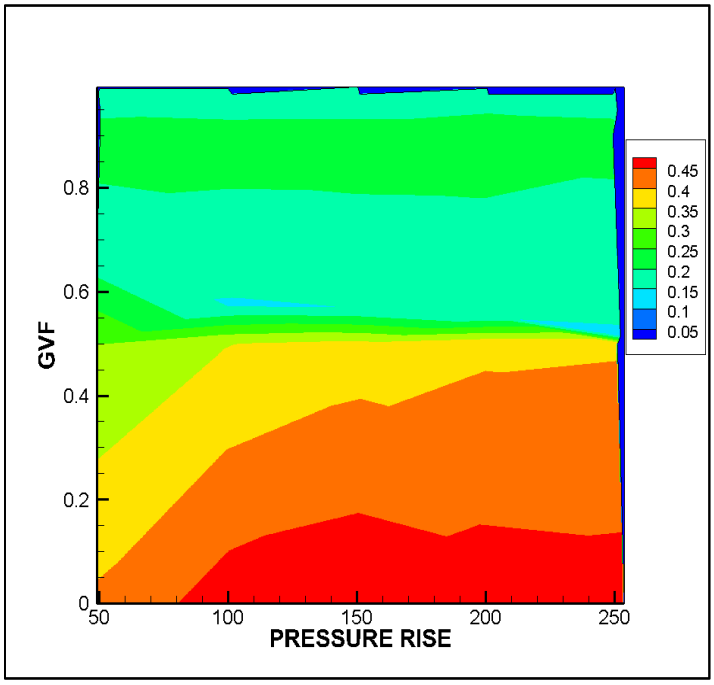

Figure 37 TAMU inlet 10 PSI pump based isothermal mechanical efficiency

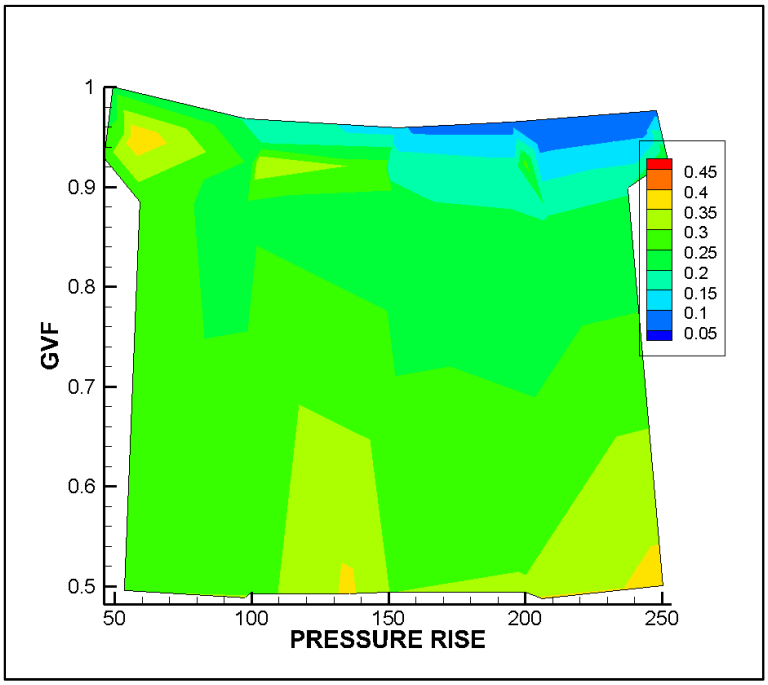

Figure 38 LSU inlet 25 PSI pump based isothermal mechanical efficiency

Figure 39 shows the pump based isothermal mechanical efficiency of TAMU Inlet 50 PSI and Figure 40 shows the pump based isothermal mechanical efficiency of LSU Inlet 65 PSI. TAMU graph represents the contour which is very similar to low pressure inlet case. The only difference is the high inlet pressure condition has larger mechanical efficiencies. Ryan Kroupa (2011) explains in his thesis that the load power does not depend on the inlet pressure; it only depends on the differential pressure. [2] With the same gas volumetric flow rate and the differential pressure, more gas power achieved in the high inlet pressure case and this increases the mechanical efficiency. Also Shell Test Facility report which conducts the LSU Experiment concludes that in the high inlet pressure condition the density change is less and in this kind, the gas part of the mixture is acting more like incompressible fluid.

In the high pressure condition the LSU pump based isothermal mechanical efficiency graph is nearly opposite of the expected results. As seen in the graph the minimum mechanical efficiency is in the low GVF and the high differential pressure rise condition and the maximum mechanical efficiency is in the high GVF area. This massive difference between TAMU and LSU data makes impossible to work on both experiments.

Figure 41 is the pump based polytropic mechanical efficiency of the TAMU Inlet 10 PSI and Figure 42 is the pump based polytropic mechanical efficiency of the LSU Inlet 50 PSI. Figure 43 is the pump based polytropic mechanical efficiency of the TAMU Inlet 50 PSI and Figure 44 is the pump based polytropic mechanical efficiency

of the LSU Inlet 65 PSI. The graphs show that in the same inlet pressure cases, the isothermal and the polytropic efficiencies are very close.

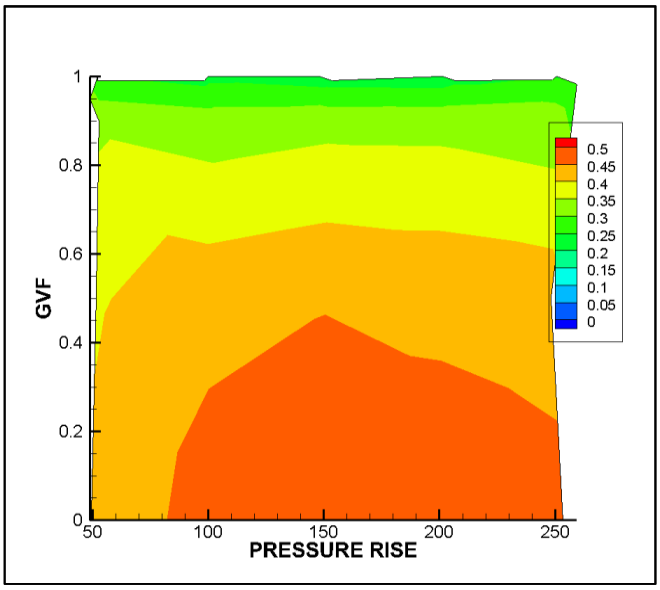

Figure 39 TAMU inlet 50 PSI pump based isothermal mechanical efficiency

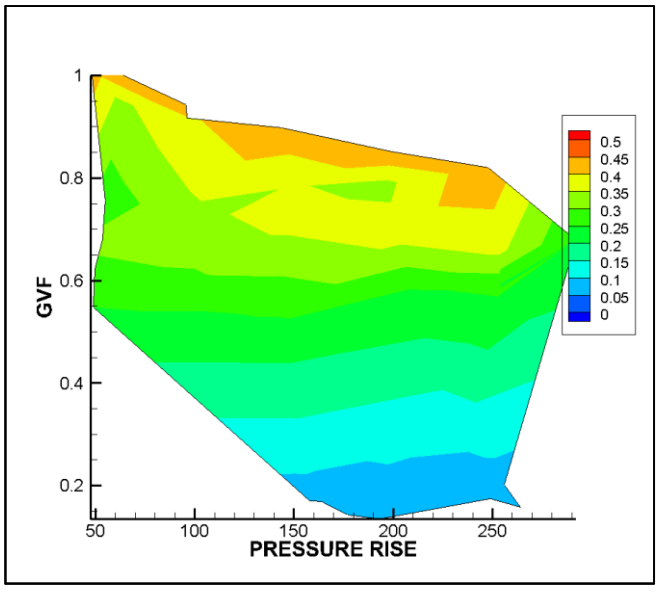

Figure 40 LSU inlet 65 PSI pump based isothermal mechanical efficiency

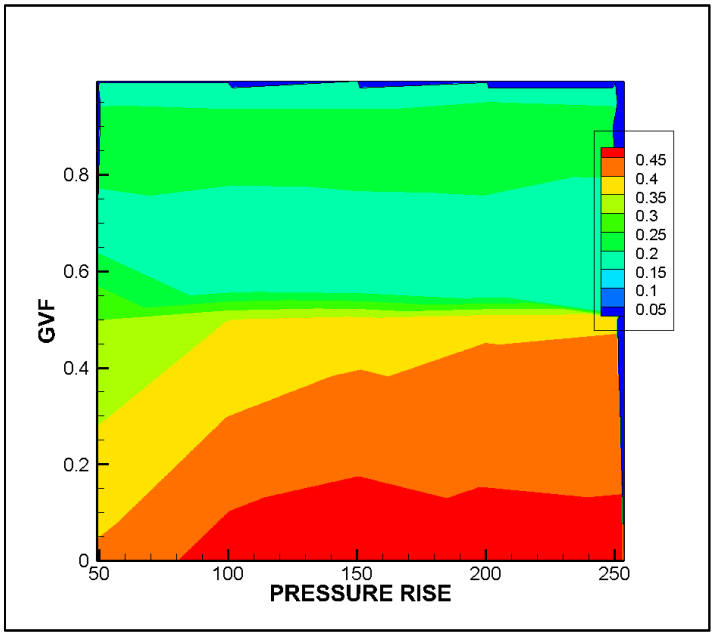

Figure 41 TAMU inlet 10 PSI pump based polytropic mechanical efficiency

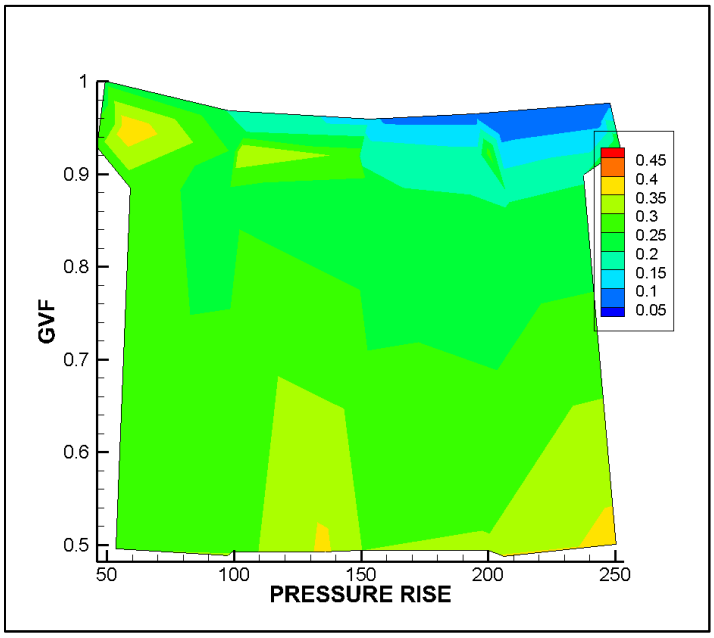

Figure 42 LSU inlet 25 PSI pump based polytropic mechanical efficiency

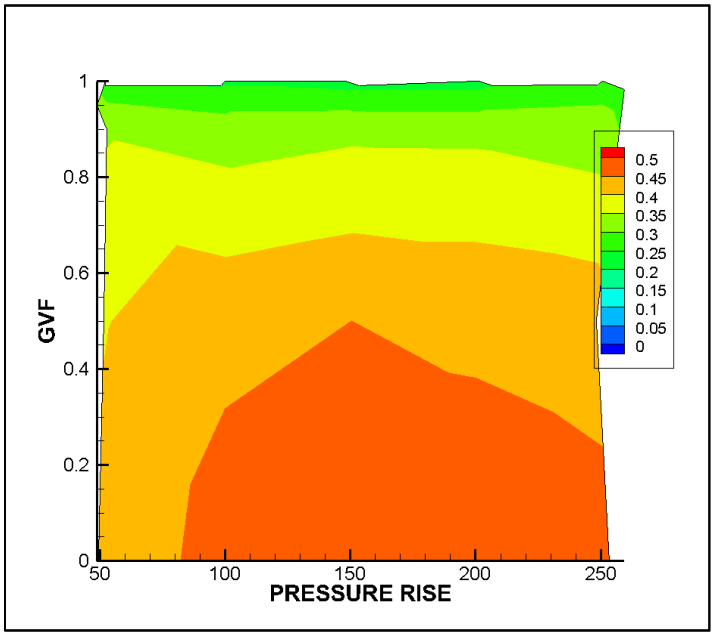

Figure 43 TAMU Inlet 50 PSI pump based polytropic mechanical efficiency

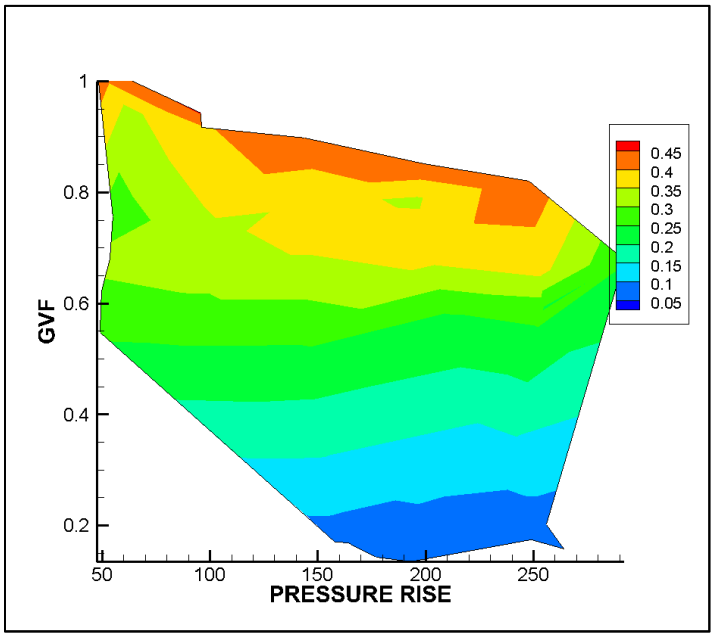

Figure 44 LSU inlet 65 PSI pump based polytropic mechanical efficiency

Figure 45 and Figure 46 give an idea about the similar results of isothermal and polytropic compression power for TAMU data. $\dot{Q}_{gas} * P_{in}$ is subtracted from the isothermal and the polytropic compression equation, the average polytropic index is used for n which is 1.036 and the following equations are assumed for the compression coefficient for the isothermal and polytropic processes. As presented with graphs with the average polytropic index, the polytropic compression and the isothermal compression powers are nearly same. Also, it should be noted that the pressure ratio, which is 2 to 26, plays a key role in this calculation. Since the maximum pressure ratio is only 26, the difference is not so large in the greatest pressure ratio point.

$$\boldsymbol{Isothermal\ Compression\ Power\ Coefficient}: \ln\left(\frac{P_{out}}{P_{in}}\right)$$

$$\boldsymbol{Polytropic\ Power\ Compression\ Coefficient}: \frac{n}{n-1} * \left[\left\{\frac{P_{out}}{P_{in}}\right\}^{\frac{n-1}{n}} - 1\right]$$

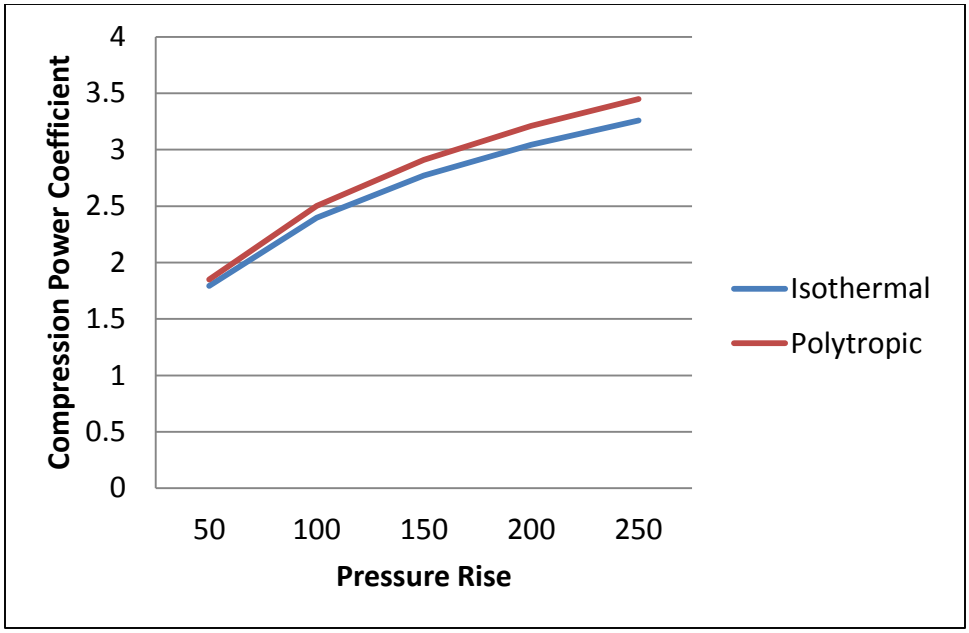

Figure 45 Isothermal and polytropic process comparison for 10 PSI inlet condition

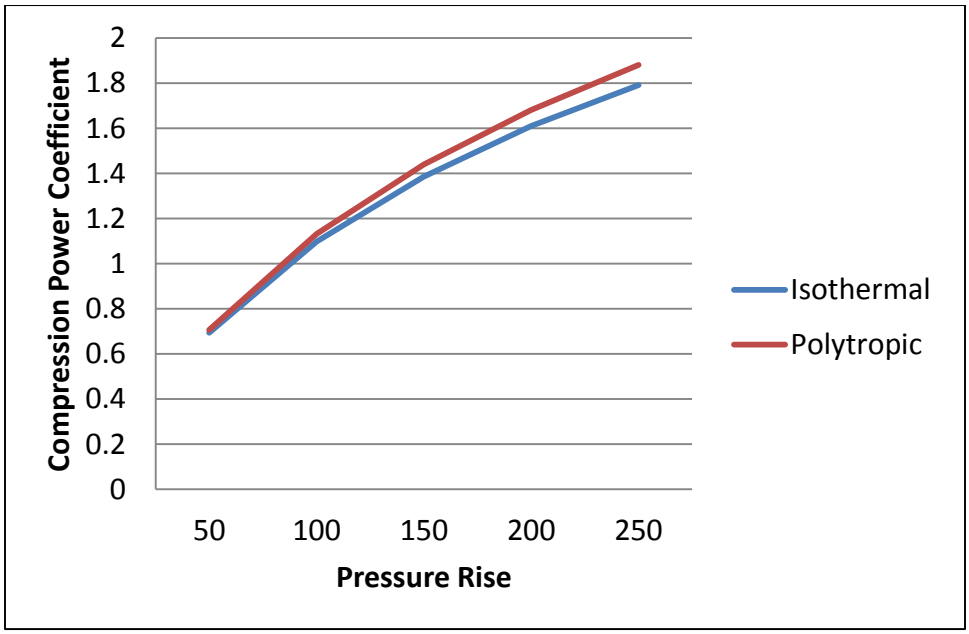

Figure 46 Isothermal and polytropic process comparison for 50 PSI inlet condition

Even though the notable difference between the LSU and the TAMU experiment is mentioned in the previous parts, the reasons of this difference will be discussed in a methodical way. Firstly, the main difference between these experiments is one of working fluid. While the TAMU experiment works with the air/water mixture, the LSU experiment works with the methane/water mixture. This requires discussing the difference between the air and methane for a thermodynamic behavior. Then, the experiment setups will be compared and discussed. Finally, based on their reports, the problems and recommendations for the experiments will be mentioned.

Figure 47 shows the comparison compression behavior of the air and the methane. Since nitrogen constitutes 78 percentage of the air, nitrogen properties are used for air. The distinctive variance between the LSU and the TAMU data in terms of efficiencies motivates observing the temperature ratio of these gases for the same pressure ratio. The compression is assumed isothermal for both cases. As presented in Figure 47, for the same pressure ratio, air temperature rise is more than methane. Therefore, in comparison with the methane case, the air case always needs more recirculation liquid in order to cool the pump and this suffers skid volumetric efficiency of the pump. However, liquid recirculation graphs, Figure 31 and Figure 34 show that the liquid re-circulation amount does not depend on the temperature rise. While the TAMU experiment liquid re-circulation amount depends on differential pressure, the LSU experiment liquid re-circulation amount depends on GVF value and it is much lower than the TAMU experiment data. In terms of the mechanical efficiency, it is expected that more heat rise suffers mechanical efficiency. The mechanical efficiency

distribution graphs show that the influence of heat rise does not affect too much because the ranges of the pump based mechanical efficiency are nearly same in experiments.

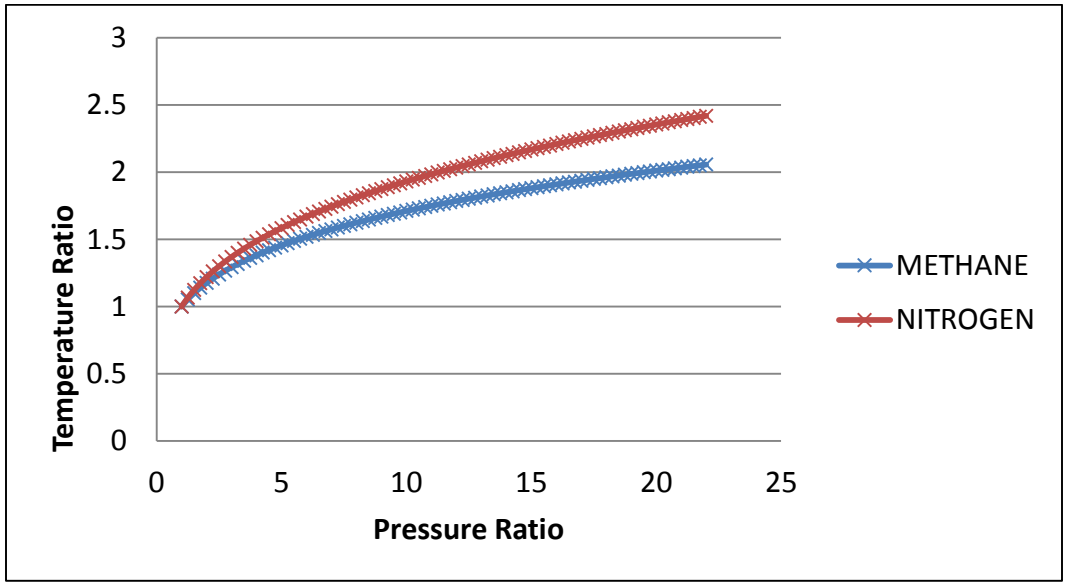

Figure 47 Methane and nitrogen compression behavior comparison

For experiment setup comparison Figure 48 and Figure 49 can be considered. Both systems are closed for the liquid but the gas part is supplied from the wells. Measurement points for temperature and pressure are located at the same place in the systems. Rather than the TAMU experiment data, different instrumentation is used in the LSU experiment which includes automatic choke valve and water base heat exchangers. The automatic choke valve sets a constant discharge pressure or backpressure for the test pump. The water base heat exchangers were hooked into the re-circulation loop in the skid to cool the fluid. If results and discussion part and recommendation part of Ryan Kroupa's thesis is considered, the deficiency of this equipment is highlighted. Therefore,

existing heat exchanger can be an advantage for the system but the effect of this could not be seen in LSU graphs [5].

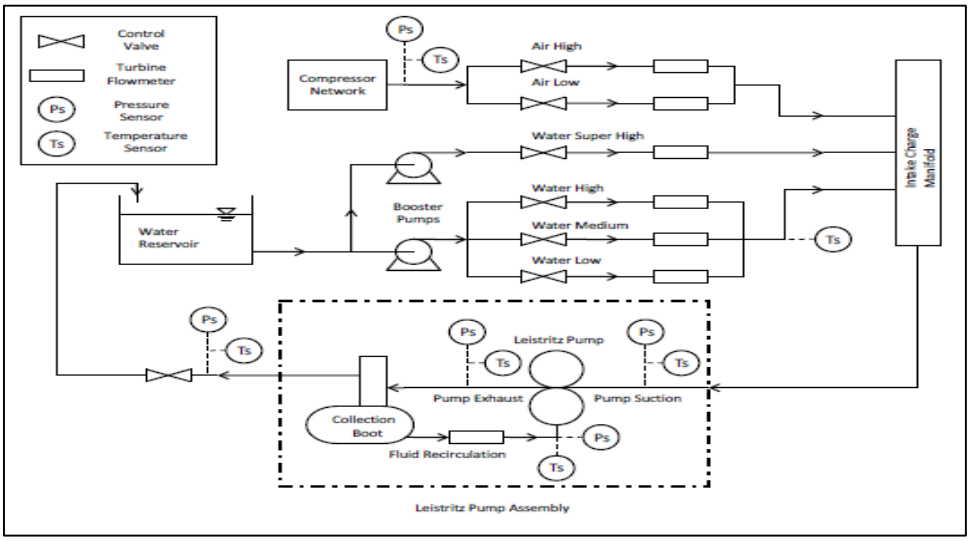

Figure 48 TAMU experiment setup [5]

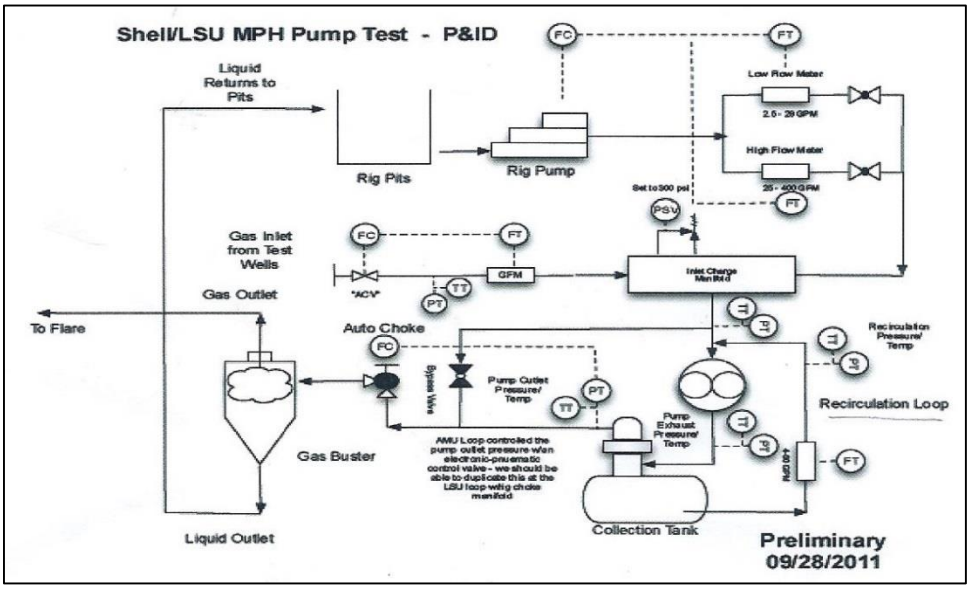

Figure 49 LSU experiment setup (Shell Test Facility Report)

The reports for these experiments mention the deficiencies of the experiments and the recommendations for future investigations. Shell Analysis Report for LSU experiment informs that the re-circulation flow supply is insufficient for the seal flush and some recommendations are given for better experiments. Also the smallness of the pump is stated. TAMU experiment reporter Ryan Kroupa states that preventing heat rise is one of the most important things to increase efficiencies. He recommends adding a heat exchanger to the system. Also, another interesting suggestion that he put into his thesis was using a kind of chemical friction reducing agents to reduce the amount of heat added to the system [5].

3.3 Leakage Flow

Leakage is a kind of flow whose direction is the opposite of the pressure side. In other words, the leakage flow moves from the pressure side to the suction side.

Figure 50 shows the slippage or leakage with red arrows. As can be seen, the main reason of this leakage is clearances. In order to prevent metal to metal contact between the screws and housing, twin-screw pumps are produced with these clearances [5].

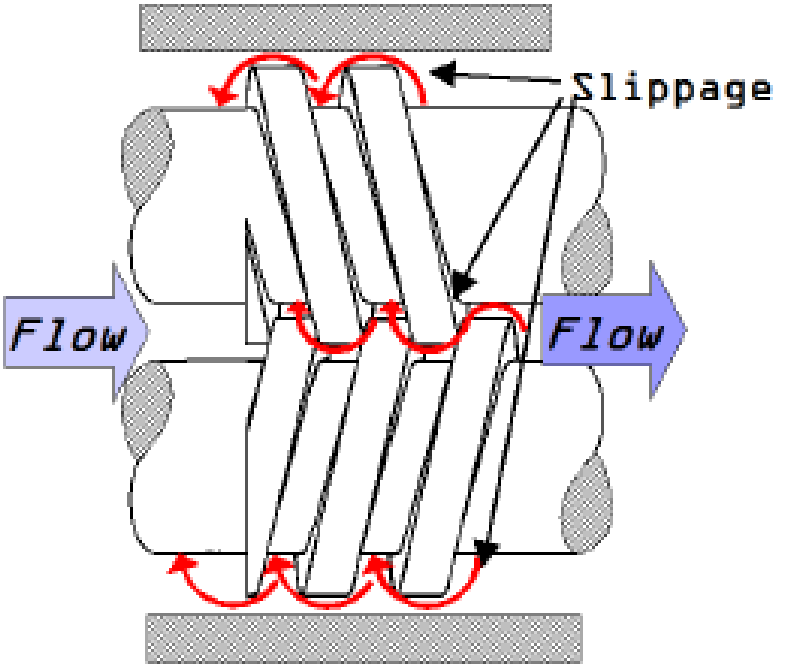

Figure 50 Visualization of different leak paths [5]

There are three kinds of clearances which are circumferential clearance, radial clearance and flank clearance. As showed in Figure 51, the circumferential clearance is between the housing and the screw. The radial and the flank clearances are located between two screws [5].

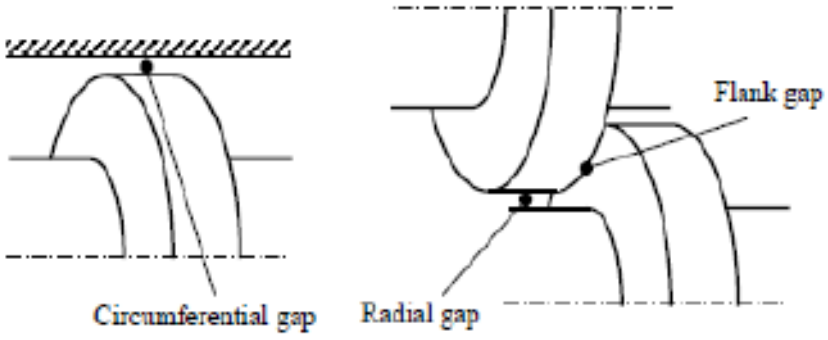

Figure 51 Clearance types of a twin-screw pump [5]

Since the leakage model contains the mass flow rate and some kind of fluid mechanics calculations, the geometry of the screw knowledge is required. Figure 52 represents some important dimensions of a screw.

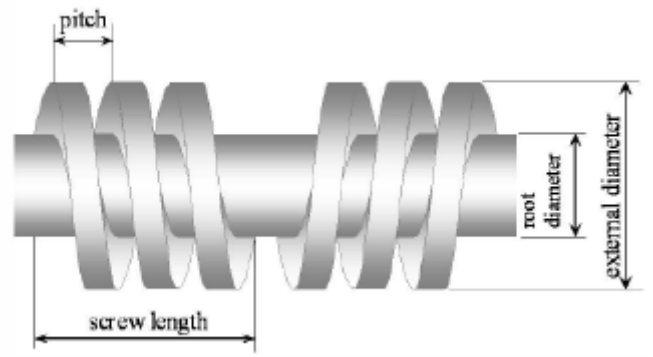

Figure 52 Screw dimensions [5]

Three different leakage models are built because, since one of them works for a specific case, the other one may be best for a different case. The TAMU experiment data is used. Models are named pipe flow leakage model, GVF inlet based leakage model and GVF exit based leakage model. Also, for a comparison, the actual leakage is found for each case. Firstly, the leakage models and their calculation steps will be explained, and then their results will be compared with the actual leakage values.

3.3.1 Leakage Flow Models

3.3.1.1 Pipe Flow Leakage Model

The pipe flow model is built with the assumptions listed below:

1. The leakage includes both gas and liquid. The flow is homogenous. Therefore, the physical properties of flow such as the density and the viscosity can be calculated by the homogenous mixture correlations.
2. The gas is assumed as an ideal gas.
3. The gas part of the working fluid is compressible. Therefore, the inlet mixture density is different than the outlet mixture density.
4. The leakage which only flows in the circumferential gap is investigated.
5. The flow is isothermal.
6. The mass is conserved: The inlet and outlet mass flow rates are equal.
7. The gas compression only occurs in the circumferential gap so the tooth thickness is used to calculate the area in order to calculate the mass flow rate.
8. Bernoulli equation is used as a governing equation.
9. The calculated tooth number is 2.825. Rather than choosing three teeth involve, two teeth involve is assumed because the leakage flow does not move in all teeth.

For a start of the pipe flow leakage model, the single phase experiment data is used. The match between the model and the actual leakage is important because it can be used as a base for the multi-phase operation calculations. The Bernoulli Equation for a pipe flow without a height change is:

$$\frac{P_{in}}{\rho_{liquid}} + \frac{1}{2}V_{in}^2 - \frac{P_{out}}{\rho_{liquid}} - \frac{1}{2}\,V_{out}^2 = \frac{1}{2}f\frac{L}{D}V_{in}^2$$

In the single-phase operation, the only working fluid is liquid and it is incompressible. Therefore the density does not change and the mass conversation yields that the inlet and outlet flow velocity does not change either. Then, the final form of the equation becomes:

$$V_{in} = \sqrt{\frac{P_{out} - P_{in}}{0.5 * f * \rho * {}^{L}/_{D_h}}}$$

where L is the tooth length and D_h is the hydraulic diameter. The friction coefficient purely depends on the Reynolds number for a pipe flow and it has different correlations for laminar and turbulent flow.

$$\text{Re} < 2300 \rightarrow \text{Laminar flow} \rightarrow f = \frac{64}{Re}$$

$$\text{Re} > 2300 \rightarrow \text{Turbulent Flow} \rightarrow f = 0.332 * Re^{-0.25}$$

Reynolds number is:

$$Re = \frac{\rho * V * D_h}{\mu}$$

In order to calculate the Reynolds number and the mass flow rate, hydraulic diameter and the area should be identified.

$$D_h = 2 * c$$

$$A = \pi * c * D$$

where c is the clearance.

In order to find the inlet velocity, the flow is assumed as turbulent and it is proved after the calculation is done. The inlet velocity is:

$$V_{in} = \frac{\dot{m}_{inlet}}{\rho_{liquid} * A}$$

If the turbulent friction coefficient is substituted into the modified Bernoulli Equation, the inlet velocity can be found by the following equation.

$$V_{in} = \left[\frac{(P_{out} - P_{in}) * \left(\frac{\rho * D_h}{\mu}\right)^{0.25}}{0.5 * 0.332 * \rho * {}^{L}/_{D_h}} \right]^{1/1.75}$$

At this point, the calculated single-phase pipe flow leakage model volumetric flow rate can be compared to the actual leakage volumetric flow rate. As expressed in the volumetric efficiency part, the leakage volumetric leakage flow rate is:

$$\dot{Q}_{leakage} = \dot{Q}_{theoretical} - \dot{Q}_{actual}$$

Figure 53 and Figure 54 are graphs for modeled and experiment leakage comparison for inlet 10 PSI and 50 PSI. As represented with graphs, the modeled leakage volumetric flow rate and the actual leakage volumetric flow rate values are almost identical and this shows that the model can be used for incompressible operation calculations. Furthermore, using the velocity that calculated in the final step is used into the Reynolds number correlation; the turbulent flow will be concluded. This indicates that the turbulent flow assumption may be appropriate for multiphase flow calculations as well.

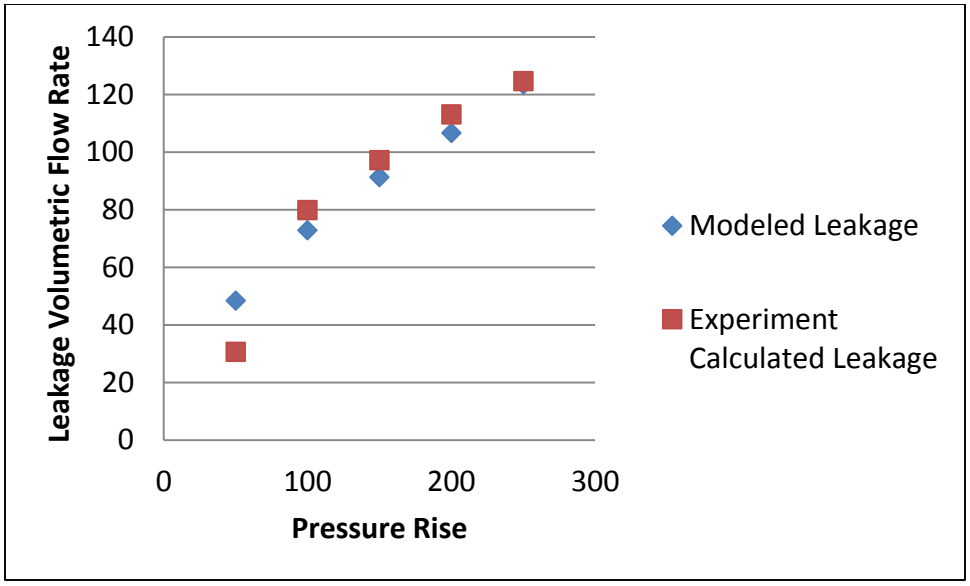

Figure 53 Modeled and experiment leakage comparison for 10 PSI inlet

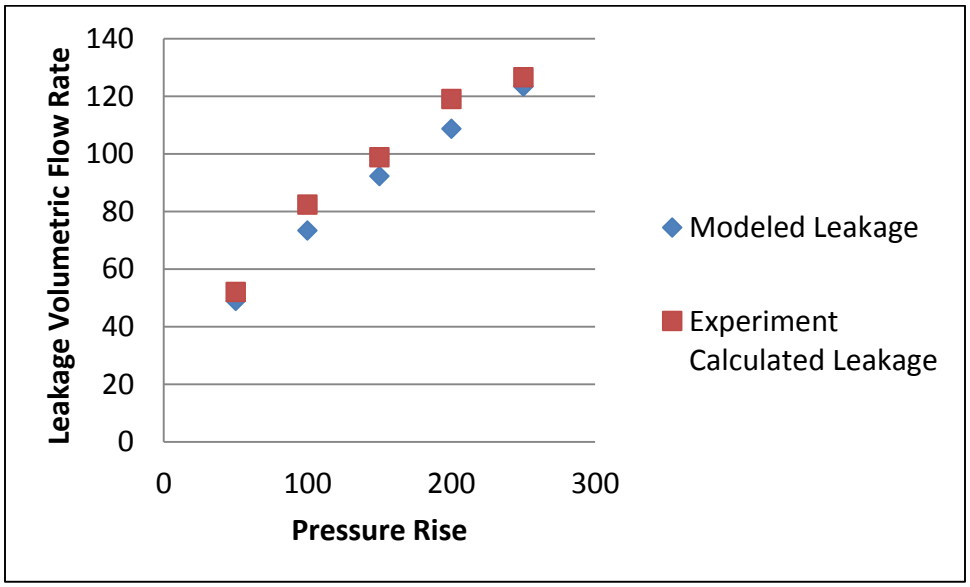

Figure 54 Modeled and experiment leakage comparison for 50 PSI inlet

The pipe flow leakage model for a multiphase flow is built step by step with equations and assumptions as will be expressed below. Bernoulli equation is used as the

governing equation and the isothermal gas compression is assumed. The modified equation is applied across one tooth.

$$\frac{P_{in}}{\rho_{in,mixture}} + \frac{1}{2}V_{in,mixture}^2 - \frac{P_{out}}{\rho_{out,mixture}} - \frac{1}{2}\,V_{out,mixture}^2 = \frac{1}{2}f\frac{L}{D}V_{in,mixture}^2$$

The experiment results yield the inlet and outlet properties of the pump which are the inlet and outlet pressures, the inlet and outlet temperatures and inlet volumetric flow rates for gas, liquid and re-circulation liquid thereby inlet and outlet physical properties can be calculated. However, the flow is assumed as isothermal so the inlet and outlet temperature are assumed equal. Therefore, unknowns in the governing equation are mixture properties, friction factor and velocities. Mixture properties are calculated with equations below,

$$x = \frac{\dot{Q}_{gas} * \rho_{gas}}{\dot{Q}_{gas} * \rho_{gas} + \left(\dot{Q}_{liquid} + \dot{Q}_{re-circulation}\right) * \rho_{liquid}}$$

where x is the gas mass fraction which will be used to calculate the mixture density and viscosity. The gas mass fraction is constant at inlet and outlet and it equals to the pump based control volume gas mass fraction.

$$\rho_{in,mixture} = \frac{\rho_{in,gas} * \rho_{in,liquid}}{x * \rho_{in,liquid} + (1-x) * \rho_{in,gas}}$$

$$\mu_{in,mixture} = \frac{\mu_{in,gas} * \mu_{in,liquid}}{x * \mu_{in,liquid} + (1-x) * \mu_{in,gas}}$$

The leakage mass flow rate does not change which yields:

$$\rho_{in,mixture} * A * V_{in.mixture} = \rho_{out,mixture} * A * V_{out.mixture}$$

where areas cancel each other because they are equal and the equation becomes,

$$\rho_{in,mixture} * V_{in.mixture} = \rho_{out,mixture} * V_{out.mixture}$$

Therefore the outlet mixture velocity equals to:

$$V_{out,mixture} = \frac{\rho_{in,mixture} * V_{in,mixture}}{\rho_{out,mixture}}$$

The friction coefficient is calculated by the following equation and correlations:

$$Re = \frac{\rho_{in,mixture} * V_{in,mixture} * D_h}{\mu_{in,mixture}}$$

Re <2300 → Laminar flow → $f = \frac{64}{Re}$

Re>2300 → Turbulent Flow → $f = 0.332 * Re^{-0.25}$

If the outlet physical properties such as the density and the viscosity are calculated with the equations used for the inlet properties, the final form of the governing equation becomes:

$$\frac{P_{\text{in}}}{\rho_{in,mixture}} + \frac{1}{2}V_{\text{in},mixture}^2 - \frac{\rho_{\text{out},gas} * R * T_{\text{out}}}{\frac{\rho_{out,gas} * \rho_{out,liquid}}{x * \rho_{out,liquid} + (1-x) * \rho_{\text{out},gas}}} - \frac{1}{2}\left\{\frac{\rho_{\text{in},mixture} * V_{\text{in},mixture}}{\frac{\rho_{2,gas} * \rho_{2,liquid}}{x * \rho_{\text{out},liquid} + (1-x) * \rho_{\text{out},gas}}}\right\}^2 =$$

$$\frac{1}{2} f \frac{L}{D} V_{\text{in},mixture}^2$$

As expressed below this modified equation is for each tooth. Unknown components of the modified equation above are the outlet gas density and the inlet mixture velocity. A software code is written for this implicit equation that starts with an estimated value for the inlet mixture velocity and it can give an outlet gas density. If the outlet pressure which is calculated by the ideal gas law is equal to the pump outlet pressure, the loop is stopped by the computer program and all outlet properties such as the outlet mixture velocity, the volumetric flow rate and the mass flow rate can be

calculated. These results are symbolized as the pipe flow leakage model. Figure 55 is the algorithm of the pipe flow model. The leakage volumetric flow rate is

$$\dot{Q}_{leakage} = V_{outlet,mixture} * A$$

The results of the pipe flow leakage model will be discussed with other leakage models which will be explained in the following sections.

3.3.1.2 GVF Inlet Based Leakage Model

In the high GVF values, the pipe flow leakage model is not sufficient to match the actual leakage results. Rather than using the pipe flow approximation, it is assumed that the leakage flow is a compressible flow and hence may be subjected to choked flow in the first tooth. Therefore, the velocity of the mixture equals to the speed of sound. The mixture calculations which are presented in the pipe flow leakage model are used in this model too. It should be added that the GVF inlet based leakage model uses to the pump inlet GVF value. Furthermore, the pump outlet properties are used for the GVF inlet based leakage model.

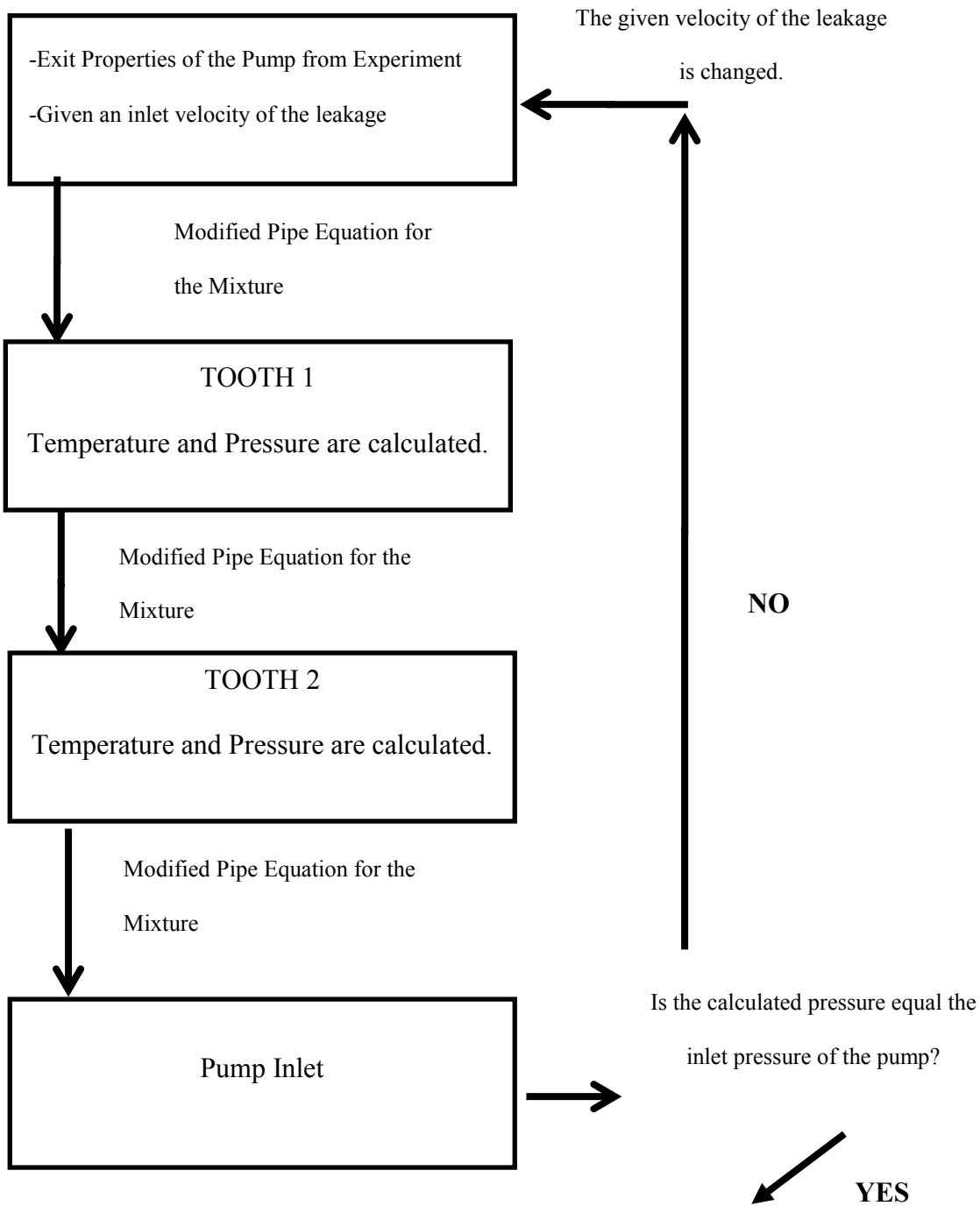

Figure 55 Pipe flow model algorithm

In the choked case with an ideal gas assumption for air the pressure, the temperature and thereby the density can be calculated by the stagnation point situation which is used in thermodynamics.

$$P_{outlet} = P_{inlet} * 0.5283$$

$$T_{outlet} = T_{inlet} * 0.8333$$

$$\rho_{outlet} = \frac{P_{outlet}}{R * T_{outlet}}$$

The speed of sound and the speed of the air and the mixture are calculated by the following equations [12]:

$$c = \sqrt{k * R * T}$$

$$c_{mixture} = \sqrt{\frac{\rho_{gas,outlet} * c^2}{\rho_{liquid} * GVF * (1 - GVF)}}$$

where c is the speed of sound of the gas and GVF that is used in this equation is based on the inlet volumetric flow rates and is found by following equation:

$$GVF = \frac{\dot{Q}_{gas}}{\dot{Q}_{gas} + \dot{Q}_{liquid} + \dot{Q}_{recirculation\ liquid}}$$

With the speed of the mixture, the mass flow rate and the volumetric flow rate directly can be found with the equations below:

$$\dot{Q}_{leakage} = A * c_{mixture}$$

$$\dot{m}_{leakage} = \rho_{mixture} * A * c_{mixture}$$

where area is calculated with the same formula used in the pipe flow leakage model.

$$A = \pi * c * D$$

Since the variable parameters in the mixture speed of sound equation are the outlet gas density and the GVF, it is very important to see how mixture speed of sound changes with respect to these parameters. The inlet pressure and the differential pressure dictate the outlet gas density. Therefore working in the high inlet pressure and differential pressure case yields larger densities. Figure 56 shows the mixture speed of sound change with respect to outlet gas density and GVF. Since the English Unit System is used in all data analysis, the gas densities are lbm/ft^3. As can be seen in the graph, the outlet gas density has a direct effect on the mixture speed of sound. The outlet gas density increment increases the mixture speed of density. Also, in very low and very large GVF operations, the vast increment of the mixture speed of sound can be observed. The data includes the high GVF operations such as %98, 99, 100 so the high leakage

mass flow rates and low volumetric efficiency can be achieved in the choked flow condition.

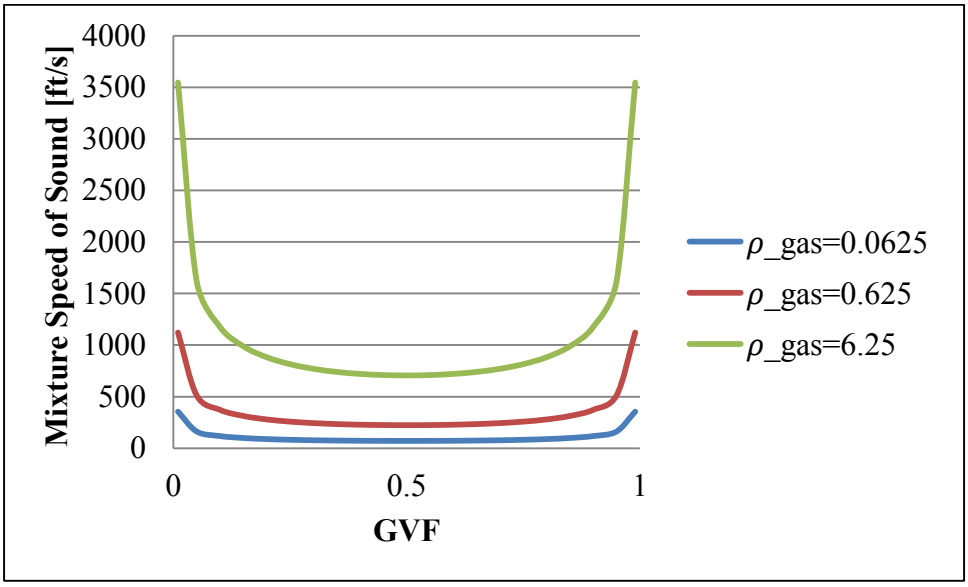

Figure 56 Mixture speed of sound change with respect to outlet gas density and GVF

This leakage mass flow rate and the volumetric flow rate are symbolized the GVF inlet based leakage model. Figure 57 shows the mixture speed of sound for 10 PSI inlet and Figure 58 shows the mixture speed of sound for 50 PSI inlet. It should be noted that the pump based GVF is used in the horizontal axis. As can be seen in the graphs, the mixture speed of sound depends on the pressure rise and the GVF. The inlet pressure increment increases the speed of sound a little bit because the gas density increases with the pressure increment. All pressure rise cases give approximately the same trends, and pressure rise increment increases the mixture speed of sound. Furthermore, the operation

GVF has a direct effect on the mixture speed of sound. GVF increment increases the mixture speed of sound. This increment affect will not be seen in the leakage mass flow rate because the GVF increment decreases the mixture density.

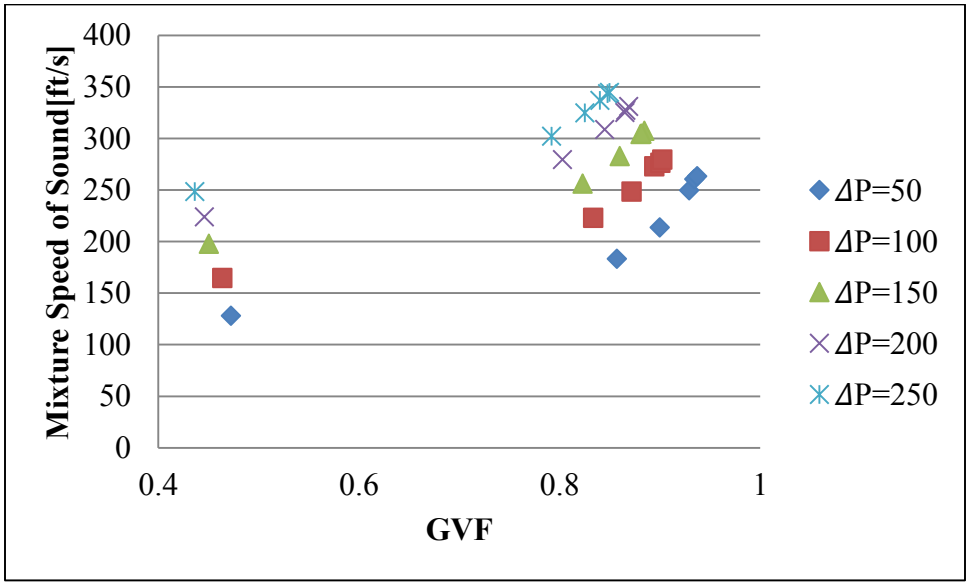

Figure 57 Inlet 10 PSI mixture speed of sound

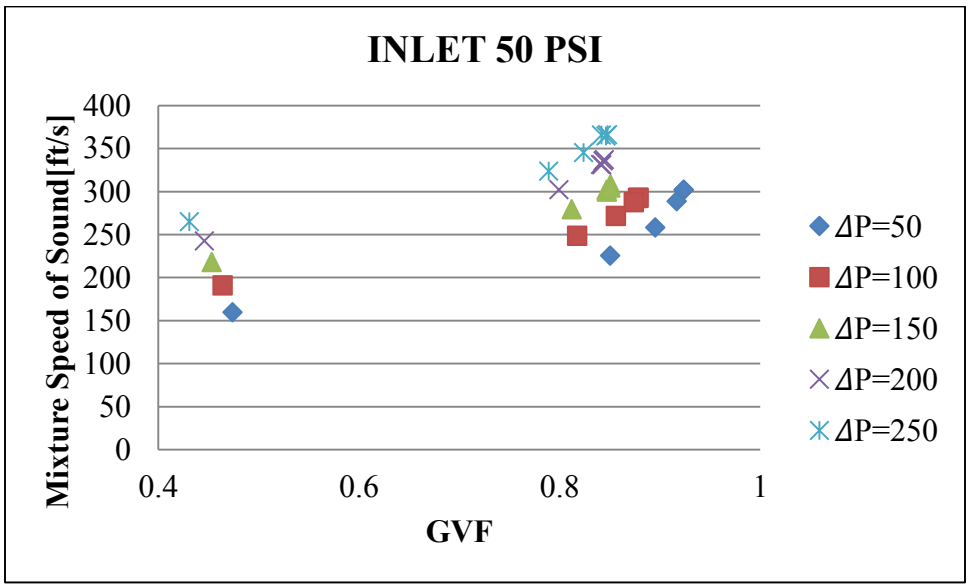

Figure 58 Inlet 50 PSI mixture speed of sound

3.3.1.3 GVF Exit Based Leakage Model

Since the pump exit properties are used for the leakage flow, the choked leakage flow should be calculated and compared with respect to the pump GVF exit value. Rather than using the GVF inlet value, the GVF exit value is calculated and used for this model. Since there is not a mass accumulation in the pump and the liquid is incompressible, the difference of the pump inlet and the outlet pressure causes different GVF value in the inlet and the outlet. The following equations are used for the outlet GVF calculation. Similar to GVF inlet model, GVF exit based leakage model uses to the pump exit GVF value. The calculated mixture speed of sound can be used to calculate the volumetric flow rate and mass flow rate.

$$\dot{Q}_{gas,inlet} * \rho_{gas,inlet} = \dot{Q}_{gas,outlet} * \rho_{gas,outlet}$$

$$\dot{Q}_{gas,outlet} = \frac{\rho_{gas,inlet}}{\rho_{gas,outlet}} * \dot{Q}_{gas,inlet}$$

$$GVF_{exit} = \frac{\dot{Q}_{gas,outlet}}{\dot{Q}_{gas,outlet} + \dot{Q}_{liquid} + \dot{Q}_{rec,liquid}}$$

$$\dot{Q}_{leakage} = A * c_{mixture}$$

$$\dot{m}_{leakage} = \rho_{mixture} * A * c_{mixture}$$

3.3.1.4 Actual Leakage Mass Flow Rate

The actual leakage mass flow rate is calculated with the same method that expressed in the pipe flow model. When the mixture density is calculated with the homogenous flow model, the actual leakage mass flow rate is calculated by the following equation:

$$\dot{m}_{leakage} = (\dot{Q}_{theoretical} - (\dot{Q}_{liquid} + \dot{Q}_{gas} + \dot{Q}_{recirculation\ liquid})) * \rho_{mixture}$$

3.3.2 Leakage Models Results and Discussion

3.3.2.1 Leakage Mass Flow Rate

The leakage mass flow rate is the first step to evaluate and compare the leakage models and its availability for further investigation. As mentioned in the previous chapters, figuring the leakage amount is basically able to detect the volumetric efficiency.

Figure 59 and Figure 60 are leakage model comparisons with actual leakage for 10 PSI inlet and 50 PSI inlet with respect to leakage mass flow rates. The GVF values that are used as heading for each graph is the skid based GVF value.

Both graphs show that the GVF inlet based leakage model gives more accurate results for all the GVF values and the inlet pressures. The GVF exit based leakage generally yields average results of pipe model and GVF inlet model. For the high differential pressures and high GVF situations, the GVF exit based leakage model mass flow rate is much lower than the actual leakage. The pipe model leakage mass flow rate amount distribution with respect to GVF values show that the model only depends on the GVF for the density mixture. Therefore, it gives similar results for all conditions. In fact, while the actual leakage mass flow rate increases, the pipe flow model leakage mass flow rate decrease can be observed. GVF inlet based leakage model gives more accurate results in low pressure inlet condition. While the leakage models yield approximately the same results in the high pressure inlet and high skid based GVF conditions, the actual leakage mass flow rate is greater than all leakage models. While the actual leakage mass flow rate yields larger results only %100 skid based GVF case in the low pressure inlet condition, above %90 skid based GVF cases yields larger actual leakage mass flow rates in high inlet pressure condition.

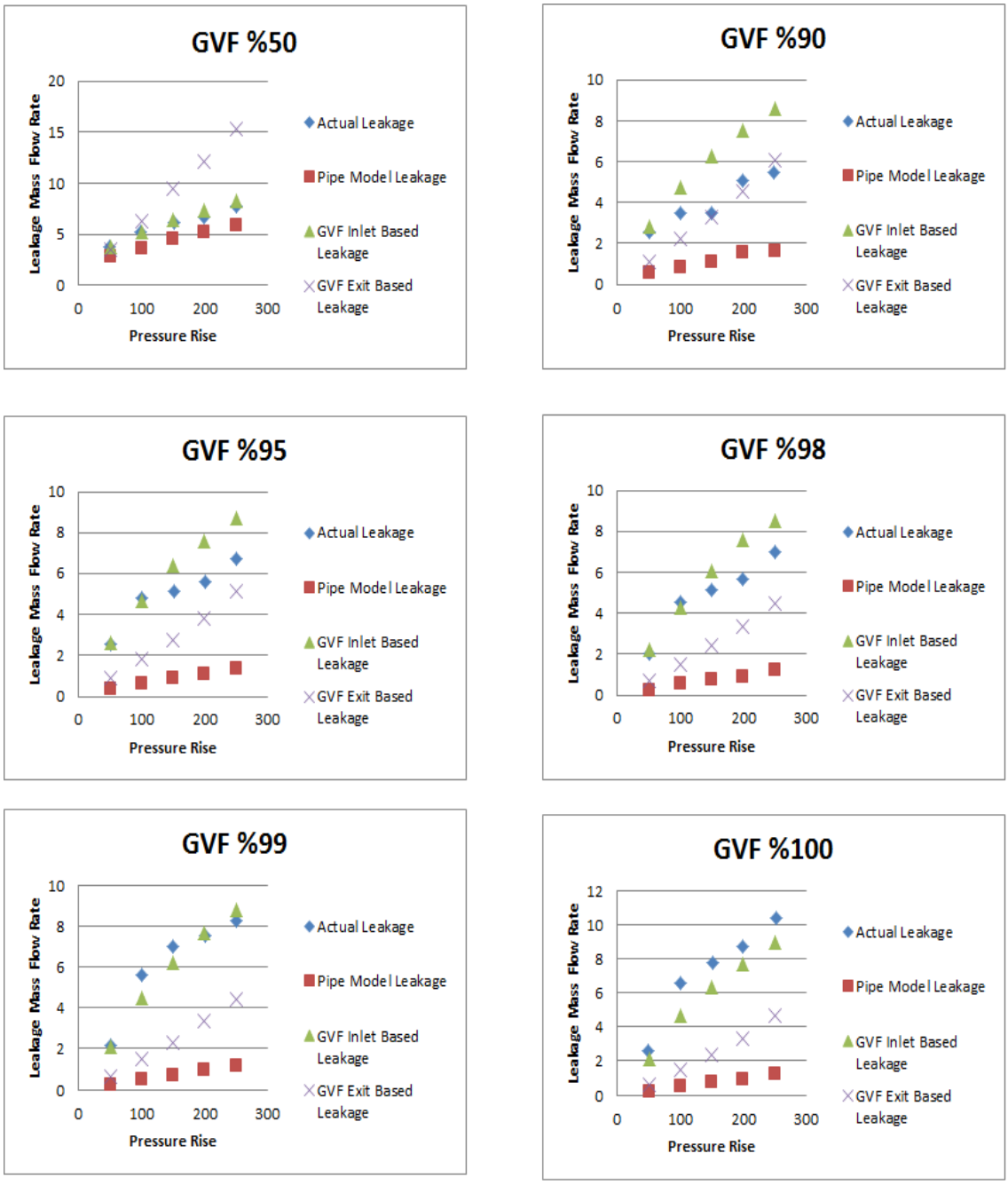

Figure 59 Inlet 10 PSI leakage model comparison with actual leakage

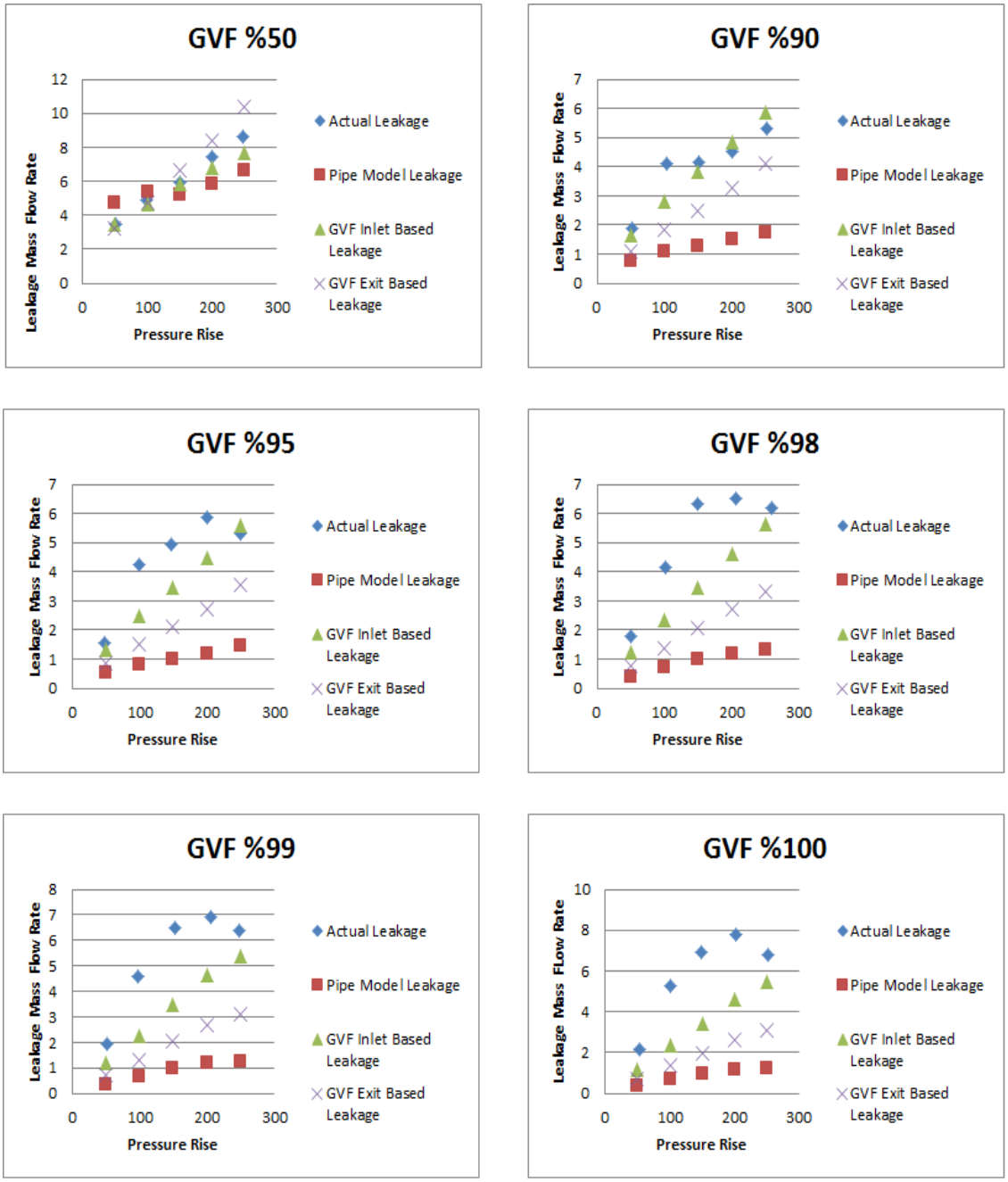

Figure 60 Inlet 50 PSI leakage model comparison with actual leakage

The mixture leakage mass flow rate in the maximum pressure rise case in different GVF cases evaluation may be beneficial for choked flow assumption. As can be seen in Figure 57 and Figure 58, the mixture speed of sound depends on the GVF and pressure rise. Figure 61 shows the actual leakage mass flow rate in the maximum differential pressure case, which is 250 PSI, with respect to the low and the high inlet pressure cases. Even though the mixture speed of sound increases with the increment of GVF and pressure rise in high GVF conditions, the actual leakage mass flow rate does not directly depend on these parameters. The actual leakage mass flow rate mostly depends on the inlet pressure. While the low inlet pressure yields larger actual leakage mass flow rates, the higher inlet pressure yields lower leakage mass flow rates. It should be added that in the high GVF operations, the leakage mass flow rate does not increase as the speed of sound for the mixture. This is because while the mixture speed of sound increases with respect to GVF, density decreases because of the increment gas portion of the mixture. For example, in the high inlet pressure case the maximum leakage mass flow rate is observed in the minimum GVF case because the density is much larger in comparison to high GVF cases.

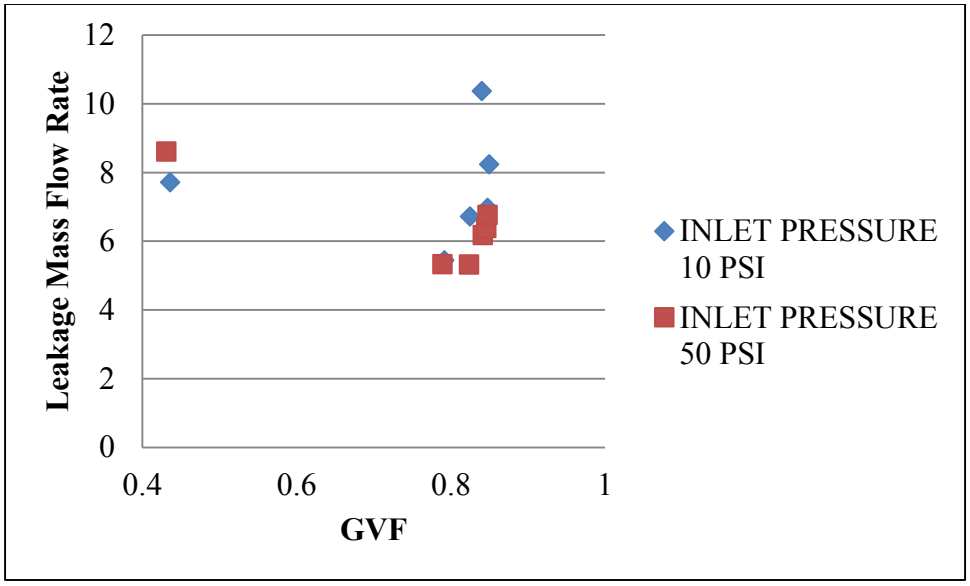

Figure 61 Actual leakage mass flow rate in 250 PSI rise conditions

3.3.2.2 Volumetric Efficiency

The volumetric efficiency comparison for these models is the main parameter to evaluate their accuracy. The effect of the models plays a key role in the calculation of the mechanical efficiency. At this point, the effect of the leakage mass flow rate comparison will be reflected in the volumetric efficiency graphs.

Figure 62 is the volumetric efficiency leakage model comparison for the inlet 10 PSI case and Figure 63 is the volumetric efficiency leakage model comparison for the inlet 50 PSI case. The actual volumetric efficiency decrease can be observed for both cases. However, the leakage models variation in different GVF conditions is lower in comparison with the actual leakage. This is because; the leakage models are based on some assumptions and the pump geometry. At the same time, the experiment result is more open to the environment and other physical situations.

For inlet 10 PSI, Figure 62 shows that the pipe flow leakage model and the GVF inlet based leakage model yields sufficient results. For first four cases, GVF %50-GVF%90-GVF %95- GVF%98, the pipe flow leakage model accuracy can be observed. For GVF %99 and GVF %100 cases the GVF inlet based leakage model gives more satisfactory results. This presents that for highest GVF values, the choked flow may occur in leakage flow. Therefore, the skid based GVF value is a crucial parameter to select the leakage model.

For inlet 50 PSI, Figure 63 shows that the best results are achieved with the GVF inlet based leakage model. Even though low GVF values yield sufficient pipe model leakage model results, the difference between pipe model leakage and the actual leakage increases in high GVF values. It is apparent that the most comprehensive result is achieved in the GVF inlet based leakage model for this inlet pressure case too. Furthermore, it can be noticed that GVF exit model and pipe flow model yields similar results. Another notable result can be observed about the leakage models and the actual leakage distribution for the high inlet pressure condition. Even though the actual leakage model gives varied results with different GVF values, the leakage models tend to give stable results. This causes the difference between the actual leakage and the leakage models. Especially, in the high inlet pressure case the actual volumetric efficiency change is not linear in a specific GVF. In fact, for a high GVF condition, it behaves like a sinusoidal trajectory. This can be explained by the experiment conditions and nature of the pump. For instance, while the liquid re-circulation system makes the system more efficient in volumetric and mechanical manner, it causes another heat rise. If leakage

models are observed, for both inlet pressure cases all leakage models change in a specific GVF is linear.

If both inlet pressure cases are compared, it is apparent that the lower inlet pressure case gives more sufficient results. Even, for the low GVF values the pipe model leakage model and for high GVF values the GVF inlet based leakage model can be suggested with a defined uncertainty. This shows that the models and their assumptions are more appropriate to determine volumetric efficiency for the low pressure case. High inlet pressure with high GVF values does not give satisfactory results. The pipe flow model becomes inapplicable in this case and for high GVF values, GVF inlet based leakage model is also varied results. The main reason is the behavior of the actual volumetric efficiency change as mentioned. Also, for the high inlet pressure case, all pump based flow becomes more incompressible with comparison to lower inlet pressure. However, all leakage models are used mainly based on the compressible effect of the gas part of the fluid.

Lastly, as can be noticed from the comparison of leakage models and volumetric efficiency in terms of their accuracy, the leakage models give more accurate results in volumetric efficiency case. This is very crucial for leakage model evaluation because the volumetric efficiency of models will be used to calculate the mechanical efficiency.

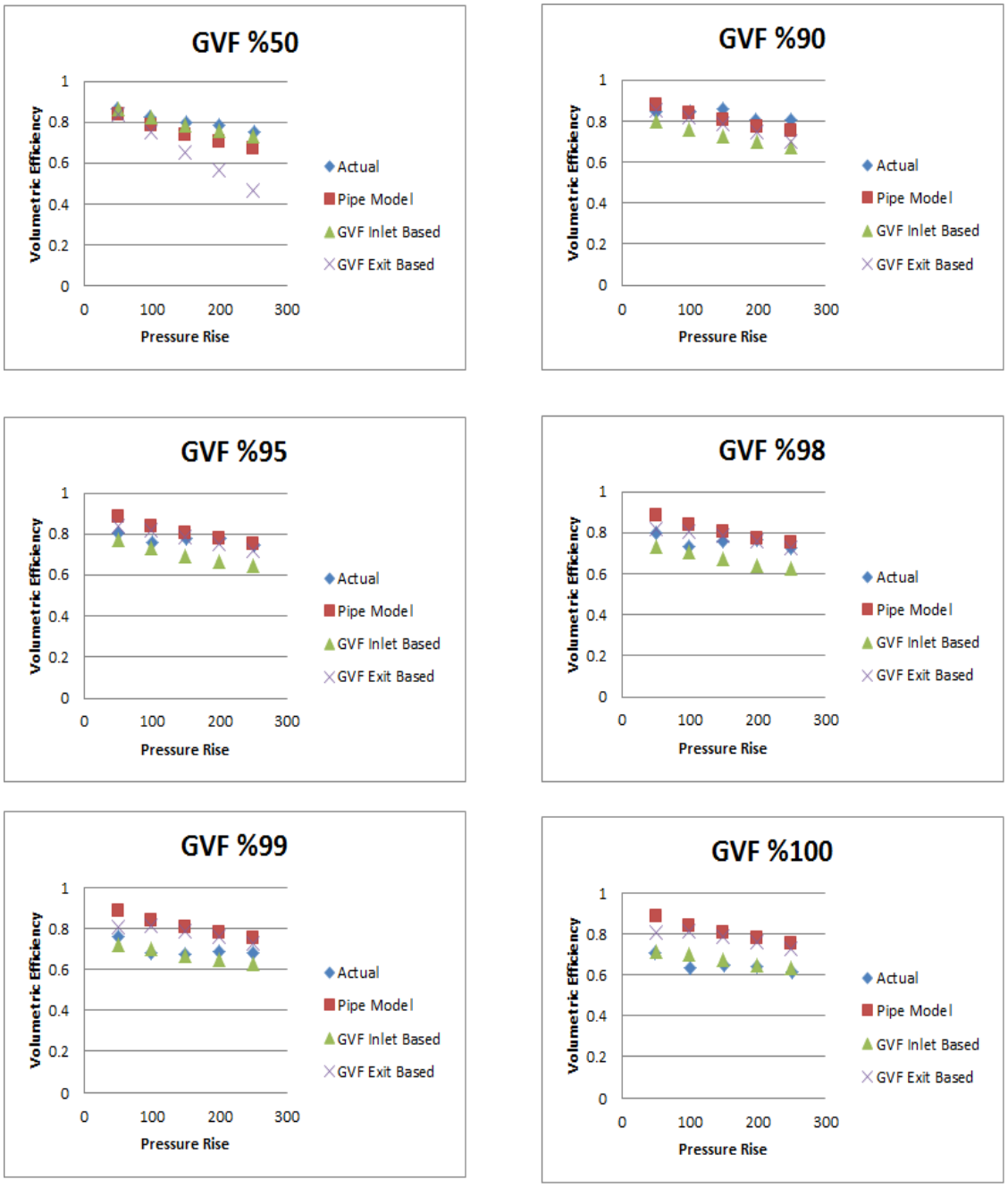

Figure 62 Inlet 10 PSI volumetric efficiency comparison with actual leakage

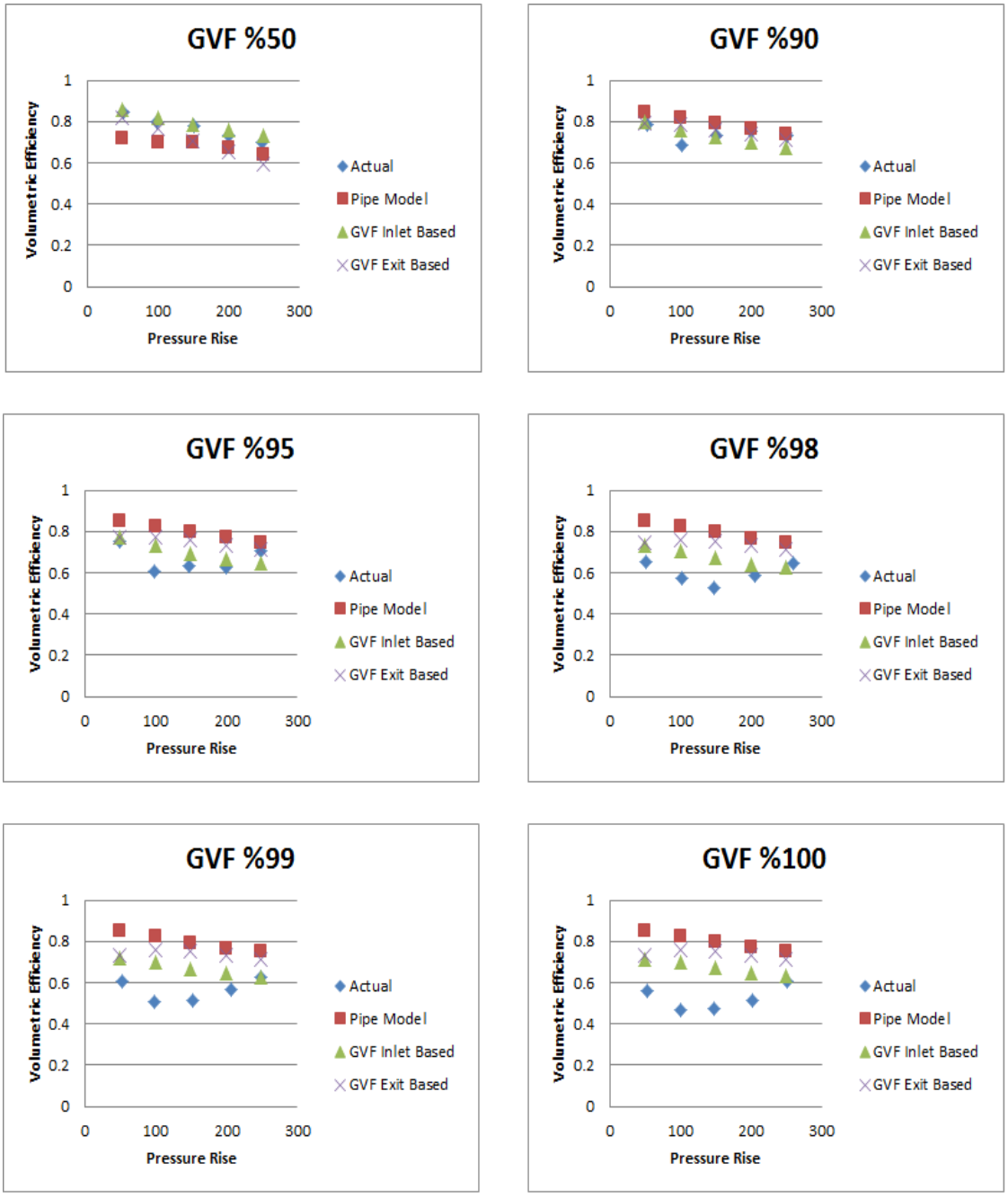

Figure 63 Inlet 50 PSI volumetric efficiency comparison with actual leakage

The volumetric efficiency ratio can be used as a tool to evaluate the leakage models with respect to the actual volumetric efficiency. The ratio is calculated by the following equation:

$$Ratio = \frac{Actual\ or\ Model\ Leakage\ Volumetric\ Efficiency_{\Delta P, GVF=50,90,95,98,99,100}}{Actual\ Volumetric\ Efficiency\ _{\Delta P, GVF=0}}$$

where the differential pressure of the numerator and denominator is same. For instance, the GVF inlet based volumetric efficiency ratio of %98 GVF and 200 PSI differential pressure case is equal to the corresponding volumetric efficiency over the single-phase operation which is GVF=0 200 PSI differential pressure case.

Figure 64 and Figure 65 show the volumetric efficiency ratios for 10 PSI and 50 PSI inlet pressure cases. In order to compare leakage models, the actual leakage volumetric efficiency should be considered as a base model. For both conditions, the general distribution of the actual volumetric efficiency and the leakage models are very similar. Actual volumetric efficiency for both inlet conditions show that the maximum results are achieved in medium GVF and the highest differential pressure case. The actual volumetric efficiency ratio depends more on the pressure rise. For the pipe model volumetric efficiency, the maximum value is achieved in the highest GVF and the highest differential pressure case. For the GVF inlet model volumetric efficiency graph represents that the maximum value is achieved in the lowest GVF but the highest differential pressure case. Both graphs show that the GVF exit based leakage model yields very similar results to pipe model volumetric efficiency. This volumetric efficiency will be used to calculate the mechanical efficiency in the mechanical efficiency part.

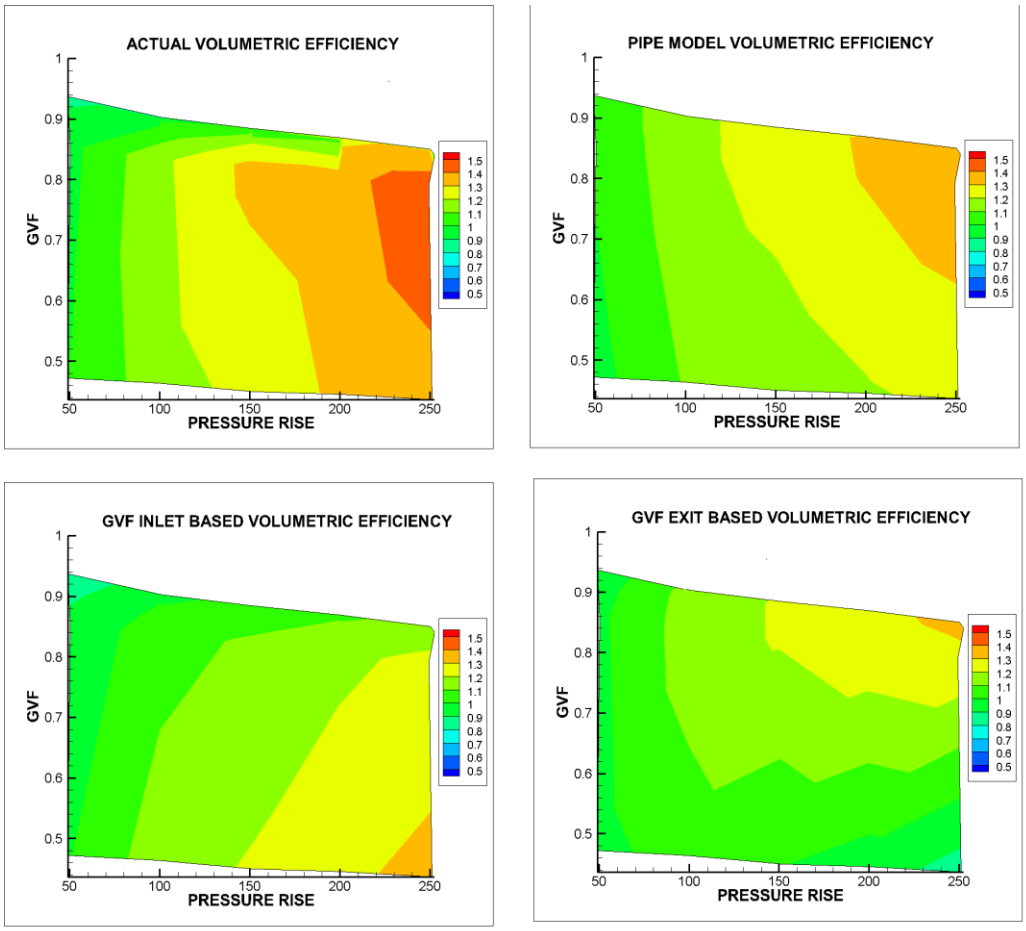

Figure 64 Inlet 10 PSI actual and leakage models volumetric efficiency ratio comparison

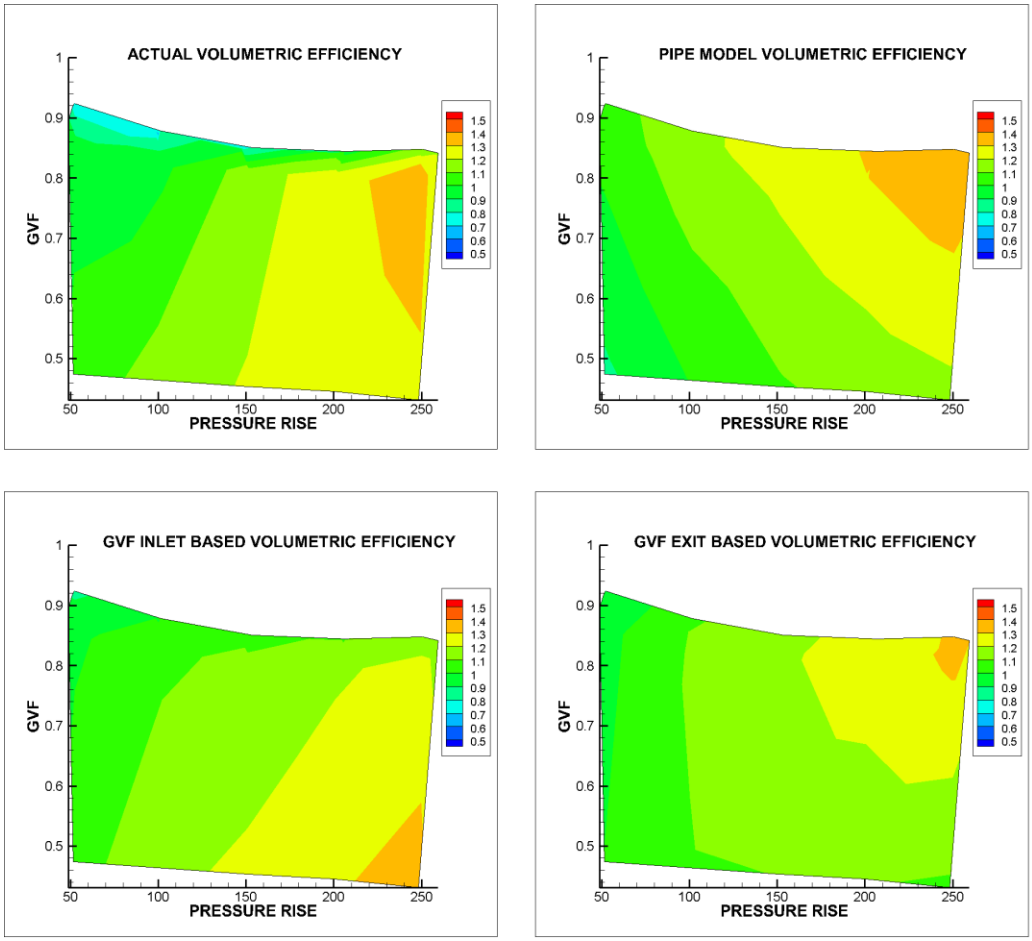

Figure 65 Inlet 50 PSI actual and leakage models volumetric efficiency ratio comparison

3.3.2.3 Mechanical Efficiency

The leakage calculation with the experiment data can be used for calculation of the mechanical efficiency. Rather than calculating the mechanical efficiency directly, using the volumetric efficiency and the effectiveness make mechanical efficiency less dependent on the experimental data. The mechanical efficiency is modified with the following equations.

$$\eta_{volumetric} = \frac{\dot{Q}_{actual}}{\dot{Q}_{design}}$$

$$GVF = \frac{\dot{Q}_{gas}}{\dot{Q}_{gas} + \dot{Q}_{liquid}}$$

$$P_{hydraulic,skid} = (\dot{Q}_{gas} + \dot{Q}_{liquid}) * \Delta P$$

Substituting the volumetric efficiency equation and the GVF equation into the hydraulic power equation yields,

$$P_{hydraulic} = \eta_{vol} * \dot{Q}_{design} * \Delta P$$

$$\eta_{effectiveness} = \frac{P_{actual}}{P_{hydraulic}}$$

For the actual power calculation, the gas compression models such as isothermal, isentropic or polytropic as presented earlier are used. Actual power is calculated by these gas compression models with the liquid compression. Then, the mechanical efficiency is defined as:

$$\eta_{mechanical} = \frac{P_{actual}}{P_{motor}}$$

The actual power is calculated by the multiplication of the modified hydraulic power calculation and the effectiveness.

$$P_{actual} = \eta_{eff} * \eta_{vol} * \dot{Q}_{design} * \Delta P$$

Substituting the modified actual power equation into the mechanical equation yields:

$$\eta_{mechanical} = \frac{\eta_{eff} * \eta_{vol} * \dot{Q}_{design} * \Delta P}{P_{motor}}$$

where the volumetric efficiency can be calculated by the leakage model and the effectiveness is the purely theoretical dimensionless value. Furthermore, $\dot{Q}_{design}$ basically depends on the geometry and the speed of the pump, so it is always known. If differential pressure is selected, only the motor power obtained from the experiment for multiphase operation is required in the modified mechanical efficiency equation.

Figure 66 presents a comparison of mechanical efficiency calculations for a polytropic process for the different leakage models for an inlet pressure of 10 PSI. The graph shows that the leakage models are applicable for the mechanical efficiency calculation. Since the only parameter for the calculation is the volumetric efficiency and its governing model, the mechanical efficiency graph yields parallel results with the volumetric efficiency graphs. As presented in Figure 59 and Figure 64, the leakage models give sufficient results for the inlet 10 PSI case. Therefore, the mechanical efficiency of all leakage models yields similar results with respect to the actual mechanical efficiency. Furthermore, since the isothermal and the polytropic gas compression models give approximately same results, the isothermal gas compression model is not added in the report.

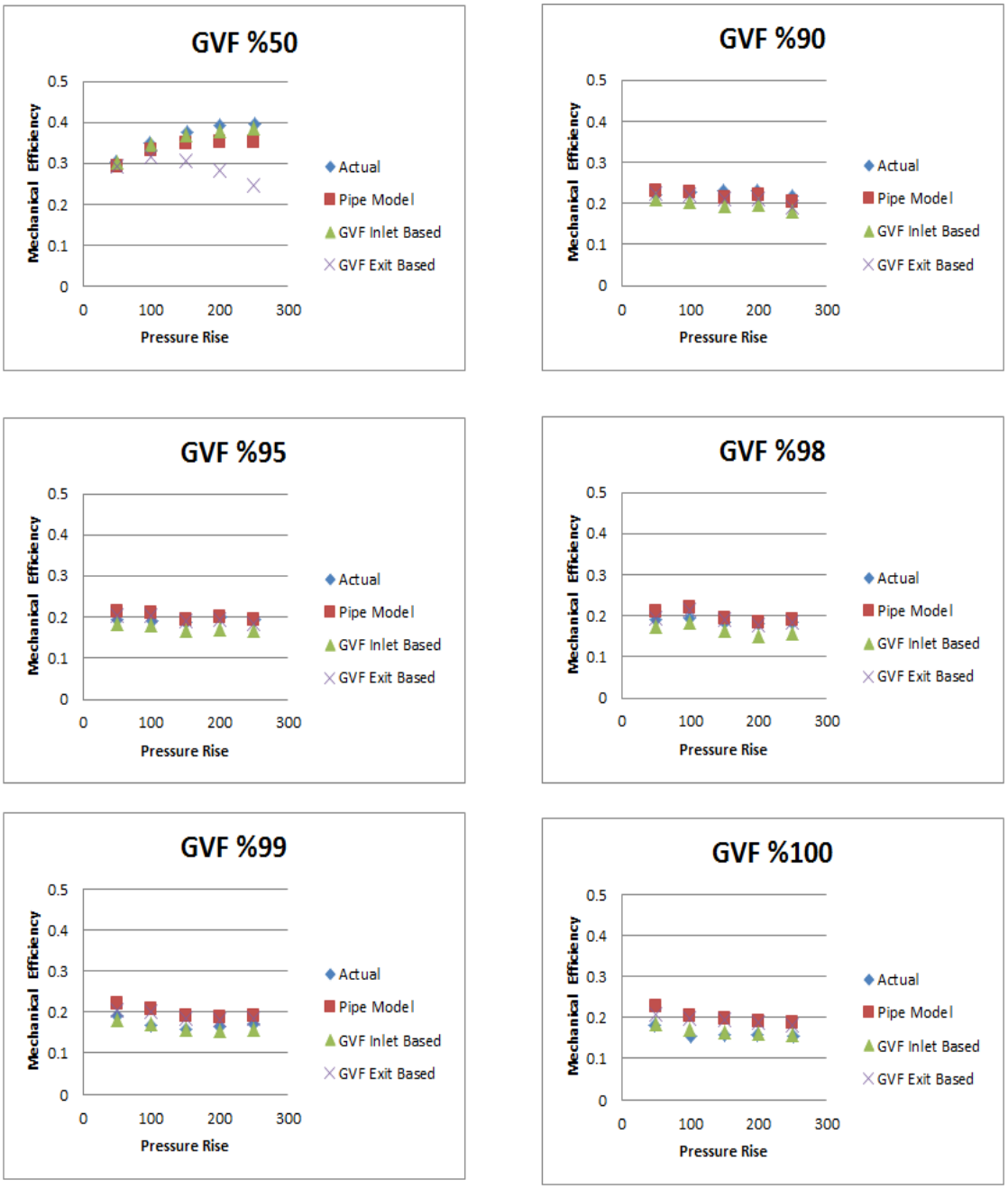

Figure 66 Inlet 10 PSI polytropic leakage model mechanical efficiency comparison

Figure 67 is the polytropic leakage model mechanical efficiency comparison for the 50 PSI inlet pressure. As mentioned in the volumetric efficiency part in the leakage model section, the mechanical efficiency accuracy is not sufficient for high GVF values. The GVF increment suffers the pipe model mechanical efficiency leakage model accuracy. Since GVF exit leakage model yields nearly same results with pipe model, the GVF exit model does not give accurate results either. At this point, take an in depth look at the GVF change with respect to skid based GVF and differential pressure may be beneficial to explain the GVF inlet based model and GVF exit based model difference. Figure 68 and Figure 69 illustrate the inlet 10 PSI pump based GVF and the outlet pump based GVF distribution with respect to the skid based GVF and the differential pressure. While the inlet pump based GVF value only depends on the skid based GVF, outlet pump based GVF depends on both skid based GVF and pressure rise across the pump. Furthermore it should be noted that the outlet pump based GVF value is always lower than the inlet pump based GVF value in the same case. This issue shows that in the high GVF and the high inlet pressure conditions, lower GVF values cause lower leakage mass flow rates.

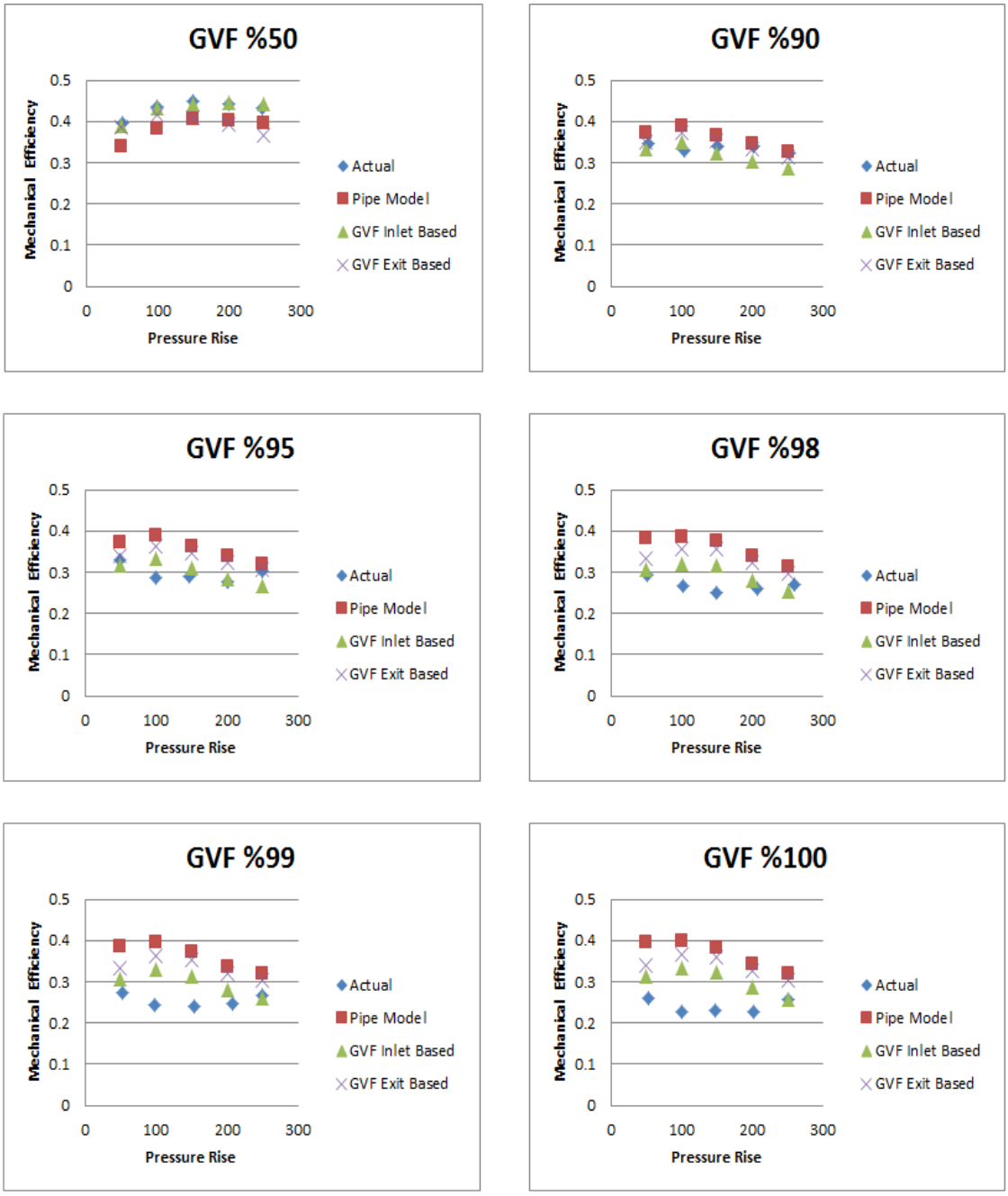

Figure 67 Inlet 50 PSI polytropic leakage model mechanical efficiency comparison

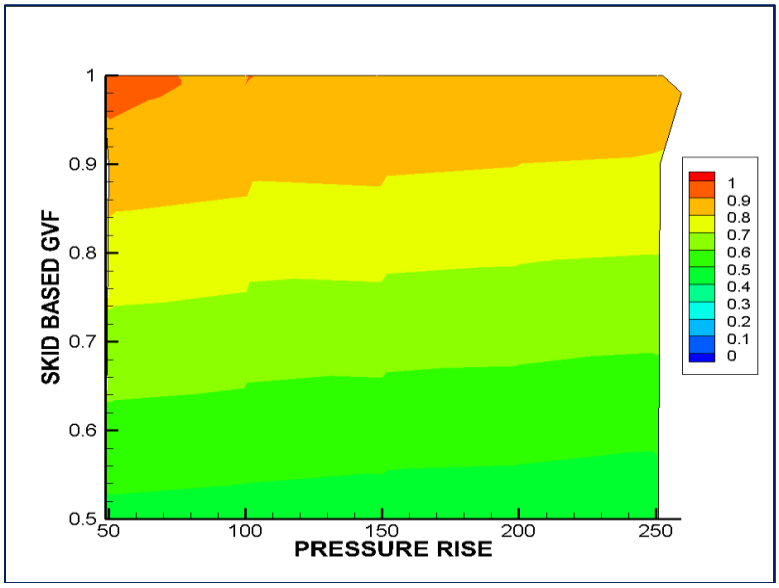

Figure 68 Inlet 10 PSI pump based inlet GVF distribution

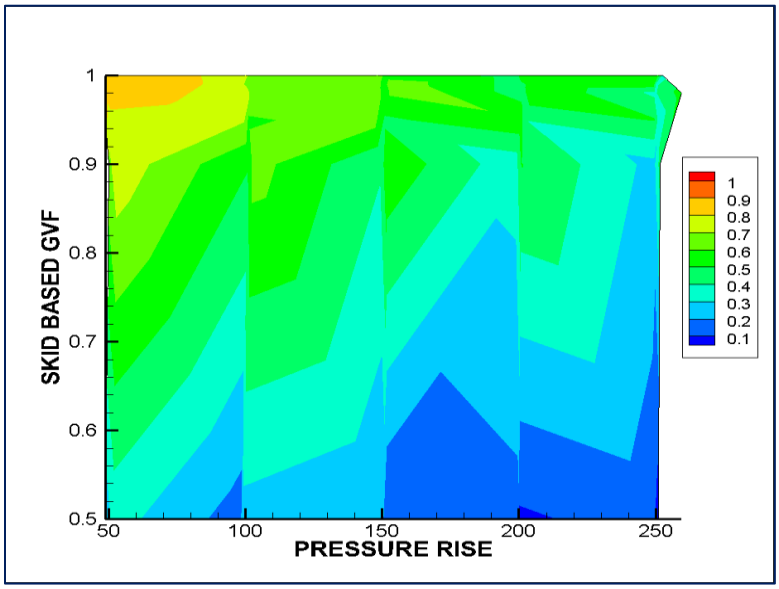

Figure 69 Inlet 10 PSI pump based outlet GVF distribution

Even though these mechanical efficiency graphs can be used as a guide to detect the mechanical efficiency and to compare with the real results, the mechanical efficiency still depends on the electrical power obtained in the multiphase experimental results. In order to make the mechanical efficiency correlation independent of experiments, the single phase operation results should be used. This enables a user of the pump to detect its mechanical efficiency before usage. Detection of the mechanical efficiency with the single phase data will be explained in the following parts. The mechanical efficiency which only depends on the dimensionless values and the single phase mechanical efficiency is calculated by the following equation:

$$\eta_{mech,\Delta P} = \eta_{mech,GVF=0,\Delta} * \eta_{process(isothermal\ or\ polytropic)} * \eta_{volumetric\ efficiency}$$

where the $\eta_{mech,GVF=0}$is the mechanical efficiency value in the dependent differential pressure case, $\eta_{process(isothermal\ or\ polytropic)}$is the effectiveness and the volumetric efficiency is calculated by the leakage models and the experimental results. The mechanical efficiency of the leakage models are calculated with their volumetric efficiency. Also, the calculated mechanical efficiency in the graph is calculated with the volumetric efficiency and the mechanical efficiency values in the experiment and the actual mechanical efficiency is directly obtained from the experiment result. As presented in the previous parts, the isothermal and polytropic compression are of interest.

This detection of the mechanical efficiency can be accounted as a starting point of the mechanical efficiency correlation. The leakage model can be criticized and its ability to detect the mechanical efficiency with a single phase mechanical efficiency

result can be evaluated. Further addition and analyze of this correlation are expressed in the following chapters.

Figure 70 and Figure 71 are the isothermal model compression mechanical efficiency comparison for the low and high inlet pressures. The graphs show that the calculated mechanical efficiency and the leakage model mechanical efficiency results are much closed. However, the actual mechanical efficiency is always much larger than models. This is because the correlation includes three different efficiency types. Especially, the single-phase mechanical efficiency usage in this correlation should be criticized because it does not exist in the modified mechanical efficiency calculation. As can be seen in the graphs, the leakage models yield approximately the same results in the low inlet pressure case. This is because the volumetric efficiency results of the leakage model are very close. However, distinctive results can be observed in the higher inlet pressure case. Especially, the calculated mechanical efficiency results are much lower than leakage model results in the high GVF operations. Pipe model and GVF exit model results are very close for the case of high inlet pressure, low differential pressure and high GVF operations. The differential pressure increment decreases the accuracy of these models. Even though, the main purpose of the calculation is to achieve actual mechanical efficiency results, the similarity between the leakage models mechanical efficiency results and calculated mechanical efficiency results show the applicability of leakage models.

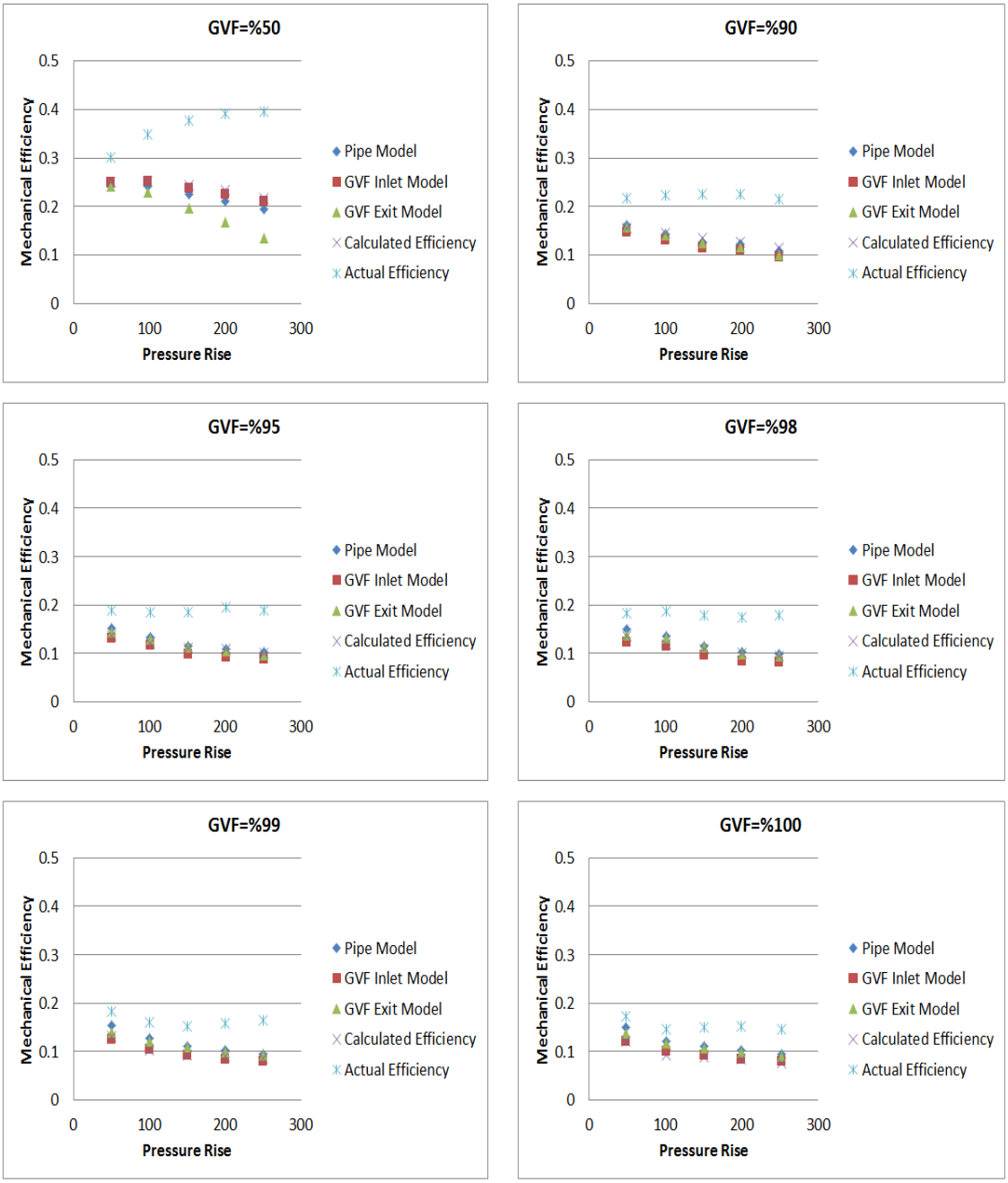

Figure 70 Inlet 10 PSI isothermal compression model leakage mechanical efficiency correlation comparison

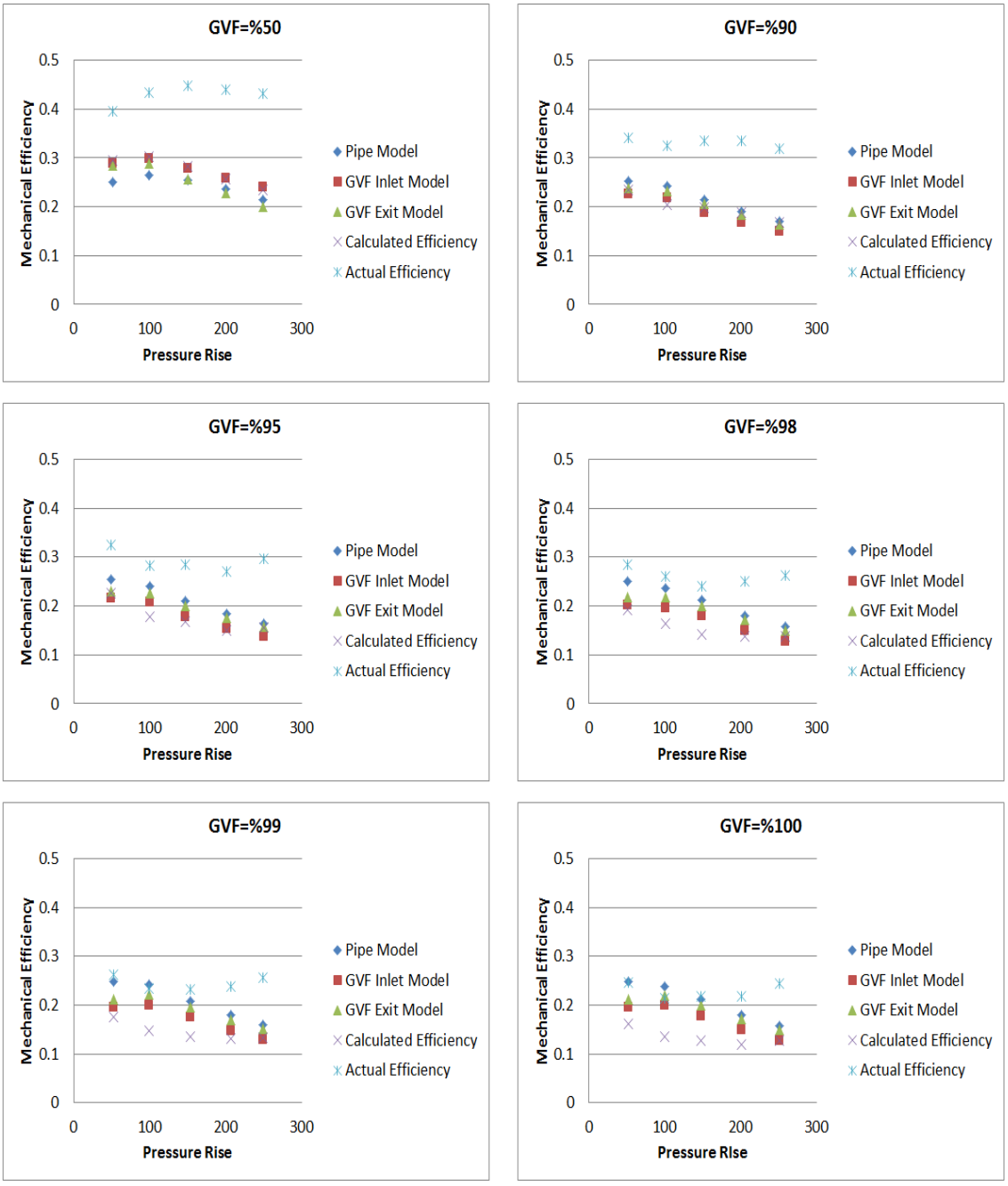

Figure 71 Inlet 50 PSI isothermal compression model leakage mechanical efficiency correlation comparison

The variation between mechanical efficiency correlation of the leakage models results and the actual mechanical efficiency motivates to the evaluation of the ratio of these two results. An appropriate coefficient can be directly used in the correlation for making the correlation more accurate. Since the leakage models mechanical efficiency correlation yields similar results, the pipe model leakage is selected for the ratio which is calculated by the following equation:

$$Ratio = \frac{Pipe\ Flow\ Leakage\ Model\ Based\ Mechanical\ Efficiency}{Actual\ Mechanical\ Efficiency}$$

Figure 72 is the inlet 10 PSI ratio comparison with respect to GVF values. As seen in the graph, the differential pressure increment causes ratio decrease as well as the leakage model accuracy for all GVF values. However, the GVF dependency of ratio is not in the direct proportion to GVF value. While the maximum ratio is achieved in GVF % 100 values, the minimum ratio is achieved in GVF %90 value.

Figure 73 is the inlet 10 PSI ratio comparison with respect to the differential pressure values. The graph shows that the ratio is inverse proportion to the differential pressure increment for a specific GVF value. GVF %50 case presents the differential pressure dependency of the ratio. As noted in the graph, GVF %50 values are similar to the average of all ratio values for a specific differential pressure.

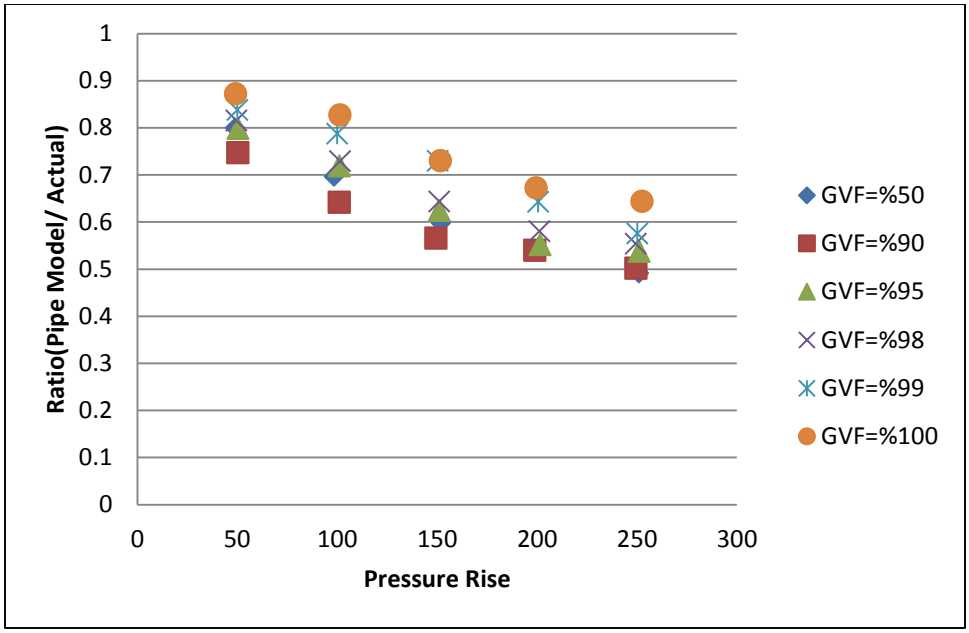

Figure 72 Inlet 10 PSI ratio comparison with respect to GVF values

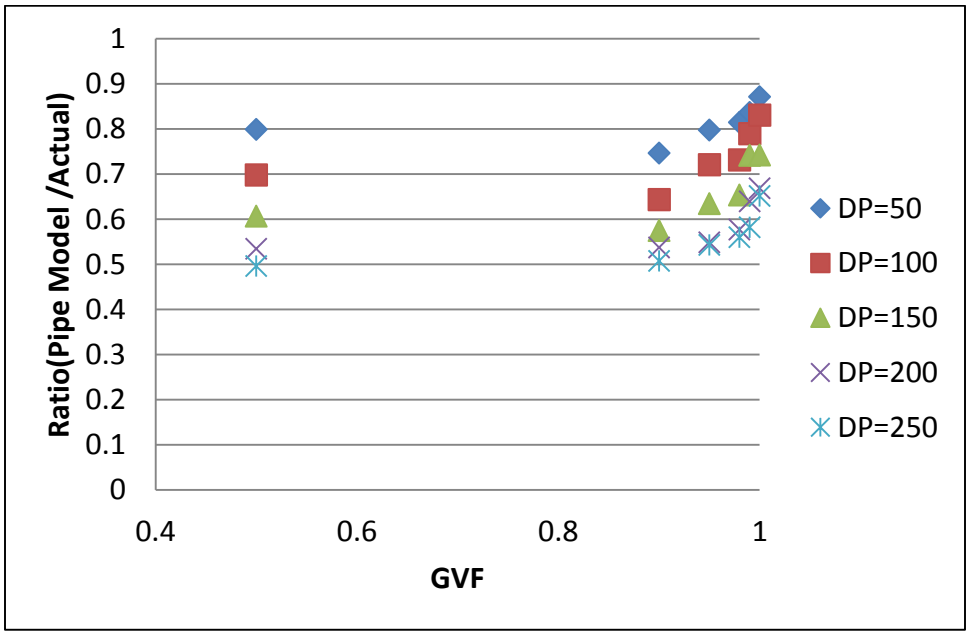

Figure 73 Inlet 10 PSI ratio comparison with respect to differential pressure values

Figure 74 is the inlet 50 PSI ratio comparison with respect to GVF values. In comparison to the inlet 10 PSI case, the inlet 50 PSI case yields more scattered results. However, in this case, the ratio is in direct proportion to GVF values. For each pressure rise, the GVF value increment yields the ratio increment as well as the accuracy of the leakage model.

Figure 75 is the inlet 50 PSI ratio comparison with respect to the differential pressure values. In comparison to the inlet 10 PSI case the graph seems more compact. This is because the pressure ratio is lower in the inlet 50 PSI case. 100 PSI differential pressure case yields the maximum ratio for this case. Even for the GVF %99 and GVF %100 cases the ratio is larger than 1.

This ratio evaluation presents that the ratio depends on the GVF value and the differential pressure of the pump operation. Generally, the leakage models for a mechanical efficiency calculation produce the best results in minimum differential pressure and the maximum GVF value case. This is due to the leakage model being based on the compressible effect of gas. Therefore, GVF increment increases the accuracy of the model.

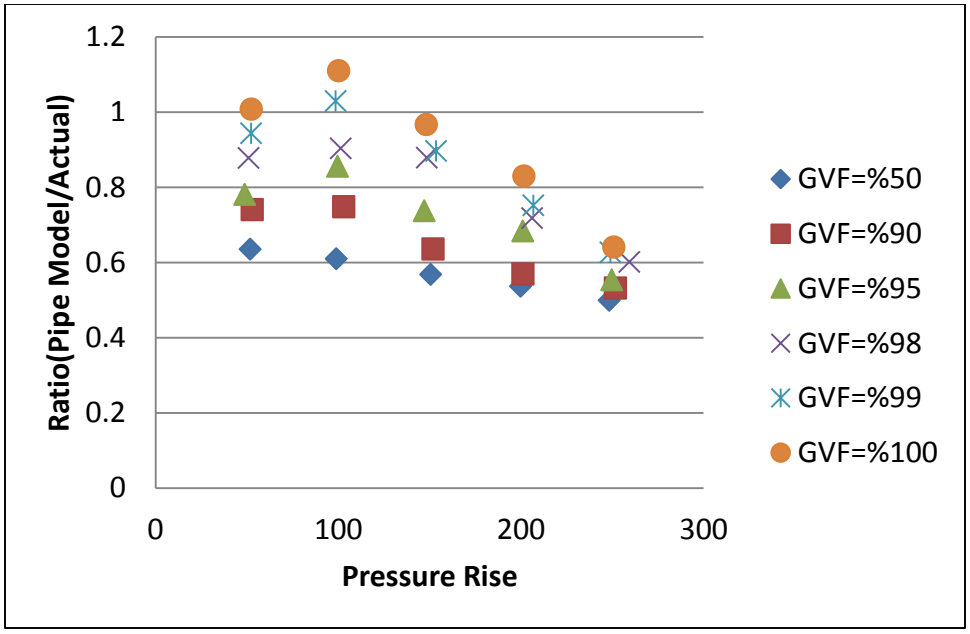

Figure 74 Inlet 50 PSI ratio comparison with respect to GVF values

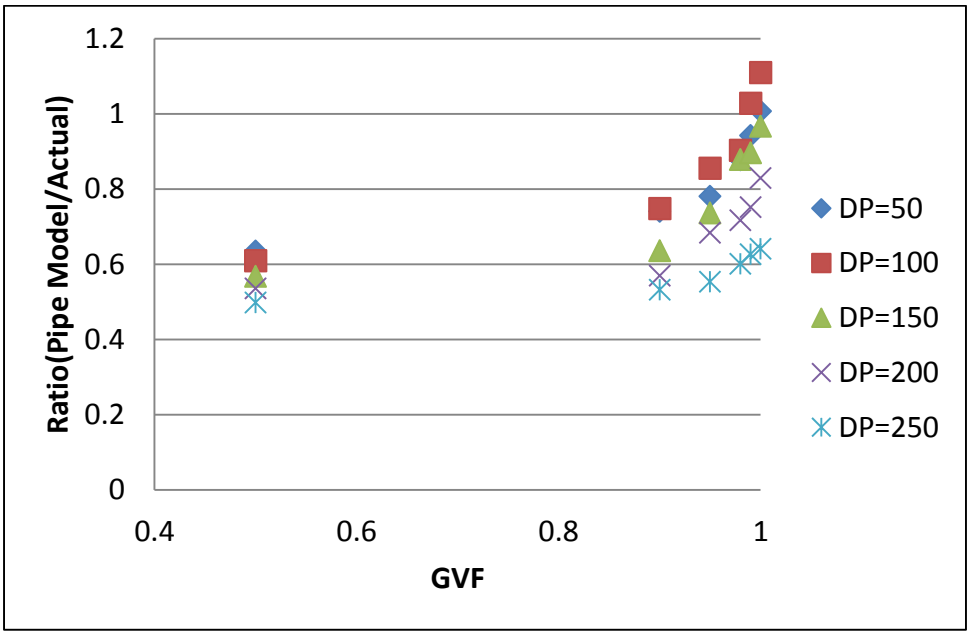

Figure 75 Inlet 50 PSI Ratio comparison with respect to differential pressure values

The applicability of the leakage model mechanical efficiency ratio is examined in the last step of the project. Since the mechanical efficiency calculation with a leakage model is the main purpose of the project, the ratio of the calculated mechanical efficiency with the pipe leakage model and isothermal mechanical efficiency from an experiment is used. This ratio is used in the vertical axis and the pressure ratio is used in the horizontal axis. The pressure ratio is calculated by the following equation:

$$Pressure\ Ratio\ (P_r) = \frac{Differential\ Pressure}{Absolute\ Inlet\ Pressure}$$

The curve fit equation is built for each case and the equation is applied to the other inlet pressure case. The purpose of this operation is to determine the behavior of the leakage model correlation and compare to the actual mechanical efficiency results.

Figure 76 presents all the ratio values for the inlet 10 PSI. A curve fit equation selected is a second order polynomial and the equation and standard its deviation are:

$$Ratio_{10\ PSI} = 0.0027P_r^2 - 0.0676P_r + 0.9534$$

$$R^2 = 0.8078$$

Figure 77 presents all the ratio values for inlet 50 PSI. The curve fit equation is selected second order polynomial and the equation and its standard deviation are:

$$Ratio_{50\ PSI} = -0.0178P_r^2 - 0.0139P_r + 0.9034$$

$$R^2 = 0.4326$$

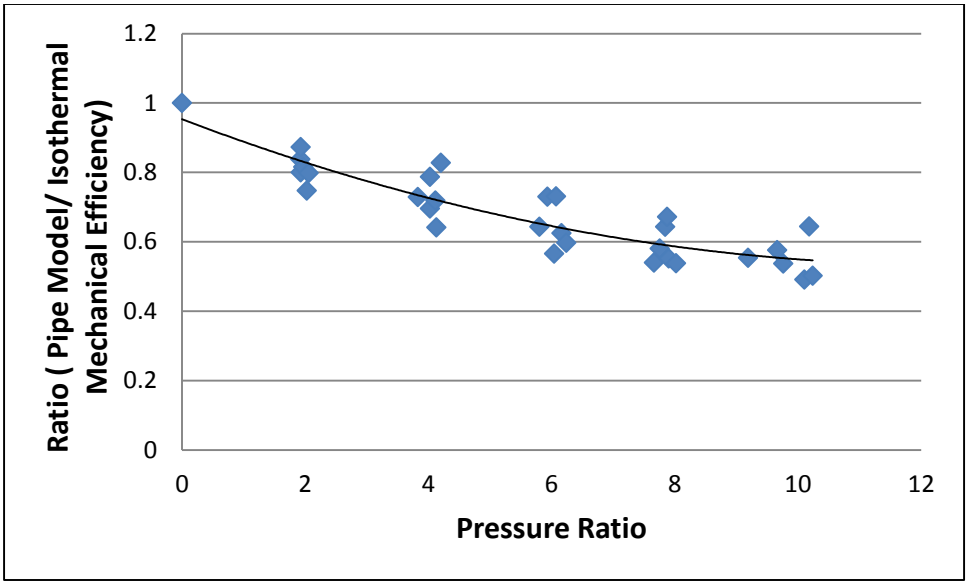

Figure 76 Inlet 10 PSI mechanical efficiency correlation ratio, curve fit applied

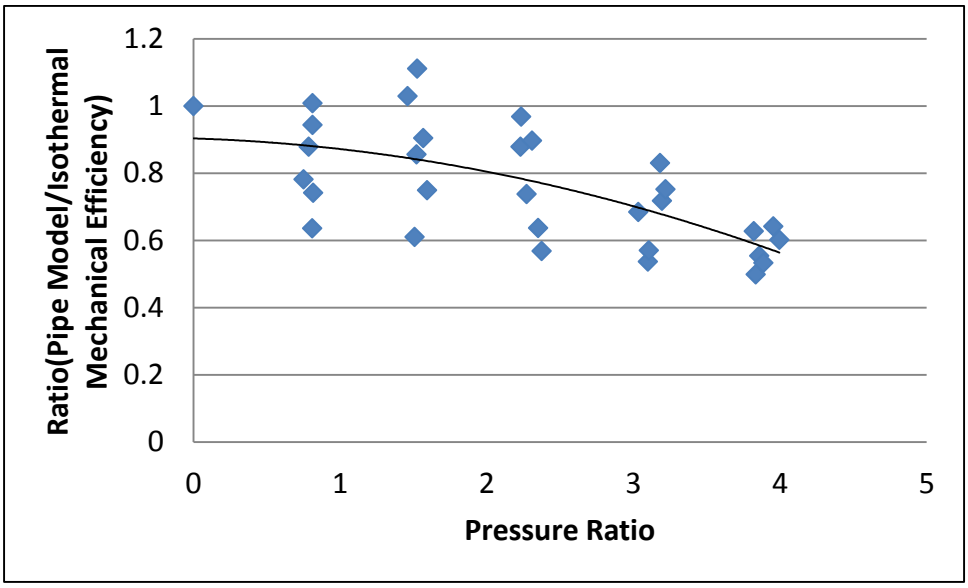

Figure 77 Inlet 50 PSI mechanical efficiency correlation ratio, curve fit applied

For each case, the curve fit equations are applied. In order to compare results with the actual mechanical efficiency values, the following method is used to actual mechanical efficiency:

$$Ratio = \frac{\eta_{pipe}}{\eta_{actual}}$$

$$10\ PSI \rightarrow\ \ \eta_{actual} = \frac{\eta_{pipe,10PSI}}{0.0027P_r^2 - 0.0676P_r + 0.9534}$$

$$50\ PSI \rightarrow\ \ \eta_{actual} = \frac{\eta_{pipe,10PSI}}{-0.0178P_r^2 - 0.0139P_r + 0.9034}$$

Figure 78 presents the inlet 10 PSI actual mechanical efficiency and the applied curve fits comparison. As noted in the graph, the 50 PSI curve fit equation gives negative results and it proves that this equation is not appropriate for the high pressure ratio cases. As expected, 10 PSI Curve Fit yields similar results with the actual mechanical efficiency.

Figure 79 presents the inlet 50 PSI actual mechanical efficiency and the applied curve fits comparison. Since the inlet 10 PSI curve fit equation is applicable in a range value, it can also be applied to the inlet 50 PSI case. However, it generally gives lower results in comparison to the actual mechanical efficiency.

The curve fit applications and the pipe model leakage ratio graphs show that mechanical efficiency correlation can be modified. If the GVF value and the differential pressure are considered, a coefficient can be added to the mechanical efficiency correlation. Furthermore, the inlet 10 PSI curve fit equation can be used for the mechanical efficiency detection for other inlet pressure cases.

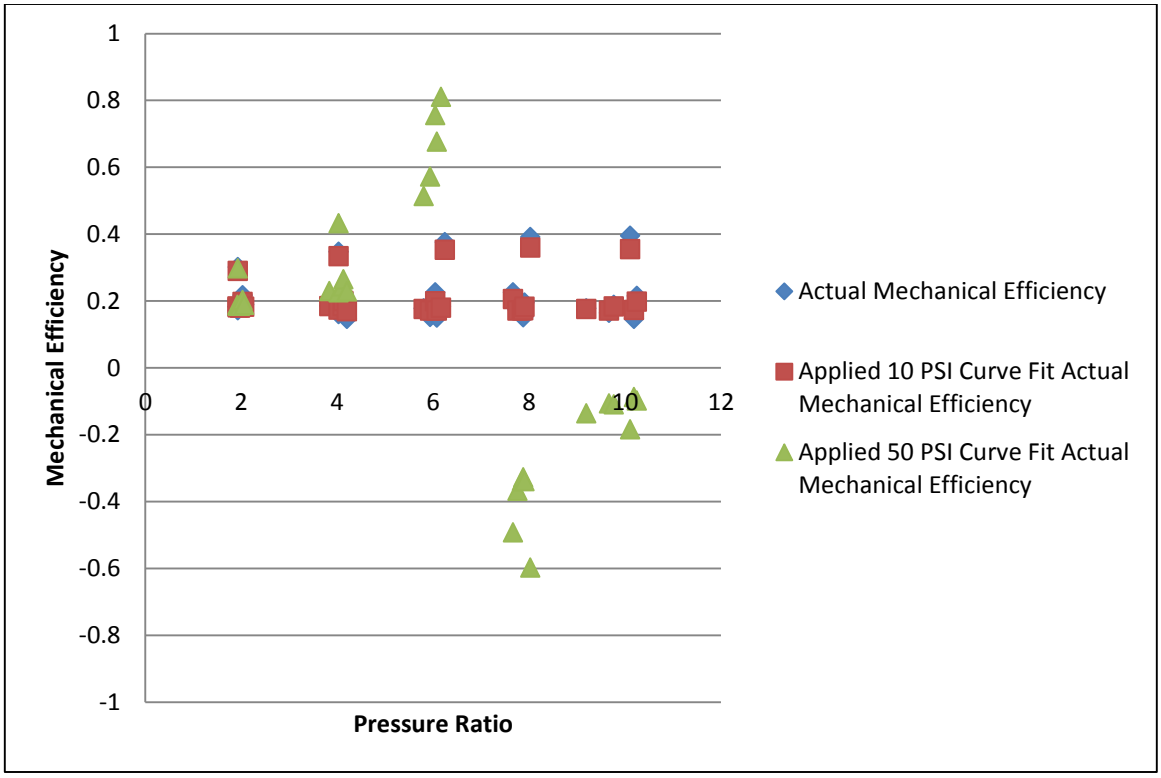

Figure 78 Inlet 10 PSI actual mechanical efficiency and applied curve fits comparison

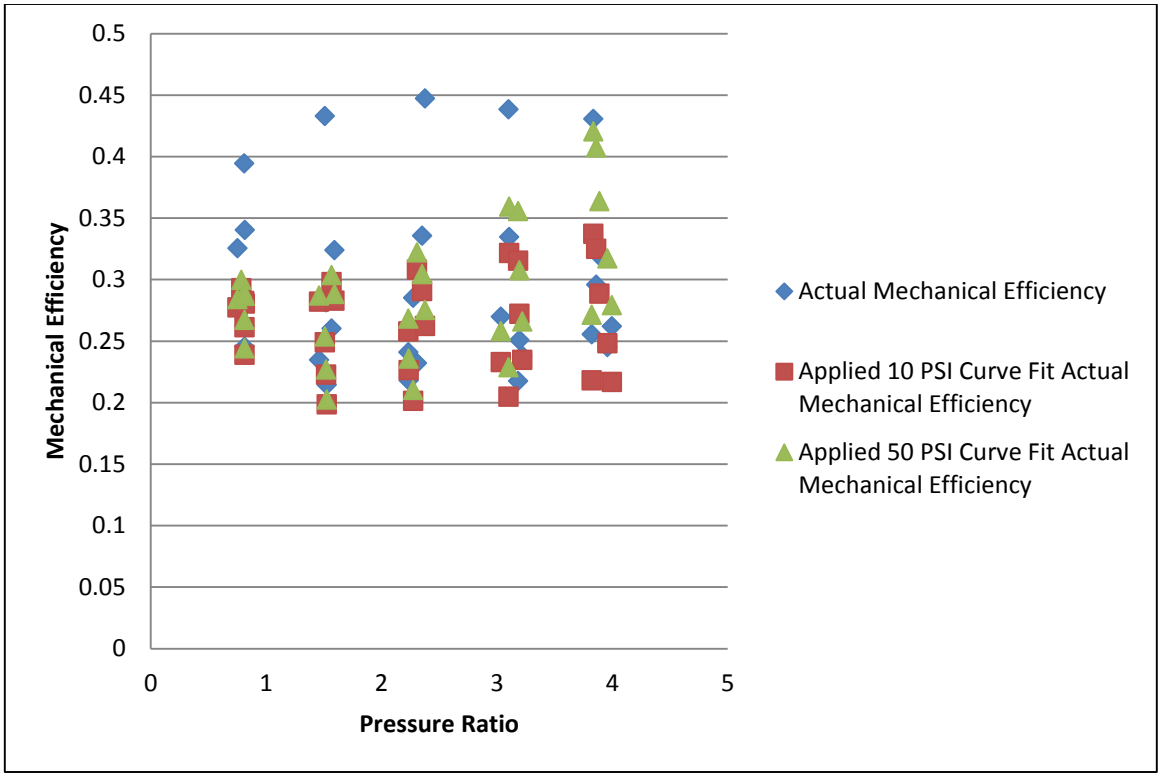

Figure 79 Inlet 50 PSI actual mechanical efficiency and applied curve fits comparison

4. RECOMMENDATIONS

For comparison of two set data with different working fluids for future work recommendations are listed below:

- The inlet pressure and the pressure rise across the pump are important parameters for evaluating and comparing two different experiments for multiphase operations. Therefore, the experiments should have the same inlet pressures and differential pressure conditions in a future study.
- As stated in the results and discussion part, the comparison of TAMU experiment and LSU experiment will be easier with the same instrumentation setup. Especially, the re-circulation system should have the same function in these different experiments.

In order to predict the leakage amount in future experiments, following recommendations can be listed:

- The leakage detection is only made for the circumferential clearance of the twin-screw pump. However, as stated in the thesis, there are also radial and flank clearances. Putting another effort to detect the leakage flow in these clearances will be very beneficial.
- If the leakage models are wanted to use for the leakage amount detection, the conclusion which is made by Vetter and Wincek (1993) may be considered.

According to their paper, the circumferential clearance is %80 of the total leakage. [7]

- For the pipe flow leakage model, the flow is assumed as turbulent. However, the viscosity of the homogenous flow is not used as turbulent viscosity.
- From the pump exit to the pump inlet, the leakage mass conservation in the circumferential clearance is assumed. However, a part of the leakage may join to the main bulk which comes from the suction. Conversely, a part of the main bulk may penetrate to the leakage amount. This should be considered in the future experiments.
- For the pipe flow leakage model, the circumferential clearance is assumed as a smooth pipe, assuming different pipe types may yield different friction coefficient. This situation may give more accurate results in the future works.
- For GVF inlet based leakage model and GVF exit based leakage model, the choked flow is assumed for all operations. However, in some cases Mach number may be less or greater than 1. A future study may cover detection of the Mach number.
- As can be noted in the mixture speed of sound distribution figure in the results and discussion part, very low GVF value cases yield same results with very high GVF cases. Therefore, liquid speed of sound term should put into the mixture speed of sound formula.

- For GVF inlet based leakage model and GVF exit based leakage model, the choked flow is assumed in the first tooth. In addition to first tooth, the other tooth should be checked in future works.
- As stated, the leakage models depend on the GVF and the differential pressure cases. Therefore, a selected leakage model with respect to GVF and differential pressure values of the operation can be used for future experiments.
- Since the actual leakage is very close to different leakage models in some cases, a correlation which includes all leakage models can be built for the leakage detection for a future study.
- As stated in the results and discussion part, the mechanical efficiency is made less dependent on the experimental result. Only the motor power from an experiment is needed to find the mechanical efficiency in multiphase operations. If the motor power is known for each condition, the mechanical efficiency can be calculated. There may be an experiment to detect the motor power with respect to the GVF and the differential pressure.
- The mechanical efficiency detection with the single-phase experimental results yields that the curve fit equation of low inlet pressure application gives accurate results. The curve fit applications can be modified with different equations and it may be used for future studies for mechanical efficiency detection.
- The ratio of the pipe model modified mechanical efficiency and the actual leakage distribution can be used to derive a formula which depends on the GVF and the differential pressure.

5. CONCLUSIONS

As presented in the results and discussion part the thesis is formed by two sections. While the first section includes the comparison of TAMU air-water experiment and LSU water-methane part, the second part includes the leakage detection of TAMU data. Therefore, the conclusion part is formed by two different sections as well.

5.1 TAMU and LSU Data Comparison

TAMU and LSU data are compared in terms of efficiencies which are the volumetric and the mechanical efficiencies. Since the inlet pressures are different in the operations, the low inlet pressure case of operations and the high inlet pressure case of operations are compared in their own right.

The volumetric efficiency distribution of TAMU and LSU data in contours are vastly different. The main reason for this difference is the liquid re-circulation operation of the experiments. In the TAMU experiment the liquid re-circulation amount is set with respect to differential pressure. Therefore, while TAMU experiment liquid re-circulation amount depends on the differential pressure, the LSU experiment liquid re-circulation system does not depend on GVF or differential pressure. It can be observed that LSU experiment yields nearly constant liquid re-circulation amount. This reduces the volumetric efficiency of the LSU experiment. The main function of the liquid re-circulation system is to prevent the pump heat rise and leakage. Hence, it can be

concluded that the TAMU experiment liquid re-circulation system is more appropriate to achieve better volumetric and mechanical efficiencies in multiphase operations.

The mechanical efficiency distribution difference can be observed in the mechanical efficiency evaluation as well. Before comparison of these experiments, the gas compression model types are discussed. Especially in the TAMU experiment, the isothermal gas compression model and the polytropic gas compression model yield very similar results. This is because the polytropic index is very close to 1 for most of the operations. Another reason of this similarity is pressure rise of operations. Since the pressure rise is not significant, both gas compression models yield similar results. The working fluid and the experiment setup differences are considered for the difference of the TAMU and the LSU experiment mechanical efficiency results. As can be seen in the results and discussion part the air compression causes more heat rise and this reduces the volumetric efficiency. However, the liquid re-circulation system of the TAMU experiment functions to eliminate this heat rise. Furthermore, as stated in the LSU experiment report, the automatic choke valve and the heat exchanger instrumentation makes the LSU experiment system more advanced. Unfortunately, the effect of this instrumentation can not be seen in the mechanical efficiency results. Lastly, it should be added that LSU experiment reporters state the smallness of the pump and the re-circulation problems of the system.

A general look of the comparison of the TAMU and LSU data reveals that the large differences of results are not caused only by the working fluid difference. If the nature of the pump is considered for multiphase operations the similar results should be

expected. However, especially in the high inlet pressure operations the LSU data does not give consistent results. Therefore, rather than looking at the instrumentation difference and the working fluid difference, the LSU experiment data accuracy should be examined.

5.2 Leakage Models

In order to detect the leakage amount for multiphase operations, different leakage models are built and evaluated in terms of efficiencies. Basically, the leakage models are built with the following assumptions.

- Pipe Flow Leakage Model: The leakage flow is moved in the circumferential gap. This gap is assumed as a smooth pipe and the mixture is assumed as homogenous mixture. Therefore, the mixture properties are calculated by the homogenous mixture formulas.
- GVF Inlet Based Leakage Model: The leakage flow is assumed as choked flow. The pump inlet pump based GVF value is used to calculate the velocity of the mixture.
- GVF Exit Based Leakage Model: The leakage flow is assumed as choked flow as well. However, the pump exit pump based GVF value is used for the GVF value for calculations.

In order to compare and evaluate the accuracy of these models, the leakage mass flow rate, the volumetric efficiency and the mechanical efficiency are used. It should be added that the pipe flow leakage model yields accurate results for single-phase operations in both inlet pressure conditions.

Leakage mass flow rate comparison yields that with the increment of the GVF, the pipe flow leakage model loses its accuracy in both inlet pressure cases. While GVF inlet based leakage model performs with good accuracy for nearly all operation conditions, GVF exit based leakage model gives similar results with other models especially in high pressure rise conditions. If the actual leakage mass flow rate is observed in different inlet pressures, the leakage mass flow rates are higher in low inlet pressure case.

The volumetric efficiency results show that especially in low inlet pressure and low GVF values, pipe flow leakage model provides accurate results. Since the pipe flow leakage model and the GVF inlet based leakage model results are close in low inlet pressure condition, both models can be used for leakage detection. GVF exit based leakage model yields larger volumetric efficiency results for both inlet pressure operations. The inlet pressure increment reduces the accuracy of models because the models are mainly based on the compressibility effect of the fluid. Furthermore, with generated contours, the pipe flow leakage model and GVF inlet based leakage model are compared with the actual leakage. The contours show that the general trend of pipe flow leakage model, GVF inlet and GVF exit based leakage model is very similar to the actual leakage. Furthermore, it is observed that the leakage does not depend on the pump speed. Therefore, higher pump speeds yield larger volumetric efficiency because the percentage of the leakage is less in these cases.

The mechanical efficiency correlation is modified and is made less dependent on the experiment results. Therefore, the leakage models can be used in this correlation.

Since the volumetric efficiency which is calculated by leakage models is used in the mechanical efficiency correlation, the volumetric efficiency and the mechanical efficiency results are very close in terms of the leakage models. The mechanical efficiency changes from 0 to 0.5 in most cases. This makes the leakage models more accurate. However, in the higher inlet pressure case the leakage models lose their accuracy in high GVF operations.

In the last part of the project, the multiphase operation mechanical efficiency is aimed to calculate with the single-phase operation data, process efficiency which is purely theoretical and the volumetric efficiency which is calculated by the leakage model. This correlation is valuable for a multiphase operation because before the operation it enables users of the pump to predict the mechanical efficiency. Even though the calculated mechanical efficiency with the actual leakage is very close to calculated mechanical efficiency with leakage models, the actual mechanical efficiency results are not close. This is because the modified mechanical efficiency calculation which is based on the single-phase operation includes three different efficiencies. If the modified mechanical efficiency calculation with other efficiencies is considered, the single-phase operation mechanical efficiency does not take place in this correlation. This situation always makes the calculated mechanical efficiency lower than the actual mechanical efficiency. The similarities between the calculated mechanical efficiency with actual leakage and leakage models motivate to add a constant to the mechanical efficiency calculation which is based on the single-phase. As can be seen in the results and discussion part an average constant for pipe flow leakage model can be applied to the

mechanical efficiency calculation with respect to GVF and pressure rise value. Furthermore, a general distribution of the ratio of the pipe flow leakage model and the isothermal mechanical efficiency of actual leakage is used and this distribution is converted to a second order polynomial for each inlet pressure case. The lower inlet pressure application of the equation gives more accurate results.

REFERENCES

[1] J. Xu, "Modeling of Wet Gas Compression in Twin-Screw Multiphase Pump", Ph.D. Dissertation, Texas A&M University, College Station, Texas, 2008.

[2] A. R. Patil, "Performance Evaluation and CFD Simulation of Multiphase Twin-Screw Pumps", Ph.D Dissertation, Texas A&M University, College Station, Texas, 2013.

[3] T. I. Hatch, "Design and Construction of a High Pressure System for Evaluating Multiphase Twin-Screw Pumps", MSc Thesis, Texas A&M University, College Station, Texas, 2013.

[4] J. R. Brennan, G. J. Czarnecki, J. K. Lippincott and A. J. Prang, "Screw Pumps," in *Pump Handbook*, New York, McGraw-Hill Professional, 2000, pp. 3.99-3.121.

[5] R. Kroupa, "Investigation of a Multiphase Twin-screw Pump Operating at High Gas Volume Fractions", MSc Thesis, Texas A&M University, College Station, Texas, 2011.

[6] F. M. White, "Borularda Surtunmeli Akis' and 'Sikistirilabilir Akis" in *Akiskanlar Mekanigi*, Istanbul,Turkey, Literatur Yayincilik, 2006,pp. 418-419, 718-719.

[7] G. Vetter and M. Wincek, "Performance Prediction of Twin Screw Pumps for Two-Phase Gas/Liquid Flow", *Pumping Machinery, 154,* pp. 331-340, 1993.

[8] C. Feng, P. Yueyuan , X. Ziwen and S. Pengcheng, "Thermodynamic Performance Simulation of a Twin Screw Pump," *Journal of Process Mechanical Engineering,* pp. 157-162, 2001.

[9] A. Martin, "Multiphase Twin-screw Pump Modeling for the Oil and Gas Industry", Ph.D. Dissertation, Texas A&M University, College Station, Texas, 2003.

[10] K. Rabiger, T. Maksoud and J. Ward, "Thermo- and Fluid Dynamic Model of a Multiphase Screw Pump, Operating at Very High Gas Volume Fractions," *Schriftenreihe der Georg-Simon-Ohm-Fachhochschule Nürnberg. Nr.35,* November 2006.

[11] M. Beijnum, "CFD simulation of multiphase twin screw pump," Graduate Project, Technische Universiteit Eindhoven-Department of Mechanical Engineering, Eindhoven, Netherlands, 2007.

[12] G.B. Wallis, “Homogenous Flow’ in *One-Dimensional Two-Phase Flow*, Arlington, Texas Mcgraw Hill, 1969, pp 24-25.